INTERBAND OPTICAL ABSORPTION IN SEMICONDUCTORS

by

INDER PAUL BATRA

B. Sc. (Honours), Delhi University (India), 1962
M. Sc. (Physics), Delhi University (India), 1964

A DISSERTATION SUBMITTED IN PARTIAL FULFILLMENT
OF THE REQUIREMENTS FOR THE DEGREE OF
DOCTOR OF PHILOSOPHY

in the Department
of
Physics

SIMON FRASER UNIVERSITY

July, 1968

EXAMINING COMMITTEE APPROVAL

R. R. Haering
Senior Supervisor

R. H. Enns
Examining Committee

D. J. Huntley
Examining Committee

P. R. Wallace
Examining Committee
Director
Theoretical Physics Institute
McGill University
Montreal, Quebec

PARTIAL COPYRIGHT LICENSE

I hereby grant to Simon Fraser University the right to lend my thesis or dissertation (the title of which is shown below) to users of the Simon Fraser University Library, and to make partial or single copies only for such users or in response to a request from the library of any other university, or other educational institution, on its own behalf or for one of its users. I further agree that permission for multiple copying of this thesis for scholarly purposes may be granted by me or the Dean of Graduate Studies. It is understood that copying or publication of this thesis for financial gain shall not be allowed without my written permission.

Title of Thesis/Dissertation:

_____

_____

_____

_____

Author: _____

(signature)

_____

(name)

_____

(date)

ABSTRACT

A unified treatment of the direct interband optical absorption in semiconductors in the presence of external static electric and magnetic fields, is presented in the framework of the 'effective mass approximation'. A general expression for the absorption coefficient is derived, which in the appropriate limits reproduces the following well known results:

(a) Zero field absorption coefficient,
(b) Magnetoabsorption coefficient,
(c) Electroabsorption and Franz-Keldysh effect,
(d) Absorption in crossed electric and magnetic fields and
(e) Photon-assisted tunneling in parallel fields.

While investigating the crossed fields absorption coefficient, special stress has been laid on the experimentally favourable situation of weak electric field. A new perturbation expansion in terms of a dimensionless parameter is developed in this connection and is used to obtain the weak electric field limit. An alternate derivation for Franz-Keldysh effect based upon W.K.B. approximation has also been given.

The effective mass treatment is also used to study the phonon-assisted transitions and Urbach's law. The absorption coefficient for phonon-assisted transitions involving the simultaneous absorption of a photon and a longitudinal optical phonon in

the presence of external electric and magnetic fields is calculated using second order perturbation theory. It is predicted that an experimental investigation of such transitions in the presence of external fields will show structure of the valence and conduction bands separately which may provide the values of effective masses in different bands. The experimental conditions, and the validity criterion for the perturbation theory, are thoroughly discussed.

Some attention is paid to the study of magnetic field induced surface states. Whereas such states have been observed recently in metals, there is no experimental or theoretical evidence as to whether or not these states exist in semiconductors. We have theoretically predicted that such states do in fact exist even in semiconductors. The experimental conditions under which surface states may be detected experimentally in semiconductors are discussed. The arguments are supported with quantitative calculations, where possible. Throughout the entire presentation we have restricted ourselves to the study of direct band gap semiconductors.

TABLE OF CONTENTS

LIST OF IMPORTANT SYMBOLS

$\vec{B}$, B	Magnetic field (Symbols with arrow represent vector quantities)
$\vec{\mathcal{E}}$, $\mathcal{E}$	Electric field
$\mathcal{E}_x, \mathcal{E}_y, \mathcal{E}_z$	Components of an electric field
η	Interband absorption coefficient
$\eta(0)$	Interband absorption coefficient in the absence of external fields
$\eta(B), \eta(\mathcal{E}), \eta(\vec{\mathcal{E}}\times\vec{B})$	Interband absorption coefficient in the presence of a magnetic field, electric field, crossed electric and magnetic fields
η_θ	Phonon-assisted absorption coefficient
$\eta_\theta(0)$	Phonon-assisted absorption coefficient in the absence of external fields
$\eta_\theta(B)$, $\eta_\theta(\vec{\mathcal{E}}\times\vec{B})$	Phonon-assisted absorption coefficient in the presence of magnetic field, crossed electric and magnetic fields
H	Hamiltonian
E	Energy
E_F	Fermi energy
E_g	Energy gap in the absence of external fields
$E_g(B), E_g(\vec{\mathcal{E}}\times\vec{B})$	Effective energy gap in the presence of fields
ω	Angular frequency of photons
ϵ	Energy
ϵ_z	Energy associated with the Z component of an electric field
$\vec{k}$	Wave vector

k	Boltzmann constant
$(k\Theta)$	Energy of a longitudinal optical phonon
α	Band index
e	Absolute value of the electronic charge
$\lambda = \left(\frac{c\hbar}{eB}\right)^{1/2}$	Magnetic length
m	Free electron mass
m^*	Effective mass
m_c	Effective mass in conduction band
m_v	Effective mass in valence band
$\alpha_{c,v} = \frac{m}{m_{c,v}}$	Dimensionless ratios
$M = m_c + m_v$	Sum of the masses
$\mu = \frac{m_c m_v}{m_c + m_v}$	Reduced mass
$\omega_c = \frac{eB}{mc}$	Cyclotron frequency involving free electron mass
$\omega_{ce} = \frac{eB}{m^* c}$	Cyclotron frequency involving an effective mass
$\omega_{cc} = \frac{eB}{m_c c} = \alpha_c \omega_c$	Cyclotron frequency involving m_c
$\omega_{cv} = \frac{eB}{m_v c} = \alpha_v \omega_c$	Cyclotron frequency involving m_v
$\omega_c^* = \frac{eB}{\mu c}$	Cyclotron frequency involving a reduced mass
$\Omega_c = \frac{eB}{Mc}$	Cyclotron frequency involving sum of the masses
$\gamma = 1 + \frac{\alpha_c}{\alpha_v}$	Dimensionless number

$V_d = \frac{\vec{E} \times \vec{B}}{B^2}$	Drift velocity
$a = V_d \frac{M\lambda^2}{\hbar}$	Length
$\delta = \frac{a}{\lambda}$	Dimensionless ratio
$\Theta_F = \left(\frac{e^2 E_z^2}{2\mu\hbar}\right)^{1/3}$	Frequency
$\beta = \frac{E_g - \hbar\omega}{\hbar\Theta_F}$	Dimensionless ratio
$\Delta = \hbar\omega + k\theta - E_g$	Energy
$\Delta(B) = \hbar\omega + k\theta - E_g(B)$	Energy
$\Delta(\vec{E}\times\vec{B}) = \hbar\omega + k\theta - E_g(\vec{E}\times\vec{B})$	Energy
$\mathcal{A} = \frac{E_g - \hbar\omega}{r}$	Energy
$\mathcal{A}(B) = \frac{E_g(B) - \hbar\omega}{r}$	Energy
$\mathcal{A}(\vec{E}\times\vec{B}) = \frac{E_g(\vec{E}\times\vec{B}) - \hbar\omega}{r}$	Energy
Ω	Volume of a unit cell
$V = L_x L_y L_z$	Volume of the crystal
$\vec{P}_{cv}$	Interband matrix elements

NOTE: We have tried to use systematic notation throughout the thesis. But due to the limited number of letters in available alphabets, we have not always been able to use the most elegant notation. However, we hope that we have succeeded in avoiding the use, in any one section, of the same symbol for different quantities.

LIST OF TABLES

LIST OF ILLUSTRATIONS

ACKNOWLEDGMENTS

The author is indebted to Dr. R. R. Haering for suggesting this topic and for his help and guidance throughout the course of the investigation. Grateful acknowledgement is also given to Drs. R. H. Enns and D. J. Huntley for reading the manuscript and for their many helpful suggestions.

The author is grateful to Dr. P. R. Wallace, Director of the Institute of Theoretical Physics at McGill University, for critically reading the manuscript. Thanks are due to Dr. Dennis Dunn for his help towards preparation of Chapter 13 of the thesis.

The author is also grateful to Mr. N. I. Robb for many useful discussions, help towards numerical computations and proof-reading several chapters of the thesis; to Dr. F. P. Kapron for sending a copy of his Ph.D. thesis; to Miss Sheila Winton and Dr. S. N. Behera for proof-reading the manuscript; to Mr. W. Schneider for drafting; and to Mrs. S. Ginetz for neat typing of the thesis.

The financial support of the National Research Council of Canada in the form of a studentship for the years 1966-67 and 1967-68 is gratefully acknowledged.

CHAPTER 1

INTRODUCTION

1.1 General

The tremendous interest in the band structure of solids in recent years has led to extensive investigation of optical absorption in solids in the presence of external electric and magnetic fields. In semiconductors, quantitative information can be obtained by studying the dependence of the interband optical absorption coefficient on the frequency of optical radiation and on external fields. In its simplest form the interband absorption process involves the promotion of an electron from a valence band to a conduction band, accompanied by the destruction of a photon and the creation of a hole in the valence band state previously occupied by the electron. The absorption is very small for photon energies much less than that corresponding to the energy gap and increases by a factor of $\sim 10^4$ or more at higher photon energies. The bulk of experimental work reported in the current literature deals with interband absorption and we shall restrict ourselves to the study of the absorption coefficient throughout the entire presentation.

The most direct way of determining the absorption coefficient is from transmission measurements, and this is generally the procedure used. Experimentally one shines light on a slab of material of thickness, d, and the ratio of transmitted intensity

to the incident intensity gives the value of absorption coefficient through the relation (if the reflection coefficient << 1)

$$I(d) = I(0) \exp(-\eta d) \qquad (1\text{-}1)$$

where I(d) is the transmitted intensity through the crystal, I(o) is the incident intensity and η is the absorption coefficient.

In the region of strong absorption, the radiation cannot be transmitted through thick samples, so thin samples of thickness $d \lesssim \frac{1}{\eta}$ should be used. Usually samples of micron thickness are adequate, but if these are hard to obtain, then reflection spectroscopy is much more suitable and then the absorption coefficient is obtained from the measured reflectivity through Kramers Kronig relations. The experiments are generally done at low temperatures using infra-red radiation.

1.2 Various Types of Interband Transitions

There are basically two types of interband transitions.

(i) Direct Transitions: The electromagnetic radiation is absorbed by a semiconducting crystal due solely to the interaction between the radiation and the electrons in the crystal.

(ii) Indirect Transitions: These involve the simultaneous interaction of the electrons with the electromagnetic radiation and with lattice vibrations.

For direct transitions, an electron in the valence band state $E_v(\vec{k})$, absorbs a photon of energy $\hbar\omega$ and wave vector $\vec{S}$, and ends up in a conduction band state, $E_c(\vec{k}')$. The transition is governed by the following two conservation laws:

(a) Energy conservation, $E_c(\vec{k}') = E_v(\vec{k}) + \hbar\omega$

(b) Momentum conservation, $\vec{k}' = \vec{k} + \vec{S}$

For electrons $k_{max} = \frac{\pi}{a} \simeq 10^7 - 10^8$ cm^{-1} ('a' is a unit cell length) but $|\vec{S}| = 10^5$ cm^{-1}, (for wavelength = 6283 Å) so $\vec{k}' \simeq \vec{k}$ and hence the name 'direct' or 'vertical' transitions. It is quite clear that the direct transitions determine the absorption edge only in a direct band gap semiconductor, such as InSb, where the valence band maximum and the conduction band minimum lie at the same point in $\vec{k}$ space. When the lowest energy state in the conduction band does not have the same value of $\vec{k}$ as the highest energy state in the valence band, direct transitions may still take place, but these are not the transitions corresponding to the lowest value of $\hbar\omega$ for which interband transitions are possible.

Direct (and also indirect) transitions are further subdivided into "allowed" and "forbidden" transitions according

to the symmetry property of the energy bands at $\vec{k} = 0$, (to be discussed later). Bardeen, Blatt and Hall[1] have derived the following expressions for the absorption coefficients, assuming parabolic bands and ignoring Coulomb effects.

Direct allowed transitions:

$$\eta_d(0) = R(\omega - \omega_g)^{\frac{1}{2}}, \quad \hbar\omega > E_g \equiv \hbar\omega_g$$

$$\eta_d(0) = 0 \qquad \text{if} \quad \hbar\omega \leq E_g ,$$

where 0 in the bracket indicates the absence of external fields.

Direct forbidden transitions:

$$\eta_d(0) = R' (\omega - \omega_g)^{\frac{3}{2}}$$

where R and R' are constants. It should be remarked that in actual practice the absorption does not strictly go to zero at $\hbar\omega = E_g$, but rather dies out exponentially. This is the so called Urbach's law[2] and we will discuss it in Section 1.4 below.

The indirect transitions dominate the absorption edge in indirect band gap semiconductors like Ge and Si where the conduction band minimum and the valence band maximum occur at different $\vec{k}$ values. An electron in initial momentum state $\vec{k}$ ends up in a final state $\vec{k}' \neq \vec{k}$ and the selection rule for conservation of momentum is satisfied by the participation of a

phonon. Thus an indirect transition is a second order transition through a virtual intermediate state which involves scattering in $\vec{k}$ space by the absorption or emission of a phonon in addition to the usual absorption of an optical photon. The absorption coefficient for indirect transitions also depends on whether the transition at $\vec{k} = 0$ is allowed or not (i.e. indirect transitions can be allowed or forbidden). For allowed indirect transitions, the absorption coefficient is given by[1]

$$\eta_i(0) \propto (\hbar\omega - E_g)^2$$

and for forbidden indirect transitions, the result[1] is

$$\eta_i(0) \propto (\hbar\omega - E_g)^3$$

When phonon absorption processes dominate over phonon emission the indirect absorption coefficient is temperature dependent through the Bose-Einstein factor $(e^{\theta/T} - 1)^{-1}$, where $k\theta$ is the energy of the phonons involved.

1.3 Effects of Static Electromagnetic Fields on Interband Transitions

Externally applied static electric and magnetic fields modify the absorption coefficient. A great deal of information about the band structure of the material can be obtained, once the field induced changes in absorption coefficient are related

to the behaviour of the electrons in the material. It is convenient to discuss the effects of electric field, magnetic field and crossed electric and magnetic fields, on the optical absorption coefficient separately.

(i) Electric Field

The simple theory of the effect of an electric field (to be discussed later) on the absorption edge of a semiconductor predicts that the change in the absorption coefficient, $\Delta\eta = \eta(\mathcal{E}) - \eta(0)$ will be exponential-like below the band gap and oscillatory above it. The former phenomenon is often called the Franz-Keldysh effect and is due to electron tunneling in the presence of an electric field. The conduction and valence band wave functions extend into the forbidden gap and the overlap integral for $\hbar\omega < E_g$ is non-vanishing. Thus the absorption coefficient has non-zero values for $\hbar\omega < E_g$. The Franz-Keldysh effect is alternatively termed as photon-assisted tunneling. The oscillatory behaviour of the absorption coefficient for $\hbar\omega > E_g$ follows from the simple theory and will be discussed later. The exponential-like tail has been confirmed by several experiments[3,4,5], but no quantitative agreement has been achieved between theory and experiment above the band gap.

(ii) Magnetic Field

A magnetic field has two striking effects on the interband absorption spectrum. It shifts the threshold for absorption

to higher photon energies and this shift is proportional to magnetic field strength, B. Secondly, in the presence of a magnetic field the absorption coefficient is oscillatory in nature for photon energies greater than that corresponding to the effective band gap. These are not too difficult to understand if one recalls that a magnetic field introduces a discrete structure in the energy level spectrum. We will see later that in the presence of a magnetic field, energy levels in conduction and valence bands are quantized and direct interband transitions obey the selection rule $\Delta n = n' - n = 0$, where n', n are the Landau quantum numbers for conduction band and valence band respectively. The discrete energy level spectrum, coupled with this interband selection rule is sufficient to explain both the above effects. There is an abundance of experimental data[21-29] and magneto-optics is extensively used in determining band parameters.

(iii) Crossed Electric and Magnetic Fields

The application of a transverse electric field, $\vec{\mathcal{E}}$, affects the magnetoabsorption basically in two ways; the energy threshold is reduced by an amount proportional to $(\mathcal{E}/B)^2$ and additional small peaks appear increasing in number and amplitude with $\mathcal{E}$. The first effect is due to the net motion of the electrons in the $\vec{\mathcal{E}} \times \vec{B}$ direction while the latter

signifies a violation of the selection rule $\Delta n = 0$. A particularly useful situation is one where the applied static electric field is weak (criterion to be discussed later). In this case the selection rule $\Delta n = 0$ is violated only slightly and the direct interband transitions obey the selection rule $\Delta n = 0, \pm 1$. The appearance of new peaks can be fruitfully exploited to obtain information about individual band effective masses. This will be discussed in a later Chapter.

1.4 Urbach's Law

It was pointed out earlier that the absorption coefficient does not strictly go to zero at the direct band gap but dies out rather slowly in a manner first reported by F. Urbach[2]. The observed absorption in the tail region ($\hbar\omega < E_g$) is temperature dependent and has the form

$$\eta_{\theta}(o) \propto \exp\{\sigma_o(\hbar\omega - E_g)/kT\} \quad (1\text{-}2)$$

where σ_o depends upon temperature and material under consideration. There have been several explanations of Urbach's Law and a complete summary of these is to be found in Chapter 9. It is now well established that the law is associated with phonon-assisted optical transition involving the absorption of one or more optical phonons of energy $k\theta$. In an ionic crystal of the direct band gap type, phonons of interest are those associated with the optical

branch and having wave vector $\vec{q} \simeq 0$. Dumke[6] calculated the absorption coefficient for such phonon-assisted transitions in the range $E_g - k\theta < \hbar\omega < E_g$ using perturbation theory and obtained a good fit with the experimental data on InSb[7]. Calculations involving higher-order phonon processes have been performed[8,9] recently but no quantitative comparison has been made with the available experimental data.

Very little attention has been paid in the past to the study of phonon-assisted transitions in the presence of external electromagnetic fields. In a recent theoretical paper we studied[10] the effect of a magnetic field on phonon-assisted transitions in the region $E_g - k\theta < \hbar\omega < E_g$ using perturbation theory. It has been shown that the absorption spectrum is oscillatory in nature and can provide useful information regarding effective masses of the electrons and holes separately. We will have occasion to study this in greater detail in Chapter 11. Also in Chapter 12, we will study the effect of simultaneous electric and magnetic fields on phonon-assisted transitions. The study of phonon-assisted transitions in the presence of an electric field is not very fruitful because the absorption edge is smeared out. Higher order transitions in the presence of external fields are extremely complex mathematically and the calculations have not been carried out so far. Throughout the entire thesis we will be calculating absorption coefficient in

various situations. It is therefore desirable to outline the general approach for calculating this quantity. This we do in the following Section.

1.5 Quantum Mechanical Expression for Absorption Coefficient

Here we express the optical absorption coefficient in terms of quantum mechanically calculable quantities and thus establish a general method for computing the absorption coefficient. In equation (1-1) we stated the relation between incident and transmitted radiation intensity in terms of the absorption coefficient for an absorbing crystal. Since the radiation intensity is proportional to the number of photons per unit volume we can immediately write

$$\gamma = -\frac{1}{N}\frac{dN}{dt} = -\frac{n_o}{c}\frac{dN}{dt} \qquad (1\text{-}3)$$

where c is the velocity of light in vacuum and n_o is the refractive index. The rate of change of photon number is related to the transition probability per unit time, W_{fi}, through the relation,

$$\frac{dN}{dt} = -\frac{1}{V}\sum_{f,i} W_{fi}$$

where

$$W_{fi} = \frac{2\pi}{\hbar} |M_{fi}|^2 \delta(E_f - E_i)$$

is the well known result in time dependent perturbation theory. Hence

$$\eta = \frac{4\Pi n_0}{cN\hbar V} \sum_{f,i} |M_{fi}|^2 \delta(E_f - E_i) \qquad (1\text{-}4)$$

where V is the volume of the crystal and a factor of two has been included for spin. For first order transitions,

$$M_{fi} = \langle f | H_1 | i \rangle \qquad (1\text{-}5)$$

is the matrix element of the photon-particle interaction Hamiltonian between the initial state i and the final state f. For second order transitions,

$$M_{fi} = \sum_j \frac{\langle f | H_2 | j \rangle \langle j | H_1 | i \rangle}{E_i - E_j} \qquad (1\text{-}6)$$

and the particle goes through a virtual intermediate state, j, before arriving in the final state f, under the influence of a

second type of interaction H_2. Throughout the entire presentation, H_1 will stand for the electron-photon interaction Hamiltonian and H_2 for the electron-phonon interaction Hamiltonian.

Thus to compute absorption coefficient, we need to know the unperturbed eigenfunctions and the corresponding eigenvalues along with the appropriate interaction Hamiltonians. The complete Hamiltonian for a particle of mass m and charge 'e' in the presence of static external electric and magnetic fields and the time dependent radiation field, is

$$H = \frac{1}{2m}(\vec{p} + e\vec{A}(r,t))^2 + e\vec{\mathcal{E}}\cdot\vec{r} + V_p(\vec{r}) + H_2 \qquad (1\text{-}7)$$

where $\vec{\mathcal{E}}$ is the static electric field and $V_p(\vec{r})$ stands for the periodic crystal potential. The vector potential $\vec{A}(\vec{r}, t)$ is decomposed into two parts in the following manner

$$\vec{A}(\vec{r}, t) = \vec{A}_o(\vec{r}) + \vec{A}_1(\vec{r}, t)$$

The time independent part, $\vec{A}_o(\vec{r})$ describes a static magnetic field, $\vec{B} = \vec{\nabla} \times \vec{A}_o(\vec{r})$, and the time dependent part describes the external radiation field. The vector potential is generally so chosen that $\vec{\nabla} \cdot \vec{A} = 0$ (Coulomb gauge), then

$$H = H_o + H_1 + H_2$$

where

$$H_o = \frac{\Pi^2}{2m} - e\vec{\mathcal{E}}\cdot\vec{r} + V_p(\vec{r}) \qquad (1\text{-}8)$$

with

$$\vec{\Pi} = \vec{p} - \frac{e}{c}\vec{A}_o(\vec{r})$$

and

$$H_1 = -\frac{e}{mc}\vec{\Pi}\cdot\vec{A}_1(\vec{r},t) + \frac{1}{2m}\left(\frac{eA_1}{c}\right)^2$$

We drop the second term of H_1, since it represents simultaneous two photon absorption and hence the electron-photon interaction Hamiltonian becomes

$$H_1 = -\frac{e}{mc}\vec{\Pi}\cdot\vec{A}_1(\vec{r},t) \qquad (1\text{-}9)$$

In the next chapter, the eigenfunctions and eigenvalues of the Hamiltonian, H_o will be calculated in the framework of the 'Effective Mass Approximation'[11]. We then proceed to evaluate the matrix elements of the electron-photon interaction, H_1.

1.6 Scope of the Thesis

As stated above, the entire problem of computing absorption coefficient hinges around obtaining proper eigenfunctions and

evaluating appropriate matrix elements. The general n-particle problem is impossible to solve, therefore we will be content with the conventional one-particle approximation. Exact solutions are not possible even for this case especially in the presence of external fields which do not possess the periodicity of the crystal lattice; therefore a further approximation is required. In the theory of optical absorption, the effective mass approximation[11] (E.M.A.) is widely used. We discuss this approximation for the case of direct band gap semiconductors in Chapter 2, and in the remaining portion of the thesis only these will be studied.

In Chapter 3 the matrix elements for the electron-photon interaction Hamiltonian are evaluated using E.M.A. wave functions and the distinction between allowed and forbidden transition is explained. This chapter also presents a unified treatment of the direct, allowed interband effects where a general expression for the optical absorption coefficient in the presence of arbitrarily oriented external electric and magnetic fields is derived, which in the appropriate limits reproduces the following well known results:

(a) Zero field absorption coefficient,
(b) Magnetoabsorption coefficient,
(c) Electroabsorption coefficient,
(d) Franz-Keldysh effect,
(e) Photon-assisted tunneling in parallel fields,
and (f) Crossed electric and magnetic fields absorption.

The task of obtaining these special cases is completed in Chapters 4 to 8, and a brief summary on the experimental situation is included at the end of each chapter. While studying the crossed fields absorption coefficient in Chapter 8, special stress has been laid on the experimentally favourable situation of weak electric field. A new perturbation expansion in terms of a dimensionless parameter is developed in this connection and is used to obtain the weak electric field limit.

Next we focus our attention on phonon-assisted transitions in direct-gap semiconductors and on Urbach's law. Chapter 9 contains a critical review of the existing explanations of Urbach's law and stresses the fact that phonon-assisted transitions are quite successful in explaining the observation. Chapter 10 serves as an introduction to the study of phonon-assisted transitions. The absorption coefficient for such transitions is calculated, stating clearly all the assumptions. In Chapters 11 and 12, the effects of external fields are investigated and the weak electric field case is emphasised. Some new effects are predicted and the experimental conditions for observing them are discussed.

Chapter 13 justifies the use of perturbation theory in calculating the absorption coefficient for phonon-assisted transitions in the range $E_g - k\theta < \hbar\omega < E_g$. Comparison is made between the perturbative and non-perturbative approach and it is shown numerically that for a realistic electron-phonon

coupling constant in InSb, many-phonon processes change the absorption coefficient only by about 2%, in the range where one-phonon processes are allowed. The range of coupling constant over which perturbation theory is valid is also discussed.

Some attention is devoted to one of the most recent developments in the field of magneto-optics, namely magnetic field induced surface states. These states have recently been observed experimentally in metals but no corresponding experiments exist in semiconductors. We have theoretically predicted the existence of such states in semiconductors and have discussed the experimental conditions under which such states may be detected in semiconductors. In order to maintain the continuity of presentation, the surface states are discussed in Appendices (H) and (I).

In the concluding chapter, some general comments and conclusions are stated. A short summary is provided in a tabular form. Some important, but mathematically involved results are given in the form of Appendices at the end of the thesis. The Gaussian system of units is followed throughout.

CHAPTER 2

BLOCH ELECTRONS IN EXTERNAL FIELDS

2.1 Effective Mass Wave Function for a Particle in External Fields

In order to study optical absorption in solids we require the solutions of the Schrödinger equation

$$\left\{ \frac{\vec{\pi}^2}{2m} + V_p(\vec{r}) + U(\vec{r}) \right\} \psi(\vec{r}) = E\,\psi(\vec{r}) \qquad (2\text{-}1)$$

where $\vec{\pi} = (\vec{p} - \frac{e}{c}\vec{A}_o)$ is the kinetic momentum, ($\vec{A}_o$ is the time independent vector potential), $V_p(\vec{r})$ is the periodic lattice potential and $U(\vec{r})$ another perturbation that can be caused for example, by a constant electric field, m is the mass of the free particle and 'e' its charge. Since no exact solutions are possible even for idealized models, we will use the effective mass approximation (E.M.A.)[11] for the specification of eigenfunctions and energy eigenvalues for electronic states in solids.

In its simplest form the E.M.A. states that for sufficiently small external fields such that the electron always remains in a single band the motion of the electron in the combined field of the lattice and the external fields can be studied in terms of the motion of a fictitious particle in the external fields only. The mass of this fictitious particle is m* (assumed isotropic)

which is different from m, and the particle is described by an envelope function $F_{\alpha\mu}(\vec{r})$ which satisfies the effective mass equation (see Appendix (A)).

$$\left\{ \frac{\Pi^2}{2m^*} + U(\vec{r}) \right\} F_{\alpha\mu}(\vec{r}) = E F_{\alpha\mu}(\vec{r}) \qquad (2\text{-}2)$$

This equation is valid near an energy band extremum, assumed for simplicity to be at $\vec{k} = 0$. The energy E is measured from the band edge E^o_α, α is the band index, and μ is a set of quantum numbers characterizing a state in band α. The complete wave function for an electron in band α is given by (see Appendix (A) equation (A-18))

$$\psi_{\alpha\mu}(\vec{r}) = \left[u_{\alpha o}(\vec{r}) + \sum_{\alpha' \neq \alpha} u_{\alpha' o}(\vec{r}) \frac{\vec{p}_{\alpha'\alpha} \cdot \vec{\Pi}}{m(E^o_\alpha - E^o_{\alpha'})} \right] F_{\alpha\mu}(\vec{r}) \qquad (2\text{-}3)$$

where $u_{\alpha o}$ is the periodic part of the Bloch function at $\vec{k} = 0$ and

$$\vec{p}_{\alpha'\alpha} = \frac{(2\pi)^3}{\Omega} \int_\Omega u^*_{\alpha' o}(\vec{r}) \left(\frac{\hbar}{i} \vec{\nabla} \right) u_{\alpha o}(\vec{r}) \, d\vec{r} \qquad (2\text{-}4)$$

Ω being the volume of a unit cell. The normalization of u's and the effective mass wave functions is discussed in the next section, the explicit forms for the envelope wave functions in various field configurations are obtained in Section 2.3.

2.2 Normalization of Effective Mass Wave Functions

In arriving at equation (2-3) we used the complete set of Kohn-Luttinger[11] wave functions

$$|\alpha, \vec{k}\rangle = e^{i\vec{k}\cdot\vec{r}} u_{\alpha}(\vec{r}) \tag{2-5}$$

The orthonormality condition satisfied by these functions is

$$\langle \alpha', \vec{k}' | \alpha, \vec{k} \rangle = \delta_{\alpha\alpha'} \delta(\vec{k} - \vec{k}') \tag{2-6}$$

From this condtion we can readily derive the orthogonality property of the Bloch functions at the band edge. We have

$$\langle \alpha', k' | \alpha, \vec{k} \rangle = \int_V e^{i(\vec{k}-\vec{k}')\cdot\vec{r}} u^*_{\alpha' o}(\vec{r})\, u_{\alpha o}(\vec{r})\, d\vec{r} \tag{2-7}$$

Since $u^*_{\alpha' o}\, u_{\alpha o}$ has the lattice periodicity, we expand it in a Fourier series as follows

$$u^*_{\alpha' o}\, u_{\alpha o} = \sum_m B_m^{\alpha'\alpha} e^{-i K_m \cdot \vec{r}} \tag{2-8}$$

where the $B_m^{\alpha'\alpha}$ are just numerical coefficients, and the $\vec{K}_m$ are the reciprocal lattice vectors. Substituting (2-8) in (2-7), we obtain

$$\langle \alpha', \vec{k}' | \alpha, \vec{k} \rangle = (2\pi)^3 \sum_m B_m^{\alpha'\alpha} \delta(\vec{k} - \vec{k}' - \vec{K}_m) \qquad (2\text{-}9)$$

However, since $\vec{k}$ and $\vec{k}'$ are both in the first Brillouin zone, $\vec{k} - \vec{k}' = \vec{K}_m$ is only possible if $m = 0$. Thus

$$\langle \alpha', \vec{k}' | \alpha, \vec{k} \rangle = \delta(\vec{k} - \vec{k}') B_0^{\alpha'\alpha} (2\pi)^3$$

Using inverse Fourier transform in (2-8), the $B_m^{\alpha'\alpha}$ are given by

$$B_m^{\alpha'\alpha} = \frac{1}{\Omega} \int_\Omega e^{i\vec{K}_m \cdot \vec{r}} u^*_{\alpha' 0} u_{\alpha 0} \, d\vec{r}$$

$$B_0^{\alpha'\alpha} = \frac{1}{\Omega} \int_\Omega u^*_{\alpha' 0} u_{\alpha 0} \, d\vec{r}$$

Hence

$$\langle \alpha', \vec{k}' | \alpha, \vec{k} \rangle = \delta(\vec{k} - \vec{k}') \frac{(2\pi)^3}{\Omega} \int_\Omega u^*_{\alpha' 0} u_{\alpha 0} \, d\vec{r} \qquad (2\text{-}10)$$

Thus comparing (2-10) and (2-6) we obtain

$$\frac{(2\pi)^3}{\Omega} \int_{\Omega} u^*_{\alpha' 0}(\vec{r})\, u_{\alpha 0}(\vec{r})\, d\vec{r} = \delta_{\alpha' \alpha} \qquad (2\text{-}11)$$

Hence the Bloch functions at the band edge are orthogonal in the band index. This is perhaps an obvious result but the factor $(2\pi)^3/\Omega$ is not easy to guess without going through the calculation.

Next we proceed to establish the orthonormality of the functions (2-3). Introducing the notation

$$\int_V \psi^*_{\beta\mu'}(\vec{r})\, \psi_{\alpha\mu}(\vec{r})\, d\vec{r} \equiv \langle \psi_{\beta\mu'} | \psi_{\alpha\mu} \rangle \qquad (2\text{-}12)$$

and

$$\vec{R}_{\alpha'\alpha} \equiv \frac{\vec{p}_{\alpha'\alpha}}{m\,[E^0_\alpha - E^0_{\alpha'}]} \equiv -\vec{R}^*_{\alpha\alpha'} \qquad (2\text{-}13)$$

where the last equality follows from the relation $\vec{p}^*_{\alpha\alpha'} = \vec{p}_{\alpha'\alpha}$. The integral (2-12) can then be written as

$$\langle \psi_{\beta\mu'} \mid \psi_{\alpha\mu} \rangle = \Big\langle u_{\beta o} F_{\beta\mu'} + \sum_{\alpha' \neq \beta} u_{\alpha' o} \vec{R}_{\alpha'\beta} \cdot \vec{\pi} \, F_{\beta\mu'} \Big|$$

$$u_{\alpha o} F_{\alpha\mu} + \sum_{\alpha' \neq \alpha} u_{\alpha' o} \vec{R}_{\alpha'\alpha} \cdot \vec{\pi} \, F_{\alpha\mu} \Big\rangle$$

$$\simeq \langle u_{\beta o} F_{\beta\mu'} \mid u_{\alpha o} F_{\alpha\mu} \rangle$$

$$+ \sum_{\alpha' \neq \alpha} \vec{R}_{\alpha'\alpha} \cdot \langle u_{\beta o} F_{\beta\mu'} \mid u_{\alpha' o} \vec{\pi} \, F_{\alpha\mu} \rangle \qquad (2\text{-}14)$$

$$- \sum_{\alpha' \neq \beta} \vec{R}_{\beta\alpha'} \cdot \langle u_{\alpha' o} \vec{\pi} \, F_{\beta\mu'} \mid u_{\alpha o} F_{\alpha\mu} \rangle + O(B^2)$$

If the functions F's are slowly varying (as is necessary for the E.M.A. to hold) the integration in all the terms of the last equation can be split into two parts, one over the unit cell and the other over the entire crystal. For example the first term can be written as

$$\langle u_{\beta o} F_{\beta\mu'} \mid u_{\alpha o} F_{\alpha\mu} \rangle \equiv \int_V F^*_{\beta\mu'} u^*_{\beta o} u_{\alpha o} F_{\alpha\mu} \, d\vec{\tau}$$

$$= \sum_m \int_\Omega F^*_{\beta\mu'} u^*_{\beta o} u_{\alpha o} F_{\alpha\mu} \, d\vec{\tau}$$

Since F's are slowly varying, they do not vary much over the dimensions of a unit cell. Therefore

$$\langle u_{\beta o} F_{\beta\mu'} | u_{\alpha o} F_{\alpha\mu} \rangle \simeq \sum_{m}{}' F^{*}_{\beta\mu'} F_{\alpha\mu} \int_{\Omega} u^{*}_{\beta o} u_{\alpha o} \, d\vec{r}$$

Now we use the fact that u's are periodic, so we can take the integral out of the sum and finally converting the sum into integral, we get

$$\langle u_{\beta o} F_{\beta\mu'} | u_{\alpha o} F_{\alpha\mu} \rangle = \frac{1}{\Omega} \int_{\Omega} u^{*}_{\beta o} u_{\alpha o} \, d\vec{r} \int_{V} F^{*}_{\beta\mu'} F_{\alpha\mu} \, d\vec{r} \qquad (2\text{-}15)$$

If we set

$$(u_{\beta o} | \hat{O} | u_{\alpha o}) \equiv \frac{(2\pi)^3}{\Omega} \int_{\Omega} u^{*}_{\beta o}(\vec{r}) \, \hat{O} \, u_{\alpha o}(\vec{r}) \, d\vec{r} \qquad (2\text{-}16)$$

for any operator $\hat{O}$, then equation (2-15) becomes

$$\begin{aligned} \langle u_{\beta o} F_{\beta\mu'} | u_{\alpha o} F_{\alpha\mu} \rangle &= (2\pi)^{-3} (u_{\beta o} | 1 | u_{\alpha o}) \langle F_{\beta\mu'} | F_{\alpha\mu} \rangle \\ &= (2\pi)^{-3} \langle F_{\alpha\mu'} | F_{\alpha\mu} \rangle \delta_{\beta\alpha} \end{aligned} \qquad (2\text{-}17)$$

where the condition (2-11) has been used in arriving at the last equation.

Similarly

$$\left\langle u_{\beta 0} F_{\beta\mu'} \middle| u_{\alpha' 0} \vec{\pi} F_{\alpha\mu} \right\rangle = (2\pi)^{-3} \delta_{\beta\alpha'} \left\langle F_{\beta\mu'} \middle| \vec{\pi} F_{\alpha\mu} \right\rangle$$

and

$$\left\langle u_{\alpha' 0} \vec{\pi} F_{\beta\mu'} \middle| u_{\alpha 0} F_{\alpha\mu} \right\rangle = (2\pi)^{-3} \delta_{\alpha'\alpha} \left\langle F_{\beta\mu'} \middle| \vec{\pi} F_{\alpha\mu} \right\rangle$$

since $\vec{\pi}$ is hermitian. Hence the equation (2-14) gives

$$\left\langle \psi_{\beta\mu'} \middle| \psi_{\alpha\mu} \right\rangle = (2\pi)^{-3} \left\langle F_{\alpha\mu'} \middle| F_{\alpha\mu} \right\rangle \delta_{\beta\alpha} = \delta_{\mu'\mu} \delta_{\beta\alpha} \qquad (2\text{-}18)$$

as required. In obtaining the last step, we have used the following orthogonality condition,

$$\int_V F^*_{\alpha\mu'}(\vec{r}) \, F_{\alpha\mu}(\vec{r}) \, d\vec{r} = (2\pi)^3 \delta_{\mu'\mu} \qquad (2\text{-}19)$$

In this relation, there is a cumbersome factor of $(2\pi)^3$. In future, we will use $\int_V F^*_{\mu'}(\vec{r}) \, F_{\mu}(\vec{r}) \, d\vec{r} = \delta_{\mu\mu'}$ (i.e. without the factor $(2\pi)^3$), when the F's represent discrete states. This would mean that while splitting the integral into two parts as in equation (2-17), (also see Appendix (B)) the factor of $(2\pi)^{-3}$ will be left out. For problems involving continuous states (e.g. electron

in static electric field) an alternate normalization involving the Dirac delta function rather than the Kronecker delta function, is more convenient (see Section 2.3(a)). Care must be taken in this case when evaluating sums over energy states.

2.3 Solution of the Effective Mass Equation in External Static Fields

In this section we obtain solutions of the effective mass equation (2-2) in various configurations of the external electric and magnetic fields. It should be pointed out that for equation (2-2) to be valid the potential $U(\vec{r})$ and the envelope functions $F_{\alpha\mu}(\vec{r})$ must vary slowly over the dimensions of a unit cell. The limits of the E.M.A. have been investigated by Zak and Zawadzki[12]. They conclude that for most semiconductors, E.M.A. holds even when $B \sim 10^5$ gauss and $\mathcal{E} \sim 5 \times 10^4$ V/cm. For lower field values the approximation is of course applicable. Throughout our analysis, we will consider the fields to have values such that the E.M.A. holds. It is convenient to discuss the various field configurations in separate subsections below.

2.3a Arbitrarily Oriented Electric and Magnetic Fields

We wish to solve the effective mass Schrödinger equation (2-2) for a particle of mass m*, charge 'e' in the presence of static electric and magnetic fields, where the relative

orientation of the fields is arbitrary[13]. Solutions will be obtained in non-relativistic approximation, the relativistic generalization has been made by Rajagopal[14] in crossed electric and magnetic fields.

Suppose the static magnetic field is along the Z-direction, described by the vector potential $\vec{A}_o = (0, Bx, 0)$ and the electric field lies in the X-Z plane. Notice that the electric field has a component $\mathcal{E}_z$ parallel to the magnetic field. Then suppressing the band indices equation (2-2) becomes

$$\left[\frac{1}{2m^*}\left(\vec{p} - \frac{e}{c}\vec{A}_o\right)^2 - e\mathcal{E}_x x - e\mathcal{E}_z z\right] F(\vec{r}) = E F(\vec{r})$$

or

$$\left[\left\{-\frac{d^2}{dx^2} + \left(-i\frac{d}{dy} - \frac{eB}{c\hbar}x\right)^2 - \frac{2m^*}{\hbar^2} e\mathcal{E}_x x\right\} - \left\{\frac{d^2}{dz^2} + \frac{2m^*}{\hbar^2} e\mathcal{E}_z z\right\}\right] F(\vec{r}) = \frac{2m^*}{\hbar^2} E F(\vec{r}) \tag{2-20}$$

This equation is readily separable according to the scheme $F(\vec{r}) = F(x,y)\, F(z)$ and we obtain

$$\left[-\frac{\hbar^2}{2m^*}\frac{d^2}{dx^2} + \frac{\hbar^2}{2m^*}\left\{\left(-i\frac{d}{dy} - \frac{eB}{c\hbar}x\right)^2 - \frac{2m^*}{\hbar^2} e\mathcal{E}_x x\right\}\right] F(x,y) = E' F(x,y) \tag{2-21}$$

and

$$\frac{d^2F(z)}{dz^2} + \left(\frac{2m^*e\mathcal{E}_z}{\hbar^2}\right)\left\{ z + \frac{\epsilon_z}{e\mathcal{E}_z} \right\} F(z) = 0 \qquad (2\text{-}22)$$

where ϵ_z represents the particle's kinetic energy in the electric field direction parallel to the magnetic field.

Solutions for (2-21) are obtained by setting

$$F(x,y) = \text{constant} \times \exp(ik_y y)\, F(x)$$

when we get

$$-\frac{\hbar^2}{2m^*}\frac{d^2F(x)}{dx^2} + \frac{1}{2}m^*\omega_{ce}^2\left(x - \frac{\hbar}{m^*\omega_{ce}} - \frac{V_d}{\omega_{ce}}\right)F(x) = \left(E' + \frac{1}{2}m^*V_d^2 + \hbar V_d k_y\right)F(x) \qquad (2\text{-}23)$$

where $\omega_{ce} = \frac{eB}{m^*c}$, $V_d = \frac{c\mathcal{E}_x}{B} \ll c$ (Non-relativistic case)

Equation (2-23) is the equation for linear harmonic oscillator centred at

$$x_o = \frac{\hbar}{m^*\omega_{ce}}k_y + \frac{V_d}{\omega_{ce}} = \lambda^2 k_y + \frac{V_d}{\omega_{ce}} \qquad (2\text{-}24)$$

where $\lambda = \sqrt{\frac{c\hbar}{eB}}$, is the magnetic length. Thus the eigenvalues[15] are given as

$$E' = \left(n + \frac{1}{2}\right)\hbar\omega_{cc} - \frac{1}{2}mV_d^2 - \hbar V_d k_y \qquad (2\text{-}25)$$

and the corresponding eigenfunctions[15] are harmonic oscillator wave functions $\Phi_n (x - x_o)$, n = 0, 1, 2, ... (see Appendix C). For a volume of dimensions L_x, L_y, L_z the x and y dependent terms give rise to the normalized eigenfunctions

$$F(x,y) = \frac{1}{\sqrt{L_y}} \exp(ik_y y)\ \Phi_n(x - x_o) \qquad (2\text{-}26)$$

where use has been made of the orthonormality conditions

$$\frac{1}{L_y}\int_{-L_y/2}^{L_y/2} \exp i\left[(k_y - k_y')\, y\right] dy = \delta_{k_y, k_y'}$$

and

$$\int_{-\infty}^{\infty} \Phi_{n'}(x)\ \Phi_n(x)\, dx = \delta_{n,n'}$$

Equation (2-22) can be solved[16] by introducing the dimensionless variable

$$\xi = \beta \left(z + \frac{\epsilon_z}{e \mathcal{E}_z} \right) \quad \text{where} \quad \beta = \left(\frac{2 m^* e \mathcal{E}_z}{\hbar^2} \right)^{1/3} \qquad (2\text{-}27)$$

Equation (2-22) then takes the form

$$\frac{d^2 F(\xi)}{d \xi^2} + \xi F(\xi) = 0$$

The solution of this equation which is finite for all values of z has the form

$$F(\xi) = a \, Ai(-\xi)$$

where

$$Ai(u) = \frac{1}{\nu} \int_0^\infty \cos\left(\frac{s^3}{3} + su \right) ds \qquad (2\text{-}28)$$

is the Airy function[16], and 'a' is the normalization constant which will be determined below. The constant, ν is taken as $\pi^{\frac{1}{2}}$ or π. It will be left as ν in the following so the results will be applicable to either choice. For positive values of u, Ai(u) decreases rapidly as u increases. For negative values of

u, Ai(u) is oscillatory in nature, the amplitude of the oscillations decreases as u becomes more and more negative. As $\xi \rightarrow -\infty$, the function $F(\xi)$ tends exponentially to zero. The asymptotic expression for $F(\xi)$ for large negative values of ξ is[16]

$$F(\xi) \simeq \frac{\sqrt{\pi}}{\nu} \frac{a}{2.|\xi|^{1/4}} \exp\left[-\frac{2}{3}|\xi|^{3/2}\right] \qquad (2\text{-}29)$$

For large positive values of ξ, the asymptotic expression for $F(\xi)$ is[16]

$$F(\xi) \simeq \frac{\sqrt{\pi}}{\nu} \frac{a}{\xi^{1/4}} \sin\left(\frac{2}{3}\xi^{3/2} + \frac{\pi}{4}\right) \qquad (2\text{-}30)$$

According to the well known rule for the normalization of eigenfunctions of a continuous spectrum, we introduce the Dirac delta function normalization condition

$$\int_{-\infty}^{\infty} F(\xi)\, F(\xi')\, dz = \delta(\epsilon'_z - \epsilon_z) \qquad (2\text{-}31)$$

We will use a simple but elegant method[16] of determining the normalization coefficient by means of the asymptotic expression for the wave functions. The method demands that the asymptotic

expression for the wave function be represented in the form of a sum of two plane waves travelling in opposite directions, the normalization coefficient can then be chosen in such a way that the probability current density in the wave travelling towards (or away from) the origin is $1/2\pi\hbar$. Following this method, we represent the function (2-30) as the sum of two travelling waves:

$$F(\xi) = \frac{\sqrt{\pi}}{\nu}\left[\frac{1}{2}\, a\, \xi^{-1/4} \exp\left\{i\left(\frac{2}{3}\,\xi^{3/2} - \frac{\pi}{4}\right)\right\}\right. \\ \left. + \frac{1}{2}\, a\, \xi^{-1/4} \exp\left\{-i\left(\frac{2}{3}\,\xi^{3/2} - \frac{\pi}{4}\right)\right\}\right] \tag{2-32}$$

In order to calculate probablility current density $V|F|^2$, we need to know the velocity, V, which can be obtained from the relation $\frac{1}{2}m^*V^2$ = Total energy - Potential energy = $\epsilon_z + e\mathcal{E}_z Z$ or

$$V = \sqrt{\frac{2\,(\epsilon_z + e\mathcal{E}_z Z)}{m^*}} \tag{2-33}$$

The quantity $V|F|^2$ calculated from each of the two terms of (2-32), must be $1/2\pi\hbar$:

$$\sqrt{\frac{2e\mathcal{E}_z\left[Z + (\epsilon_z)/e\mathcal{E}_z\right]}{m^*}} \cdot \frac{\pi}{4\nu^2} \cdot \frac{a^2}{\xi^{1/2}} = \frac{1}{2\pi\hbar}$$

which gives

$$a = \frac{\nu}{\pi} \frac{(\beta)}{(e\mathcal{E}_z)^{1/2}} \tag{2-34}$$

where equation (2-27) has been used.

Hence the Z-dependent term gives rise to the normalized eigenfunction

$$F(z) = \frac{\nu}{\pi} \frac{(\beta)}{(e\mathcal{E}_z)^{1/2}} \, Ai\left[-\beta\left(z + \frac{\epsilon_z}{e\mathcal{E}_z}\right)\right] \tag{2-35}$$

Finally one has, for the eigenfunctions and eigenvalues of the effective mass equation, the following expressions:

$$F_{(n, k_y, \epsilon_z)}(\vec{r}) = \frac{\nu}{\pi} \frac{(\beta)}{(e\mathcal{E}_z)^{1/2}} \frac{1}{\sqrt{L_y}} e^{i k_y y} \Phi_n\left(x - \lambda^2 k_y - \frac{V_d}{\omega_{ce}}\right) \times Ai\left[-\beta\left(z + \frac{\epsilon_z}{e\mathcal{E}_z}\right)\right] \tag{2-36}$$

$$E(n, k_y, \epsilon_z) = \epsilon_z + \left(n + \frac{1}{2}\right)\hbar\omega_{ce} - \frac{1}{2} m^* V_d^2 - \hbar k_y V_d \tag{2-37}$$

The quantum numbers of the electrons in the electric and magnetic fields are (n, k_y, ϵ_z). Note that only the limit

$\frac{\mathcal{E}_x}{B} \to 0$ can formally be taken.

2.3b Crossed Electric and Magnetic Fields and Magnetic Field Alone

The effective mass Schrödinger equation in crossed electric and magnetic fields can be obtained from (a) by setting $\mathcal{E}_z = 0$ in equation (2-20) and we get

$$\left[-\frac{d^2}{dx^2} + \left(-i\frac{d}{dy} - \frac{eB}{c\hbar} x \right)^2 - \frac{2m^*}{\hbar^2} e\mathcal{E}_x x - \frac{d^2}{dz^2} \right] F(\vec{r}) = \frac{2m^*}{\hbar^2} E\, F(\vec{r}) \tag{2-38}$$

Solutions of this equation are obtained by the method quite similar to one used for solving (2-21) and we just state results

$$F_{(n,k_y,k_z)}(\vec{r}) = \frac{1}{\sqrt{L_y L_z}} \exp\left[i(k_y y + k_z z) \right] \times \Phi_n(x - x_0) \tag{2-39}$$

$$E(n, k_y, k_z) = \frac{\hbar^2 k_z^2}{2m^*} + \left(n + \frac{1}{2} \right) \hbar\omega_{ce} - \frac{1}{2} m^* V_d^2 - \hbar k_y V_d \tag{2-40}$$

The case of magnetic field alone follows from (2-39) and (2-40) by setting $V_d = 0$.

2.3c Electric Field

The effective mass Schrödinger equation in the presence of the electric field alone is another interesting problem, whose solutions can be obtained from (a) by slight modification. If the electric field is along the Z-direction the motion along this axis will be governed by (2-22) whose solutions are given by (2-35). The x and y dependent terms would be plane wave states and the following results are obtained for normalized eigenfunctions and eigenvalues

$$F_{(\epsilon_z, k_y, k_z)}(\vec{r}) = \frac{\nu}{\pi}\frac{\beta}{(e\mathcal{E}_z)^{1/2}}\frac{1}{\sqrt{L_y L_z}}\exp\left[i(k_x x + k_y y)\right] \times Ai\left[-\beta\left(z + \frac{\epsilon_z}{e\mathcal{E}_z}\right)\right] \quad (2\text{-}41)$$

$$E(\epsilon_z, k_y, k_z) = \epsilon_z + \frac{\hbar^2 k_x^2}{2m^*} + \frac{\hbar^2 k_y^2}{2m^*} \quad (2\text{-}42)$$

The envelope functions (2-36), (2-39) and (2-41) will be used in subsequent chapters.

CHAPTER 3

GENERAL FORMULATION FOR DIRECT INTERBAND ABSORPTION COEFFICIENT

3.1 Introduction

In this chapter we wish to derive a general expression for the direct (allowed) absorption coefficient in the presence of external electric and magnetic fields. It was pointed out in Chapter 1, that the first step in calculating the absorption coefficient consists of evaluating appropriate matrix elements, which are subsequently used to calculate transition rates. The calculation will be done in two stages in the following two sections. The first section will be devoted to the evaluation of first order interband matrix elements of electron-photon interaction using effective mass wave functions. Here we will take an opportunity to discuss the various parts of the matrix elements and explain which ones are needed for allowed and forbidden transitions respectively. In Section 3.3, the interband absorption coefficient will be calculated using only that part of the matrix element which gives rise to direct allowed transitions.

3.2 Evaluation of First Order Interband Matrix Elements

For first order transitions, the matrix elements of the electron-photon interaction between an initial state in the valence band and a final state in the conduction band are needed.

The unperturbed wavefunctions in E.M.A. (see equation (2-3)) for the electrons in the conduction and valence bands are

$$\psi_{\alpha\mu}(\vec{r}) = \left[u_{\alpha 0}(\vec{r}) + \sum_{\alpha' \neq \alpha} \vec{R}_{\alpha'\alpha} \cdot \vec{\Pi} \right] F_{\alpha\mu}(\vec{r}) \quad (3\text{-}1)$$

where μ denotes the quantum numbers other than the band, 0 denotes the band edge, α = (c or v) for conduction and valence band respectively and $\vec{R}_{\alpha'\alpha}$ is defined by equation (2-13).

The electron-photon interaction Hamiltonian was derived in Chapter 1 (equation (1-9)) and is given by

$$H_1 = -\frac{e}{mc} \vec{\Pi} \cdot \vec{A}_1(\vec{r}, t) \quad (3\text{-}2)$$

where two photon processes have been ignored. The perturbation can be described by a time varying field, whose space variation can be neglected (dipole approximation[17]) since the wavelength is long compared to the electronic wavelengths involved[18]. Equation (3-2) can then be written as

$$H_1 = -\frac{e}{m} \sqrt{\frac{2\pi\hbar N}{\omega n_0^2}} \vec{\Pi} \cdot \left[\hat{\xi} e^{i\omega t} + \hat{\xi} e^{-i\omega t} \right] \quad (3\text{-}3)$$

where $\hat{\xi}$ is a unit polarization vector of the photon (may be taken

as complex in the case of circular polarization), n_o, the index of refraction (assumed constant) and N is the number of photons per unit volume.

The first order interband matrix elements, $M_{cv} \equiv \langle \psi_{c\mu'} | H_1 | \psi_{v\mu} \rangle$ can now be evaluated. For a process involving photon absorption, these are given by

$$M_{cv} = -\frac{e}{m}\sqrt{\frac{2\pi\hbar N}{\omega n_o^2}}\,\langle \psi_{c\mu'} | \vec{\pi}\cdot\hat{\xi} | \psi_{v\mu} \rangle \qquad (3\text{-}4)$$

where equation (3-3) has been used for the electron-photon interaction and the time dependent factor of modulus unity has been left out. Using the expression (3-1) for ψ's we can evaluate the quantity $\langle \psi_{c\mu'} | \vec{\pi}\cdot\hat{\xi} | \psi_{v\mu} \rangle$. This calculation is carried out in Appendix (B) and we finally obtain

$$M_{cv} = -\frac{e}{m}\sqrt{\frac{2\pi\hbar N}{\omega n_o^2}}\left[\left\{(\vec{p}_{cv}\cdot\hat{\xi}) + \frac{i\hbar\vec{\omega}_c}{E_g}\cdot(\vec{p}_{cv}\times\hat{\xi})\right\} \times \langle F_{c\mu'} | F_{v\mu} \rangle + \vec{\Pi}_{cv}\cdot\langle F_{c\mu'} | \vec{\Pi} | F_{v\mu} \rangle\right] \qquad (3\text{-}5)$$

where

$$\vec{\Pi}_{cv} = \frac{1}{m}\sum_{\beta\neq(c,v)}\left\{\frac{\vec{p}_{\beta v}(\vec{p}_{c\beta}\cdot\hat{\xi})}{E_v^o - E_\beta^o} + \frac{\vec{p}_{c\beta}(\vec{p}_{\beta v}\cdot\hat{\xi})}{E_c^o - E_\beta^o}\right\}, \qquad (3\text{-}6)$$

$\omega_c = \frac{eB}{mc}$ is the cyclotron frequency and $E_g = E_c^o - E_v^o$ is the forbiddent energy gap. For most semiconductors the ratio, $\frac{\hbar\omega_c}{E_g} \sim 10^{-3}$ or 10^{-4} at $B \simeq 10^4$ gauss and hence the term containing it makes negligible contribution towards the absorption coefficient. Thus it is sufficient to write

$$M_{cv} \simeq -\frac{e}{m}\sqrt{\frac{2\pi\hbar N}{\omega n_o^2}}\left[(\vec{p}_{cv}\cdot\hat{\xi})\langle F_{c\mu'}|F_{v\mu}\rangle + \vec{\Gamma}_{cv}\cdot\langle F_{c\mu'}|\vec{\Pi}|F_{v\mu}\rangle\right] \qquad (3\text{-}7)$$

One term of (3-7) will in general vanish if the crystal has a centre of symmetry and we have two types of direct transitions which we discuss below.

3.2a Allowed Transitions

It can be shown quite easily that for $\vec{p}_{cv}$ to be non-vanishing, the bands c and v must have different parity. Thus if $u_{co}(\vec{r}) = -u_{co}(-\vec{r})$ (odd parity), then $u_{vo}(\vec{r})$ must have even parity or else $\vec{p}_{cv}$ vanishes. However if the bands have opposite parity then $\vec{\Gamma}_{cv}$ vanishes because any intermediate band β must have the same parity as either c or v and the corresponding momentum matrix element must be zero (see equation (3-6)). The vertical transitions between c and v in this case are called 'Allowed' and the matrix element for direct allowed transitions

is given by

$$M_{cv}^{(A)} = -\frac{e}{m}\sqrt{\frac{2\pi\hbar N}{\omega n_o^2}}\left(\vec{p}_{cv}\cdot\hat{\xi}\right)\int_V F^*_{c\mu'}(\vec{r})\,F_{v\mu}(\vec{r})\,d\vec{r} \quad (3\text{-}8)$$

3.2b Forbidden Transitions

If the bands c and v have the same parity so that $\vec{p}_{cv}$ vanishes, then intermediate states having parity opposite to c and v may exist so that the second order term, $\vec{\Gamma}_{cv}$ does not vanish. The transitions associated with this term are called 'Forbidden' and the corresponding matrix element is given by

$$M_{cv}^{(F)} = -\frac{e}{m}\sqrt{\frac{2\pi\hbar N}{\omega n_o^2}}\;\vec{\Gamma}_{cv}\cdot\int_V F^*_{c\mu'}(\vec{r})\,\vec{\Pi}\,F_{v\mu}(\vec{r})\,d\vec{r} \quad (3\text{-}9)$$

If a centre of symmetry does not exist, then the bands c and v can no longer be classified according to parity and nonzero contributions may arise from both terms in (3-7). Such transitions are generally called 'Mixed' but will not concern us here. We will be mainly concerned with allowed transitions, a calculation of the absorption coefficient for forbidden transitions is carried out in Appendix (B).

3.3 Calculation of Direct Allowed Absorption Coefficient in Electric and Magnetic Fields

Here we compute the optical absorption coefficient, in semiconductors due to direct allowed interband transitions between simple parabolic valence and conduction bands having their extrema at the centre of the Brillouin zone ($\vec{k} = 0$), in the presence of arbitrarily oriented electric and magnetic fields. We suppose that the magnetic field is along the Z-direction and the static electric field lies in the X-Z plane i.e. $\vec{\mathcal{E}} = (\mathcal{E}_x, 0, \mathcal{E}_z)$.

For non-degenerate parabolic bands, the envelope functions in electric and magnetic fields have been obtained in Section 2.3 and are given by

$$F_{c\mu'}(\vec{r}) = \frac{\nu}{\pi} \frac{\beta_c}{(e\mathcal{E}_z)^{1/2}} \frac{1}{\sqrt{L_y}} e^{ik'_y y} \Phi_{n'}\left(x - \lambda^2 k'_y - \frac{V_d}{\omega_{cc}}\right) \times Ai\left[-\beta_c\left(z + \frac{\epsilon'_z}{e\mathcal{E}_z}\right)\right], \tag{3-10a}$$

$$F_{v\mu'} = \frac{\nu}{\pi} \frac{\beta_v}{(e\mathcal{E}_z)^{1/2}} \frac{1}{\sqrt{L_y}} e^{ik_y y} \Phi_n\left(x - \lambda^2 k_y + \frac{V_d}{\omega_{cv}}\right) \cdot Ai\left[\beta_v\left(z + \frac{\epsilon_z}{e\mathcal{E}_z}\right)\right] \tag{3-10b}$$

where $\omega_{cc} = \frac{eB}{m_c c}$ and $\omega_{cv} = \frac{eB}{m_v c}$ are the cyclotron frequencies and m_c, m_v are the effective masses in the two bands. Further,

$V_d = \frac{c\mathcal{E}_x}{B}$, $\beta_c = (\frac{2m_c e\mathcal{E}_z}{\hbar^2})^{1/3}$ and $\beta_v = (\frac{2m_v e\mathcal{E}_z}{\hbar^2})^{1/3}$. In these expressions 'e' stands for the absolute value of the charge of the particle. It is assumed that the bands c and v have opposite curvature i.e. the sign of $\partial^2 E/\partial k^2$ is opposite for the two bands. The energy eigenvalues of the electrons in the conduction and valence bands are (Section 2.3)

$$E_c(\mu') = E_c^o + \epsilon_z' + (n' + \tfrac{1}{2})\hbar\omega_{cc} - \frac{1}{2} m_c V_d^2 - \hbar k_y' V_d \quad (3\text{-}11a)$$

and

$$E_v(\mu) = E_v^o + \epsilon_z - (n + \tfrac{1}{2})\hbar\omega_{cv} + \frac{1}{2} m_v V_d^2 - \hbar k_y V_d \quad (3\text{-}11b)$$

where E_c^o and E_v^o are the energies of the conduction and valence bands at $\vec{k} = 0$, $\mu \equiv (n, k_y, \epsilon_z)$ and $E_c^o - E_v^o = E_g$.

The absorption coefficient for direct allowed transitions can now be computed using equation (1-4) and we have

$$\eta(\vec{\mathcal{E}}, \vec{B}) = \frac{4\pi n_o}{cN\hbar V} \sum_{\mu', \mu} \left| M_{cv}^{(A)} \right|^2 \delta\left(E_c(\mu') - E_v(\mu) - \hbar\omega\right) \quad (3\text{-}12)$$

where the matrix element for allowed transitions is given by (3-8).

Substituting (3-8) in (3-12) we obtain

$$\eta(\vec{\mathcal{E}},\vec{B}) = \frac{2(2\pi)^2 e^2 |(\vec{p}_{cv}\cdot\hat{\xi})|^2}{c m^2 n_o \omega V} \sum_{\mu',\mu} |I_{\mu'\mu}|^2 \delta\left(E_c(\mu') - E_v(\mu) - \hbar\omega\right) \quad (3\text{-}13)$$

where

$$I_{\mu'\mu} = \int_V F^*_{c\mu'}(\vec{r})\, F_{v\mu}(\vec{r})\, d\vec{r}$$

Our next task is to give an explicit expression for $I_{\mu'\mu}$. Substituting for $F^*_{c\mu'}$ and $F_{v\mu}$ from (3-10) we obtain

$$I_{\mu'\mu} = \frac{V^2}{\pi^2} \frac{\beta_c \beta_v}{e\mathcal{E}_z} \frac{1}{L_y} \int_{-L_y/2}^{L_y/2} \exp i(k_y - k'_y) y \, dy$$
$$\times \int_{-\infty}^{\infty} \Phi_{n'}\left(x - \lambda^2 k'_y - \frac{V_d}{\omega_{cc}}\right) \Phi_n\left(x - \lambda^2 k_y + \frac{V_d}{\omega_{cv}}\right) dx$$
$$\times \int_{-\infty}^{\infty} Ai\left[-\beta_c\left(z + \frac{\epsilon'_z}{c\mathcal{E}_z}\right)\right] Ai\left[\beta_v\left(z + \frac{\epsilon_z}{c\mathcal{E}_z}\right)\right] dz$$

or

$$I_{\mu'\mu} = \left(\frac{V}{\pi}\right) \frac{J_{n',n}(a)}{\hbar\Theta_F} \, Ai\left[\frac{\epsilon_z - \epsilon'_z}{\hbar\Theta_F}\right] \delta_{k_y,k'_y} \quad (3\text{-}14)$$

where

$$J_{n',n}(a) = \int_{-\infty}^{\infty} dx \; \Phi_{n'}(x)\, \Phi_n(x+a) \,, \quad (3\text{-}15a)$$

$$a = \frac{V_d}{\omega_{cc}} + \frac{V_d}{\omega_{cv}} = \lambda^2 \frac{M V_d}{\hbar} \,, \quad M = m_c + m_v$$

and

$$\theta_F^3 = \frac{e^2 \mathcal{E}_z^2}{2\mu\hbar} \quad , \qquad \frac{1}{\mu} = \frac{1}{m_c} + \frac{1}{m_v} \quad , \tag{3-15b}$$

μ is the reduced mass. An explicit form for $J_{n',n}(a)$ is given in Appendix (C). In arriving at equation (3-14) the integration limits on x and z have been extended to $\pm\infty$, (this introduces negligible error because the integrands fall off rapidly with distance and are vanishingly small outside a box of large dimensions.), and use has been made of the result[19].

$$\int_{-\infty}^{\infty} dt\ Ai(t+\rho_1)\, Ai(bt+\rho_2) = \frac{\pi}{(1-b^3)^{1/3}} \times Ai\left[\frac{\rho_2 - b\rho_1}{(1-b^3)^{1/3}}\right] \quad \text{for } b<1$$

Now substituting (3-14) in (3-13) we obtain

$$\eta(\vec{\mathcal{E}}, \vec{B}) = \frac{2(2\pi)^2 e^2 \left|(\vec{p}_{cv}\cdot\hat{\xi})\right|^2}{c\, m^2\, n_o\, \omega\, V} \frac{\nu^2}{\pi^2} \left(\frac{1}{\hbar\theta_F}\right)^2 \times \sum_{n,n',\epsilon_z,\epsilon'_z,k_y} J^2_{n',n}(a) \left| Ai\left[\frac{\epsilon_z - \epsilon'_z}{\hbar\theta_F}\right]\right|^2 \delta(\Delta_{n',n} + \epsilon'_z - \epsilon_z) \tag{3-16}$$

where

$$\Delta_{n',n} = E_g - \hbar\omega + (n' + \tfrac{1}{2})\hbar\omega_{cc} + (n + \tfrac{1}{2})\hbar\omega_{cv} - \frac{1}{2}MV_d^2 \quad (3\text{-}17)$$

The sum over k_y in equation (3-16) can be carried out by converting it into an integral, the limits on the integral are obtained by restricting the centre of the orbit to within the crystal length. Thus

$$\sum_{k_y} \longrightarrow \int_{-\frac{eBL_x}{2c\hbar}}^{\frac{eBL_x}{2c\hbar}} \frac{L_y\, dk_y}{2\pi} = \frac{L_x L_y}{2\pi\lambda^2}$$

Summation over ϵ_z, ϵ'_z can be easily carried out by redefining variables and making use of the Dirac delta function occuring in (3-16). The factor $\int d\epsilon_z$ contributes $e\epsilon_z L_z$ and we finally obtain for the absorption coefficient

$$\eta(\vec{\mathcal{E}}, \vec{B}) = R\,\frac{\omega_c^*}{\Theta_F^{1/2}}\left(\frac{\nu^2}{\pi}\right)\sum_{n',n} J_{n',n}^2(a)\left|Ai\left(\frac{\Delta_{n',n}}{\hbar\Theta_F}\right)\right|^2 \quad (3\text{-}18)$$

where

$$R = \frac{2e^2\left|(\vec{P}_{cv}\cdot\hat{\xi})\right|^2}{\hbar\omega\, n_0 c\, m^2}\left(\frac{2\mu}{\hbar}\right)^{3/2},$$

$$\omega_c^* = \frac{eB}{\mu c} = \omega_{cc} + \omega_{cv} \quad (3\text{-}19)$$

and all other quantities have been defined previously. The magnitude of the absorption coefficient appears to be dependent on the value chosen for ν. Actually there is no dependence since this constant merely cancels the constant implicit in the definition of the Airy function (see equation (2-28)), to give a unique value for the absorption coefficient regardless of the value chosen for ν.

Equation (3-18) is a unified result for direct allowed absorption coefficient. Most results known in the theory of direct optical transitions can be derived as various limiting cases of the equation (3-18). In particular, it will be shown in the next five chapters that the equation (3-18) in the appropriate limits reproduces the following well known results:

(i) Zero field absorption coefficient,
(ii) Magnetoabsorption coefficient,
(iii) Electroabsorption and Franz-Keldysh effect,
(iv) Absorption in crossed electric and magnetic fields
and (v) Photon-assisted tunneling in parallel fields.

The formal expression (3-18) has recently also been obtained by Spector[13] who has considered only one of the limiting cases outlined above (Case v). His general expression

differs from our equation (3-18) by a factor of π, (Equation (2-8) of the reference (13) should be divided by a factor of π) which appears to be the result of an error in the expression for the density of states employed by Spector. Other apparent differences disappear when Spector's notation is translated into our own.

CHAPTER 4

ABSORPTION IN ABSENCE OF EXTERNAL ELECTRIC AND MAGNETIC FIELDS

4.1 Derivation of Absorption Coefficient in Absence of External Fields from the General Result

The expression for field free absorption coefficient can be obtained as a special case of the general result if in equation (3-18) we first let the electric field $\vec{\mathcal{E}} \to 0$ and then take the limit $\vec{B} \to 0$. The order is important because if we first let $B \to 0$, then the drift velocity, $V_d = \frac{c\mathcal{E}_x}{B}$ approaches infinity and the non-relativistic approximation is no longer valid. However the order in which the different components of the electric field are set equal to zero is quite immaterial and in the following we first set $\mathcal{E}_x = 0$ and then let $\mathcal{E}_z \to 0$.

Setting $\mathcal{E}_x = 0$ implies that $V_d = a = 0$ and hence $J_{n',n}(a) = \delta_{n',n}$ (see Appendix (D). Substituting these in equations (3-17) and (3-18) we obtain

$$\eta = R \frac{\omega_c^*}{\theta_F^{1/2}} \left(\frac{\nu^2}{\pi}\right) \sum_n \left| Ai\left(\frac{\Delta_{n,n}}{\hbar\theta_F}\right)\right|^2 \qquad (4\text{-}1)$$

where

$$\Delta_{n,n} = E_g - \hbar\omega + \left(n + \tfrac{1}{2}\right)\hbar\omega_c^* \qquad (4\text{-}2)$$

Next we want to take the limit $\mathcal{E}_z \to 0$ which means $\theta_F \to 0$ and thus for finite values of $\Delta_{n,n}$ the argument of the Airy function becomes large. This suggests the use of Asymptotic forms for the Airy function which are given by[19]

$$\lim_{t\to\infty} \mathrm{Ai}(t) \simeq \frac{\sqrt{\pi}}{2\nu}\, t^{-1/4} \exp\left(-\frac{2}{3} t^{3/2}\right), \quad (4\text{-}3a)$$

$$\lim_{t\to\infty} \mathrm{Ai}(-t) \simeq \frac{\sqrt{\pi}}{\nu}\, t^{-1/4} \sin\left(\frac{2}{3} t^{3/2} + \frac{\pi}{4}\right) \quad (4\text{-}3b)$$

Since the asymptotic forms depend upon the sign of the argument, we split the sum over n in equation (4-1) in the following fashion:

$$\eta = R\, \frac{\omega_c^*}{\theta_F^{1/2}} \left(\frac{\nu^2}{\pi}\right)\left[\sum_{n\,(\Delta_{n,n}>0)} \left| \mathrm{Ai}\left(\frac{\Delta_{n,n}}{\hbar\theta_F}\right)\right|^2 + \sum_{n\,(\Delta_{n,n}<0)} \left| \mathrm{Ai}\left(\frac{\Delta_{n,n}}{\hbar\theta_F}\right)\right|^2 \right] \quad (4\text{-}4)$$

Now using appropriate asymptotic form in each of the sum above for $\theta_F \to 0$, we obtain

$$\eta \simeq \frac{R(\hbar\omega_c^*)}{2\pi^{1/2}} \left[\sum_{n\,(\Delta_{n,n}>0)} \frac{1}{2(\Delta_{n,n})^{1/2}} \exp\left\{-\frac{4}{3}\left(\frac{\Delta_{n,n}}{\hbar\theta_F}\right)^{3/2}\right\} + \sum_{n\,(\Delta_{n,n}<0)} \frac{1}{(-\Delta_{n,n})^{1/2}} \left\{1 + \sin\left(\frac{4}{3}\left(-\frac{\Delta_{n,n}}{\hbar\theta_F}\right)^{3/2}\right)\right\}\right] \quad (4\text{-}5)$$

When $\theta_F = 0$, the first sum does not contribute anything and in the second sum the Sine function oscillates rapidly for large argument and averages out to zero. The above result then reduces to

$$\eta = \frac{R(\hbar\omega_c^*)}{2\hbar^{1/2}} \sum_n \frac{1}{[\hbar\omega - E_g - (n+\frac{1}{2})\hbar\omega_c^*]^{1/2}} \qquad (4\text{-}6)$$

where the sum over n is restricted by the relation

$$\hbar\omega > E_g + (n + \tfrac{1}{2})\hbar\omega_c^* \qquad (4\text{-}7)$$

To obtain the limit $B \rightarrow 0$, we convert the sum over n in equation (4-4) into an integral through the relation

$$(\hbar\omega_c^*)\sum_n \longrightarrow \int_0^{\hbar\omega - E_g} dx$$

and carrying out the simple integration we obtain the expression for the zero field absorption coefficient as follows:

$$\begin{aligned} \eta(0) &= R(\omega - \omega_g)^{1/2} \quad \text{for} \quad \omega > \omega_g \\ &= 0 \quad \text{for} \quad \omega \leq \omega_g \end{aligned} \qquad (4\text{-}8)$$

where $\omega_g = E_g/\hbar$. The above result agrees with the result obtained by Bardeen, Blatt and Hall.[1]

4.2 Experimental Verification

The dependence of the above optical absorption coefficient on the energy of the incident photons has been tested in many materials like Ge, InSb[20] and has been found to be accurately proportional to the square root of the experimental frequency for $\omega > \omega_g$ as demanded by the theory. However, the other prediction that $\eta(o) = 0$ at $\omega = \omega_g$ is hard to verify experimentally due to the uncertainty involved in the measurement of the energy gap itself. Further the broadening of the energy levels due to impurity and phonon scattering tend to smear the absorption edge, making the experimental task even more difficult.

For a quantitative fit it is necessary to take this broadening into account. Since this is generally difficult, one usually does this only phenomenologically by introducing a damping time. We will not go into the details of this and shall restrict ourselves to 'pure' materials where scattering, etc. is small.

CHAPTER 5

MAGNETOABSORPTION

5.1 Derivation of the Magnetoabsorption Coefficient from the General Result

The case of the magnetoabsorption is extremely important and has been thoroughly investigated both theoretically and experimentally, during the last decade. We will first give a theoretical expression, for the absorption coefficient in a magnetic field, $\eta(B)$ starting from the fundamental equation (3-18), and then briefly review the experimental situation. We should be able to obtain $\eta(B)$, by setting $\mathcal{E}_x = \mathcal{E}_z = 0$ in equation (3-18) in either order. This was in fact done in Chapter 4 where we obtained (see equations (4-6) and (4-7))

$$\eta(\hbar\omega) = \frac{K(\hbar\omega_c^*)}{2\hbar^{1/2}} \sum_n \left| \hbar\omega - E_g - (n+\tfrac{1}{2})\hbar\omega_c^* \right|^{-1/2} \qquad (5\text{-}1)$$

where the sum over n is to be carried out in accordance with the condition

$$\hbar\omega > E_g + (n+\tfrac{1}{2})\hbar\omega_c^* \qquad (5\text{-}2)$$

In obtaining (5-1) we set a = 0 which implies that $J_{n',n}(a) = \delta_{n',n}$ (see Appendix (D)) and the optical transitions in the

presence of a magnetic field satisfy the selection rule n' = n. The above result agrees with the results reported in the literature.(21-29)

It is obvious from the condition (5-2) that there is no absorption until

$$\hbar\omega > E_g + \frac{1}{2}\hbar\omega_c^* \equiv E_g(B) \qquad (5\text{-}3)$$

and n takes values from 0 to Max $\left(\frac{\hbar\omega - E_g(B)}{\hbar\omega_c^*}\right)$ where Max (u) = maximum integer $\leq$ u. $E_g(B)$ can be thought of as the effective energy gap in the presence of a magnetic field. The effect of a magnetic field is to increase the true energy gap of the material by an amount equal to the sum of the zero point energies of the valence and conduction bands (Fig. 1). This magneto-optical band gap effect was first seen experimentally in InSb(21) and InAs(22). The result (5-1) has been derived by other methods(9,23,24) before and has been the subject of several review articles.(25-29)

In the limit of zero magnetic field, equation (5-1) reduces to the expression for field free absorption coefficient obtained in the last chapter (equation 4-8). The energy dependence of the magnetoabsorption coefficient, $\eta(B)$ has been displayed schematically in Fig. (2). Also on the same graph we have plotted $\eta(o)$ using

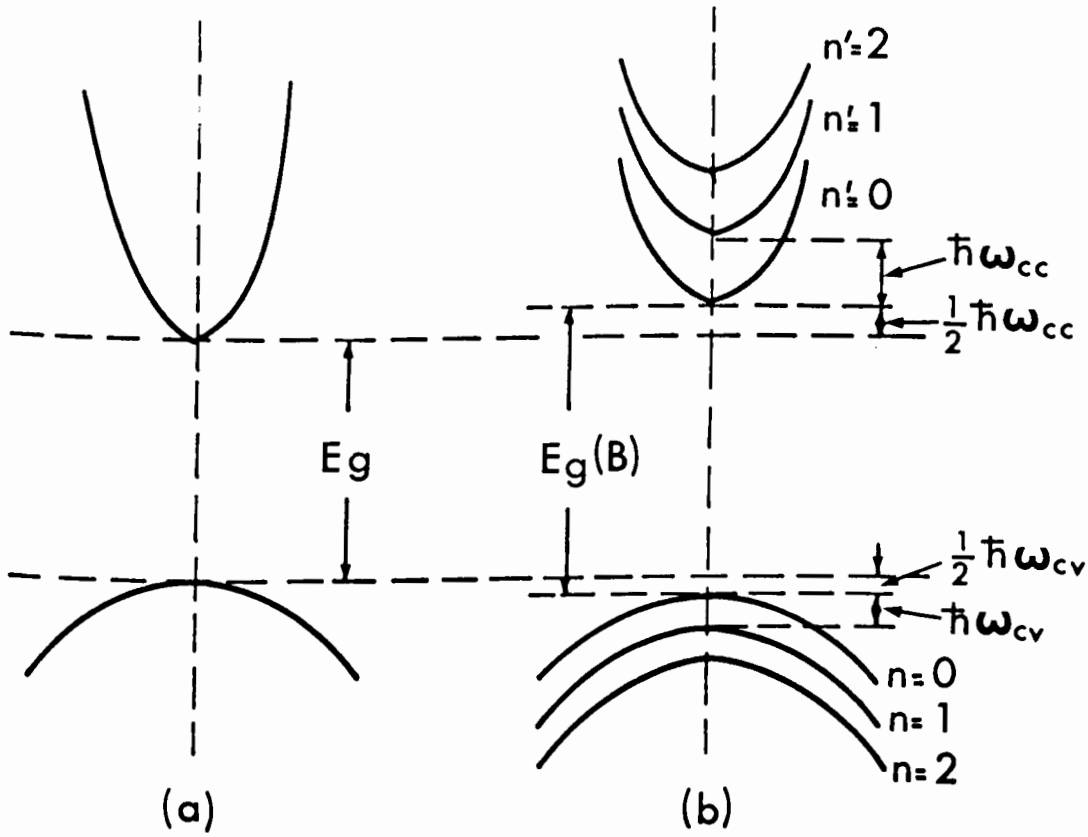

Figure 1. Energy bands for a semiconductor in the absence and presence of a magnetic field, B. (a) B = 0, (b) B ≠ 0.

equation (4-8) for comparison. The zero field absorption coefficient starts out with value zero at $\hbar\omega = E_g$ and increases as the square root of the frequency in accordance with equation (4-8).

A magnetic field has two striking effects on the absorption spectrum

(i) The energy gap shifts towards shorter wavelength (see equation (5-3) and Fig. 1), and there is no absorption until $\hbar\omega = E_g + \frac{1}{2}\hbar\omega_c^*$. Notice that by plotting the threshold for absorption as a function B, one can obtain the value of E_g by extrapolating to B = 0.

(ii) The absorption is oscillatory in nature for $\hbar\omega > E_g(B)$, and the separation, between the absorption peaks, is $\hbar\omega_c^*$ which involves the reduced mass for the two bands due to the selection rule $\Delta_{n',n} = 0$.

In the theoretical curve for $\eta(B)$, there is a singularity at $\hbar\omega = E_g(B) + n\hbar\omega_c^*$ which results from the quantization of the magnetic levels and also because the density of states at the bottom of each of the magnetic subbands has a singularity. This singularity will not occur in a real physical system, and a broadening or relaxation parameter is generally introduced, to obtain quantitative agreement between the theory and experiment.

The expected separation between the absorption peaks is

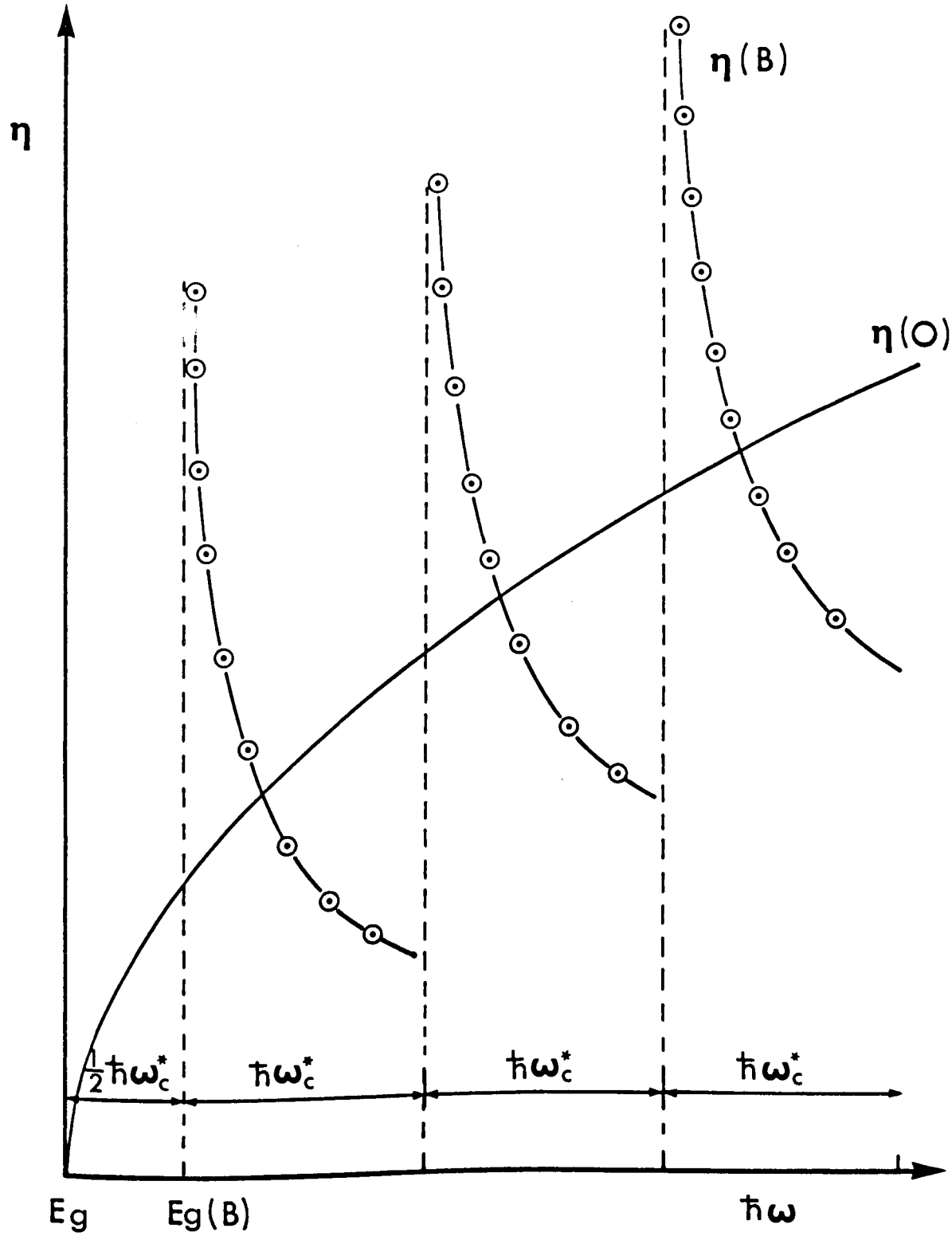

Figure 2. Schematic representation of the interband absorption spectrum for B = 0 and B ≠ 0 as a function of photon energy.

$$\delta = \hbar\omega_c^* = \frac{eB}{\mu c} \simeq 1.16 \times 10^{-8} \frac{B}{(\mu/m)} \quad eV$$

where B is in gauss and m is mass of the free electron. If $\mu = \frac{1}{20}$ m and B = 5 x 10^4 gauss, then $\delta \simeq 0.01$ eV. If the applied magnetic field is very small, the separation between the absorption peaks would not be measurable. No oscillatory absorption has so far been detected below several kilogauss and in the next section, the condition governing the lower limit on the magnetic field will be discussed.

5.2 Comparison of Theory and Experiment

The theory of magnetoabsorption has been tested by several[23,30,31,32] experimental groups on materials like germanium, indium atimonide, indium and cuprous oxide, etc. Below we discuss the results of the magnetoabsorption in a single crystal of germanium by Zwerdling et al[32]. They displayed their experimental findings in the form of a graph by plotting, the ratio of the transmitted intensity with a given magnetic field to that at zero magnetic field, as a function of photon energy (Fig. 3). It follows from the definition of the absorption coefficient that

$$\frac{I(B)}{I(B=0)} = e^{-[\eta(B)-\eta(0)]d} \qquad (5\text{-}4)$$

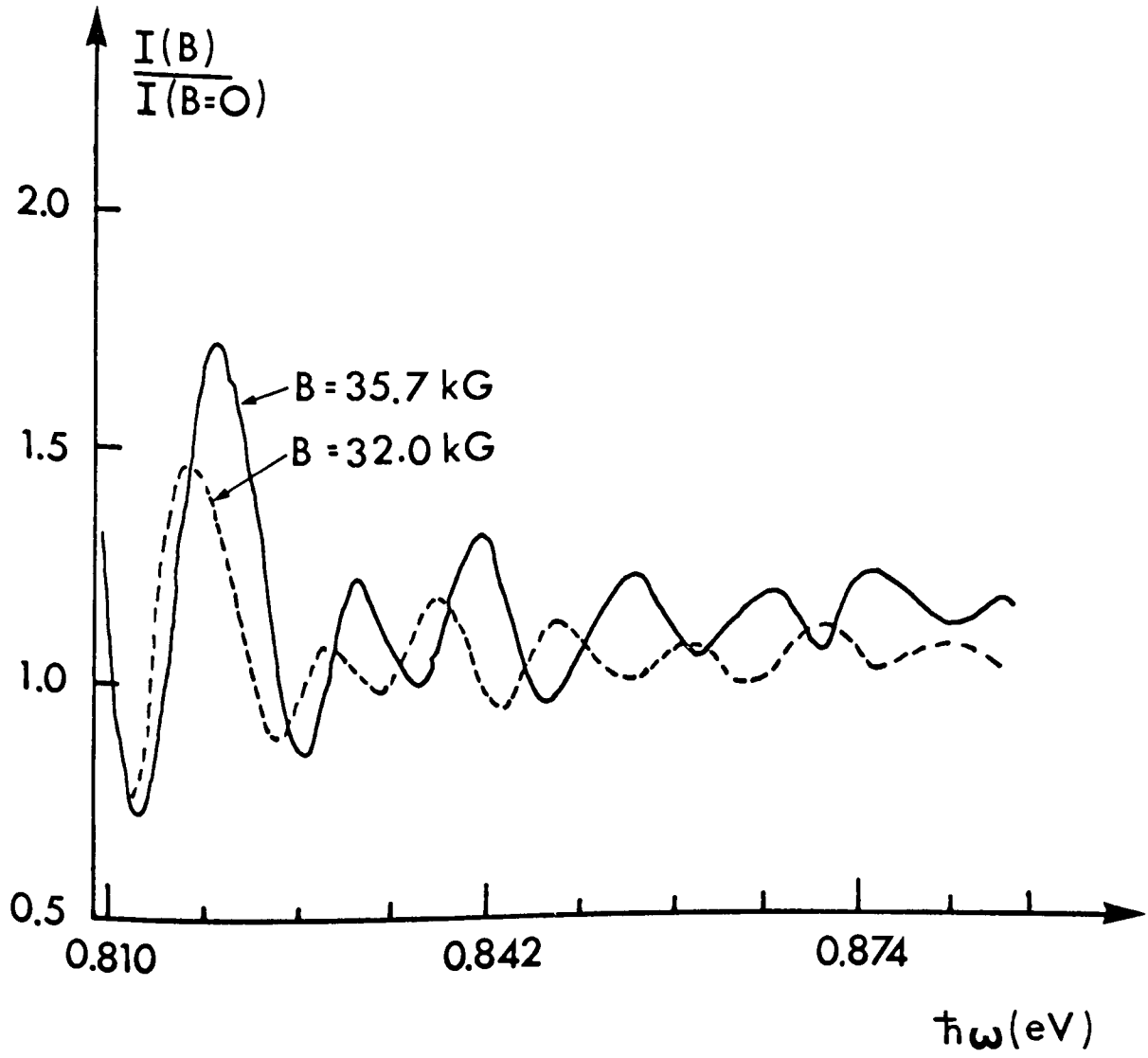

Figure 3. Oscillatory magnetoabsorption in Ge. The ratio of the transmitted signals with and without a magnetic field versus $\hbar\omega$ for two different values of magnetic field. (Zwerdling et al.[32])

provided the reflection losses can be ignored, and where d is the sample thickness. The minima of this ratio, then essentially correspond to those photon energies for which the differential absorption coefficient $[\eta(B) - \eta(0)]$ has maxima. These maxima correspond to the electron transitions between the quantized magnetic or Landau levels from the valence to the conduction bands. The above ratio has been plotted for two different values of the magnetic field in Fig. (3). One can clearly see the oscillatory behavior, as expected and the separation between maxima $\approx$ 0.015 eV in accord with the theory.

Further, from the theory, one expects that the ratio, $\frac{I(B)}{I(B=0)}$ goes through a minimum whenever

$$\hbar\omega = E_g + (n + \tfrac{1}{2})\hbar\omega_c^*$$

Thus if one plots the position of the various transmission minima n = 0, 1, 2, ... in terms of photon energy, as a function of magnetic field, straight lines should result, which when extrapolated to B = 0, should yield the value of E_g. Zwerdling et al's[32] experimental results for the position of the minima as a function of B for Ge at 298°K are shown in Fig. 4 and one sees that the functional dependence is indeed linear and that the lines converge to the energy gap of the transition. For Ge, the energy gap values obtained are 0.803 ± 0.001 eV at ~ 298°K. Also from Fig. 4 one can clearly see the shift in the absorption edge due to presence of the magnetic field (see n = 0 line).

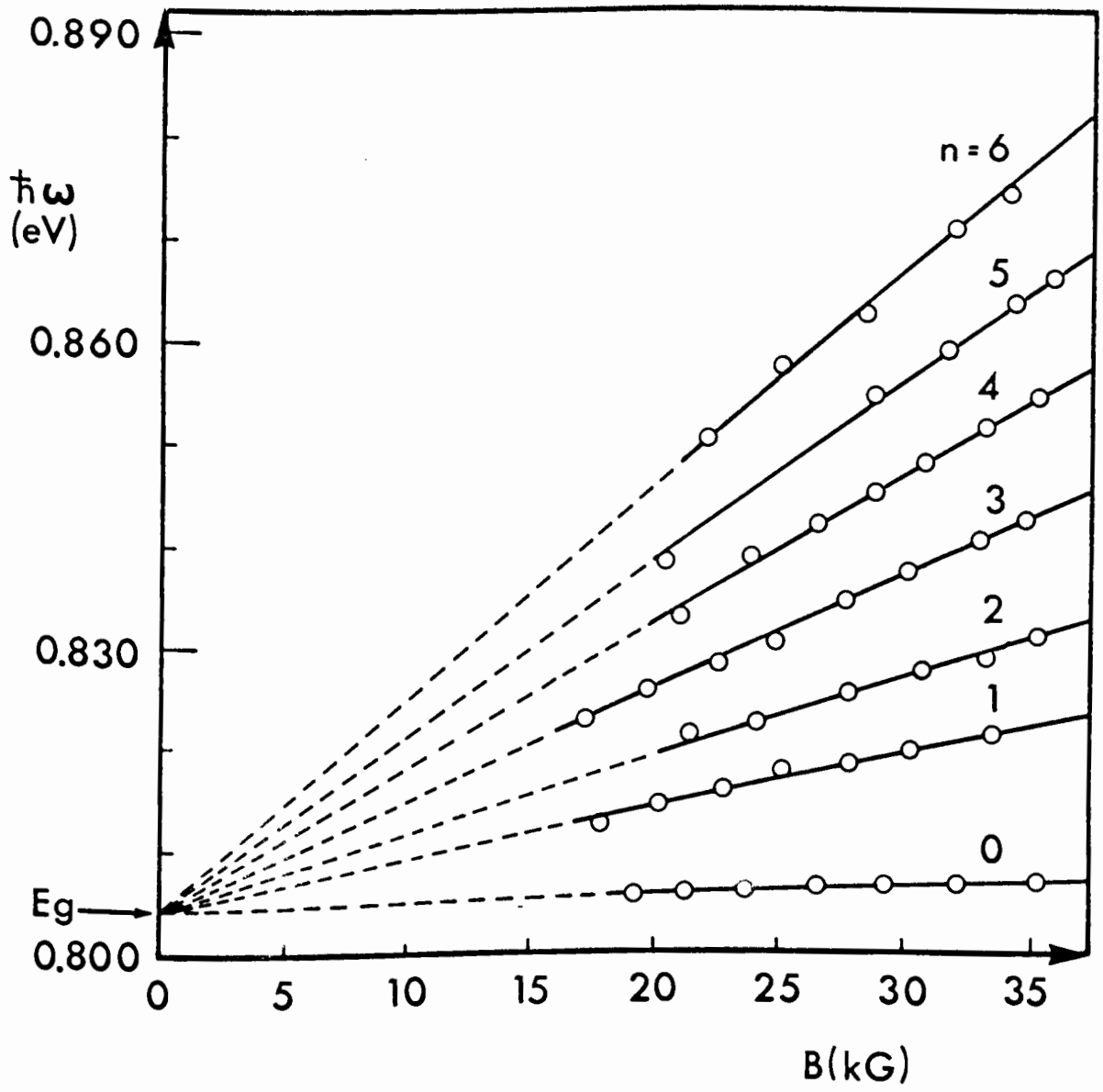

Figure 4. Photon energy of the transmission minima versus magnetic field for Ge at 298° K. The lines converge to a photon energy corresponding to the energy gap of the transition. For Ge, $E_g = 0.803 \pm 0.001$ eV at 298° K. (Zwerdling et al. (32))

Thus both aspects of the theory are supported by experiment.

A necessary condition for observing well defined structure is that the spacing between the Landau levels ($\hbar\omega_{ce}$) be greater than the broadening ($\frac{\hbar}{\tau}$) of the levels, where τ represents some average scattering time due to phonons and impurities. Hence the condition $\omega_{ce}\tau > 1$ must be satisfied for each band if the structure of both bands is to be seen. If only one band satisfies this criterion only its structure will be seen. This condition can be satisfied only by using high magnetic fields ($\sim 10^4$ gauss) and by working at low temperatures.

CHAPTER 6

ELECTROABSORPTION AND FRANZ-KELDYSH EFFECT

6.1 Derivation of the Electroabsorption Coefficient from the General Result

To obtain the optical absorption coefficient in the presence of an electric field from the general expression (3-18), one cannot proceed by setting B = 0 directly because then the drift speed $V_d = \frac{c\mathcal{E}_x}{B} \rightarrow \infty$ and the non-relativistic approximation is no longer valid. However, if we first set $\mathcal{E}_x = 0$ and then take the limit $B \rightarrow 0$, we arrive at the desired expression which contains only electric field, directed along the Z-direction, and we have not violated any validity conditions in doing so. We follow this scheme here. Setting $\mathcal{E}_x = 0$ in equation (3-18), we obtain

$$\eta = R \frac{\omega_c^*}{\Theta_F^{1/2}} \left(\frac{\nu^2}{\pi}\right) \sum_n \left| Ai\left(\frac{\Delta_{n,n}}{\hbar\Theta_F}\right)\right|^2$$

(see equation 4-1)). Now we let $B \rightarrow 0$ and thus convert the sum over n into integral, giving

$$\eta(\mathcal{E}) = \frac{R}{\hbar\Theta_F^{1/2}} \left(\frac{\nu^2}{\pi}\right) \int_0^\infty dx \left| Ai\left(\frac{E_g + x - \hbar\omega}{\hbar\Theta_F}\right)\right|^2$$

By a simple change of variable we can rewrite the above result in the following form

$$\eta(\mathcal{E}) = R\Theta_F^{1/2} \left(\frac{\nu^2}{\pi}\right) \int_\beta^\infty |Ai(t)|^2 \, dt \qquad (6\text{-}1)$$

where

$$\beta = \frac{E_g - \hbar\omega}{\hbar\theta_F}$$

The integral over 't' can now be completed using the result[19]

$$\int_\beta^\infty |Ai(t)|^2 dt = |Ai'(\beta)|^2 - \beta |Ai(\beta)|^2$$

where prime denotes differentiation with respect to the argument. Substituting the above result in (6-1) we obtain

$$\eta(\varepsilon) = R\theta_F^{1/2} \left[\left(\frac{\nu^2}{\pi}\right) \left\{ |Ai'(\beta)|^2 - \beta |Ai(\beta)|^2 \right\} \right] \quad (6\text{-}2)$$

This result is valid for $\hbar\omega \gtrless E_g$ and was first obtained by Tharmalingam[33] using exciton notation. A similar expression has been obtained by Callaway[34] and the case of an anisotropic solid has been investigated by Aspnes[19]. It is convenient to discuss the effect of electric field on the absorption spectrum in the regions $\hbar\omega > E_g$ and $\hbar\omega < E_g$, separately.

6.1a Electroabsorption above the Edge

It is convenient to start with equation (6-1) which for $\hbar\omega > E_g$ (implies $\beta < 0$) can be written in the form

$$\eta(\varepsilon) = R\theta_F^{1/2} \left(\frac{\nu^2}{\pi}\right) \left[\int_0^{-\beta} |Ai(-t)|^2 dt + \int_0^\infty |Ai(t)|^2 dt \right] \quad (6\text{-}3)$$

The integral $\int_0^\infty |Ai(t)|^2 dt$ can be evaluated approximately by breaking the region of integration into two parts as follows:

$$\int_0^\infty |Ai(t)|^2 dt = \int_0^1 |Ai(t)|^2 dt + \int_1^\infty |Ai(t)|^2 dt$$

The integral from 0 to 1 can be evaluated numerically and the integral from 1 to ∞ can be completed by replacing Ai(t) by its asymptotic form (4-3a) and using Appendix E(ii). According to this procedure we obtain

$$\int_0^\infty |Ai(t)|^2 dt \simeq 0.23 \left(\frac{\pi}{\nu^2}\right)$$

Hence the equation (6-3) becomes

$$\eta(\varepsilon) = R\theta_F^{1/2} \left[\left(\frac{\nu^2}{\pi}\right) \int_0^{-\beta} |Ai(-t)|^2 dt + 0.23 \right] \quad (6\text{-}4)$$

The upper limit on the first integral ($-\beta > 0$) depends upon $\hbar\omega$ and this term makes an oscillatory contribution to the absorption spectrum. The second term is independendent of $\hbar\omega$ and contributes only a small enhancement associated with $\varepsilon_z (\equiv \varepsilon)$.

In the limit of zero electric field, $-\beta \gg 1$, and we can use the asymptotic expression (4-3b) for the Airy function in the integral (6-4) to obtain

$$\eta(\varepsilon) \simeq R\theta_F^{1/2} \int_0^{-\beta} \frac{1}{t^{1/2}} \sin^2\left(\frac{2}{3}t^{3/2} + \frac{\pi}{4}\right) dt + 0.23 R\theta_F^{1/2}$$

The above integral has been evaluated in Appendix E(ii) and we have

$$\eta(\varepsilon) \simeq R(\omega - \omega_g)^{1/2} + 0.23 R\theta_F^{1/2}$$

When the electric field is set equal to zero ($\theta_F \to 0$), the above equation reduces to

$$\eta(\omega) = R(\omega - \omega_g)^{1/2}, \quad \omega > \omega_g$$

which is the expression for field free absorption coefficient in the region $\omega > \omega_g$ and was obtained earlier (Chapter 4).

6.1b Electroabsorption Below the Edge or Franz-Keldysh Effect

Once again we start with equation (6-1) and note that $\beta > 0$ for $\hbar\omega < E_g$ and thus the argument of the Airy function is positive throughout the integration range. Experimentally the condition $\beta >> 1$ is generally satisfied because even for $\mathcal{E} = 10^3$ volts/cm., $\hbar\theta_F$ is only about 0.005 eV and so we can replace the Airy function in (6-1) by its asymptotic form (4-3a) to obtain

$$\eta(\mathcal{E}) \simeq R\theta_F^{1/2} \int_{\beta}^{\infty} \frac{1}{4t^{1/2}} \exp\left(-\frac{4}{3}t^{3/2}\right) dt$$

Substituting the value for integral from Appendix E(i), we obtain

$$\eta(\mathcal{E}) = R \frac{\theta_F^{3/2}}{8(\omega_g - \omega)} \exp\left[-\frac{4}{3}\left(\frac{\omega_g - \omega}{\theta_F}\right)^{3/2}\right], \quad \omega < \omega_g \quad (6\text{-}5)$$

The absorption coefficient vanishes for $\hbar\omega < E_g$ if the electric field is set equal to zero. The effect of the electric field is to smear the otherwise sharp absorption edge and make the absorption possible for $\hbar\omega < E_g$ (Fig. 5). This is called the Franz-Keldysh[35,36] effect or photon-assisted tunneling after the two theorists who independently predicted it in 1958. In Appendix (F) the F-K effect is also derived using an alternate method similar to one used by Haering and Adams[37].

In Fig. 5 we have schematically displayed the variation of $\eta(\mathcal{E})$ and $\eta(0)$ with the energy of the incident photon using equations (6-2) and (4-8). $\eta(\mathcal{E})$ is oscillatory above the edge and exponential like below it whereas $\eta(0)$ attains non-vanishing values only for $\hbar\omega > E_g$.

Since the experimental results are almost always given in terms of the field induced differential absorption coefficient

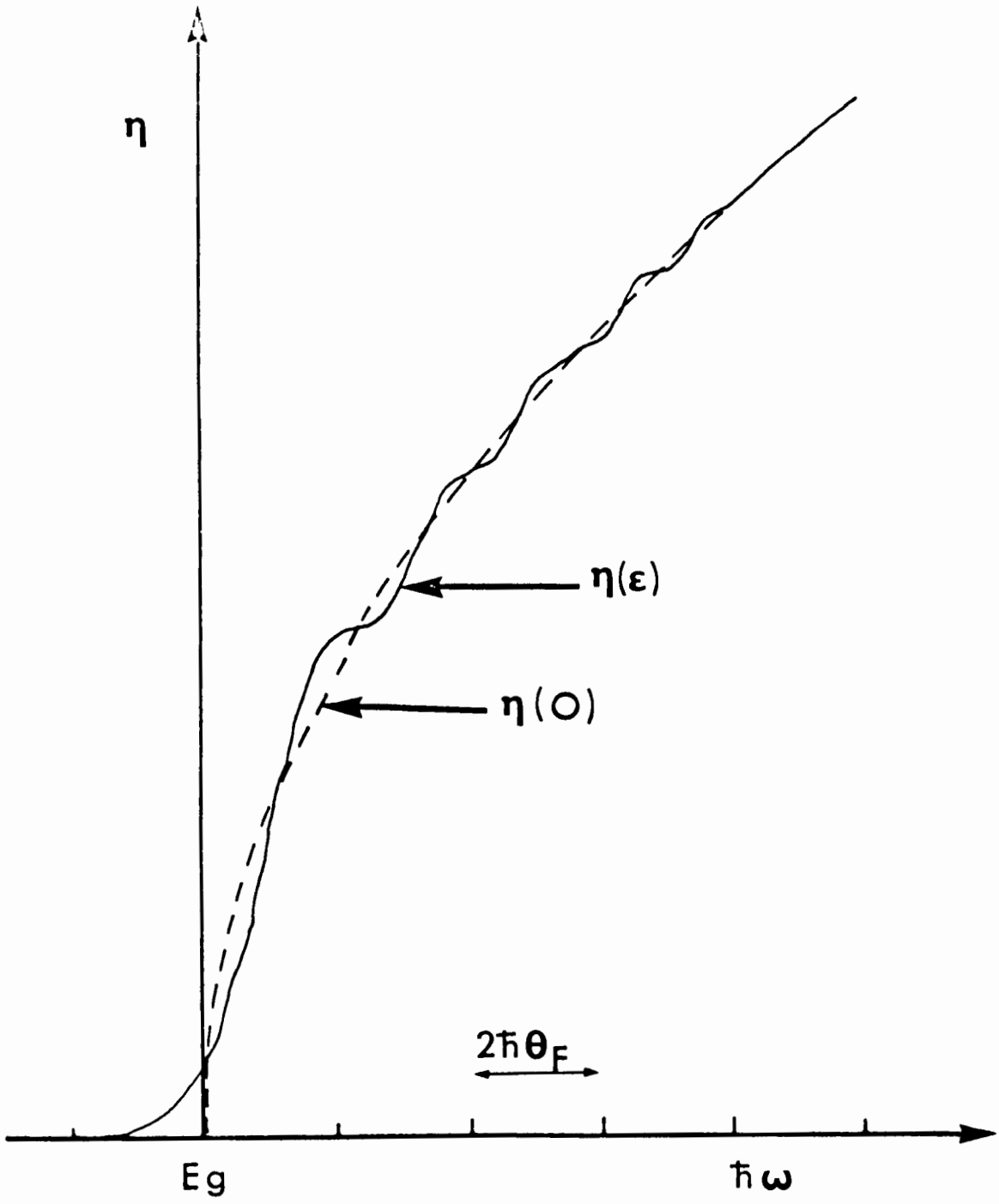

Figure 5. Energy dependence of the interband absorption coefficient for $\varepsilon = 0$ and $\varepsilon \neq 0$. Note the exponential decay of $\eta(\varepsilon)$ into the forbidden gap.

$\Delta\eta = \eta(\mathcal{E}) - \eta(0)$, it is instructive, to show the theoretical behaviour of such a quantity. From (6-2) and (4-8), we have

$$\Delta\eta = R\theta_F^{1/2}\left[\,|Ai'(\beta)|^2 - \beta|Ai(\beta)|^2 - \sqrt{-\beta}\,H(-\beta)\right] \qquad (6\text{-}6)$$

where H(x) is unit step function defined as follows:

$$H(x) = 1 \qquad x > 0$$
$$= 0 \qquad x \leq 0$$

The schematic variation of $\Delta\eta$ with the photon energy is shown in Fig. 6. The simple theory described above predicts that the change in the absorption, $\Delta\eta$ will be exponential-like below the edge and oscillatory above it.

6.2 The Experimental Situation

There are a large number of experiments[3,4,5,38,39] available, which only qualitatively support the above theory. The results of all these experiments are in good agreement with the simple theory below the edge, but there is disagreement around the edge. The experiment on GaAs first performed by Moss[3] showed an exponential decay of the absorption coefficient below the edge, but failed to record any oscillatory behaviour above the edge.

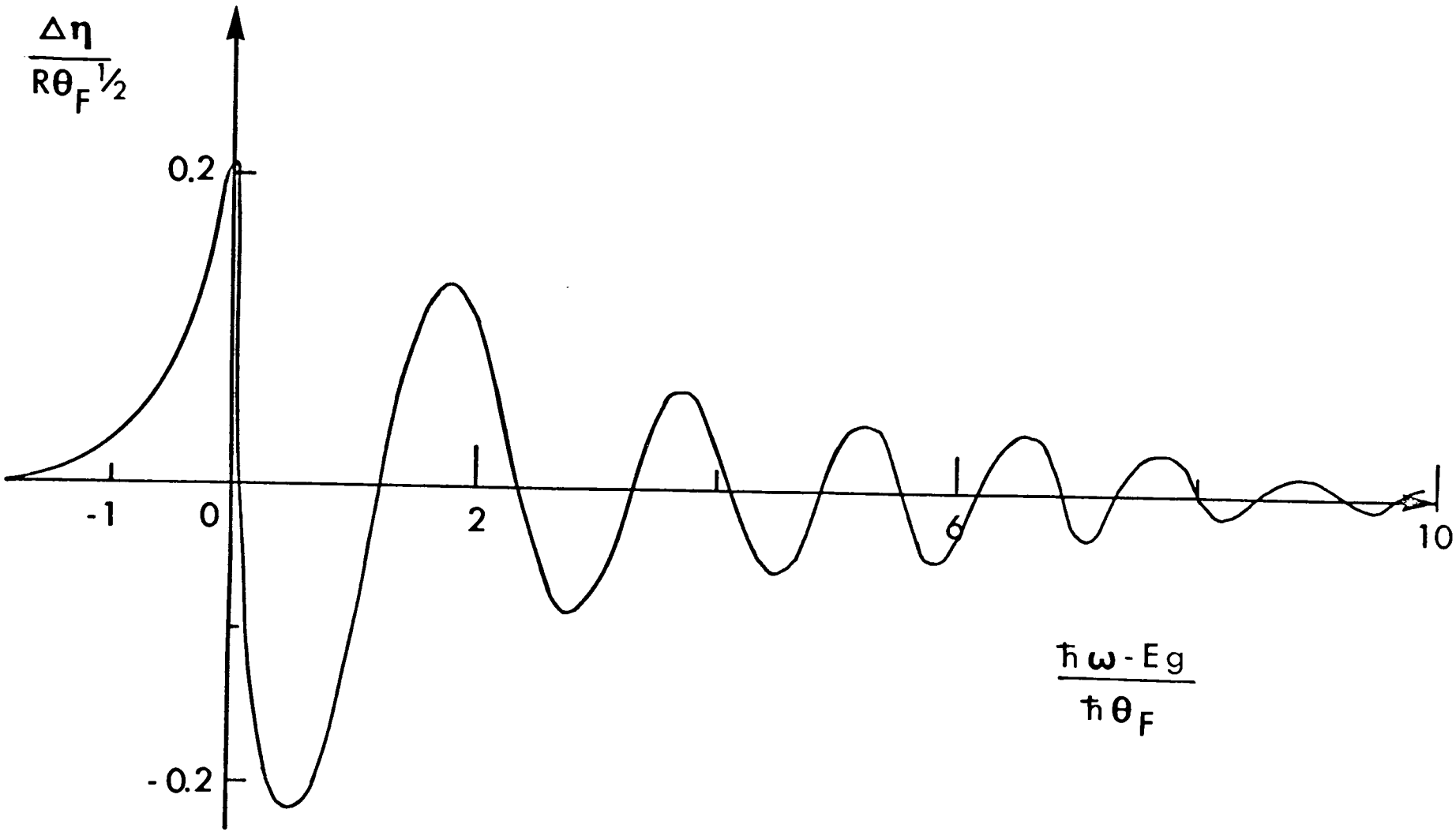

Figure 6. Difference of absorption coefficients $[\eta(\varepsilon) - \eta(0)] \equiv \Delta\eta$ as a function of photon energy.

The experiments of Frova et al.[38] are much more conclusive in nature because of the improved resolution and the wider range of incident radiation energy. Apart from measuring the change, $\Delta\eta$ for the direct absorption edge in germanium, their experiments also explored the indirect absorption edges of silicon and germanium, which will not concern us here, as we are only interested in direct transitions. They detect the change in the absorption coefficient due to an electric field, by passing a monochromatic light beam normally through the plane of a p-n junction across which both a large d.c. reverse bias and a small a.c. voltage have been applied. The d.c. voltage determines the maximum value of the electric field in the junction, while the a.c. voltage, by changing the field, modulates the light passing through the junction. This modulation ΔI of the light by the electric field and the total intensity I are measured simultaneously. Then

$$\Delta\eta = \frac{\Delta I}{\Delta V}\frac{\mathcal{E}}{I}\phi(\omega,\mathcal{E}) \qquad (6\text{-}7)$$

where ΔV is the peak-to-peak value of the modulating a.c. voltage and $\mathcal{E}$ is the maximum electric field. The function ϕ is very close to unity, and is determined by the shape of the junction.

Their experiments confirmed the characteristic exponential-

like behaviour for $\hbar\omega < E_g$, the slope of the curves decreasing with increasing electric field, as expected from the theory (see equation (6-5)). Furthermore at $\hbar\omega \simeq E_g$, the field induced change in absorption goes through zero and reaches a negative peak. This is in agreement with equation (6-5) (see Fig. 6). However, according to this equation the peak varies with the electric field as $\mathcal{E}^{1/3}$. It is this feature of the theory that is not being supported by the experiment, which favours a very weak dependence on $\mathcal{E}$. This disagreement is apparently caused by the effects of an exciton[39] and thermal broadening, which are not included in the simple theory.

CHAPTER 7

ABSORPTION IN CROSSED ELECTRIC AND MAGNETIC FIELDS AND WEAK FIELD APPROXIMATION

7.1 Derivation of the Crossed Fields Absorption Coefficient from the General Result

In order to obtain results for the crossed fields situation, we find it convenient to split the sum in (3-18) into two parts as follows:

$$\eta(\vec{\mathcal{E}},\vec{B}) = R\,\frac{\omega_c^*}{\theta_F^{1/2}}\left(\frac{\mathcal{V}^2}{\pi}\right)\left[\sum_{\substack{n',n\\(\Delta_{n',n}>0)}} J^2_{n',n}(a)\left|Ai\left(\frac{\Delta_{n',n}}{\hbar\theta_F}\right)\right|^2 + \sum_{\substack{n',n\\(\Delta_{n',n}<0)}} J^2_{n',n}(a)\left|Ai\left(\frac{\Delta_{n',n}}{\hbar\theta_F}\right)\right|^2\right] \tag{7-1}$$

Now if in each of the above two terms we set $\mathcal{E}_z = 0$, the resulting expression would contain an electric field along the X-direction and a magnetic field along the Z-direction, the configuration we are interested in. So letting $\mathcal{E}_z \to 0$ ($\Rightarrow \theta_F \to 0$) and replacing the Airy functions in (7-1) by their asymptotic forms (4-3) we obtain

$$\eta(\vec{\mathcal{E}},\vec{B}) \simeq \frac{R(\hbar\omega_c^*)}{2\hbar^{1/2}}\left[\sum_{\substack{n',n\\(\Delta_{n',n}>0)}} \frac{J^2_{n',n}(a)}{(\Delta_{n',n})^{1/2}}\exp\left\{-\frac{4}{3}\left(\frac{\Delta_{n',n}}{\hbar\theta_F}\right)^{3/2}\right\} + \sum_{\substack{n',n\\(\Delta_{n',n}<0)}} \frac{J^2_{n',n}(a)}{(-\Delta_{n',n})^{1/2}}\left\{1+\sin\left(\frac{4}{3}\left(-\frac{\Delta_{n',n}}{\hbar\theta_F}\right)^{3/2}\right)\right\}\right]$$

When $\theta_F = 0$, the first sum does not contribute anything and in the second sum the Sine function oscillates rapidly for large argument and averages out to zero. Then substituting for $\Delta_{n',n}$ from (3-17) we obtain

$$\eta(\vec{\mathcal{E}}\times\vec{B}) = \frac{R(\hbar\omega_c^*)}{2\hbar^{1/2}} \times \sum_{n',n} \frac{J^2_{n',n}(a)}{\left[\hbar\omega - E_g - \hbar\omega_{cc}(n'+\frac{1}{2}) - \hbar\omega_{cv}(n+\frac{1}{2}) + \frac{1}{2}MV_d^2\right]^{1/2}} \quad (7\text{-}2)$$

where n and n' are restricted by the relation

$$n'\hbar\omega_{cc} + n\hbar\omega_{cv} < \hbar\omega - E_g - \frac{1}{2}\hbar\omega_{cc} - \frac{1}{2}\hbar\omega_{cv} + \frac{1}{2}MV_d^2 \quad (7\text{-}3)$$

This restriction implies that there is no absorption until

$$\hbar\omega > E_g + \frac{1}{2}\hbar\omega_{cc} + \frac{1}{2}\hbar\omega_{cv} - \frac{1}{2}MV_d^2 \equiv E_g(\vec{\mathcal{E}}\times\vec{B}) \quad (7\text{-}4)$$

The right-hand side of this equation can be thought of as the effective energy gap in the presence of crossed electric and magnetic fields.

To express the result (7-2) in a standard form we use the closed form expression for $J_{n',n}(a)$ which has been derived in Appendix (C). According to equation (C-4) of the Appendix (C)

we have

$$J_{n',n}(a) = \frac{e^{-(1/4\,\gamma^2)}}{(2^{n+n'}\,n!\,n'!)^{1/2}} \times \sum_{\ell=0}^{\min\{n',n\}} \frac{(-1)^{n'-\ell}\, n!\, n'!\, 2^{\ell}\, \gamma^{n+n'-2\ell}}{\ell!\,(n-\ell)!\,(n'-\ell)!} \tag{7-5}$$

where

$$\gamma = \frac{a}{\lambda} = \frac{e\,\mathcal{E}_x\,\lambda}{\hbar\Omega_c}$$

is a dimensionless quantity, $\Omega_c = \frac{eB}{Mc} = \frac{\omega_{cc}\,\omega_{cv}}{\omega_{cc}+\omega_{cv}}$. The summation over ℓ extends to n or n' whichever is smaller. Substituting (7-5) in (7-2) we get

$$\eta(\vec{\mathcal{E}}\times\vec{B}) = \frac{R(\hbar\omega_c^{*})}{2\hbar^{1/2}} \sum_{n',n} \left[\frac{e^{-(\gamma^2/2)}}{(2^{n+n'}\,n!\,n'!)} \times \left| \sum_{\ell=0}^{\min\{n,n'\}} b_{\ell}(n,n')\,\gamma^{n+n'-2\ell} \right|^2 (\hbar\omega - E_{n,n'})^{-1/2} \right] \tag{7-6}$$

where

$$b_{\ell}(n,n') = \frac{(-1)^{n'-\ell}\, n!\, n'!\, 2^{\ell}}{\ell!\,(n-\ell)!\,(n'-\ell)!} \tag{7-7}$$

and

$$E_{n,n'} = E_g + \hbar\omega_{cc}\left(n'+\tfrac{1}{2}\right) + \hbar\omega_{cv}\left(n+\tfrac{1}{2}\right) - \tfrac{1}{2}MV_d^2 \quad (7\text{-}8)$$

The result (7-6), apart from some numerical factors was first obtained theoretically by Aronov[40] and was subsequently corrected for some factors by Vrehen[41]. The result (7-6) has also been obtained by Spector[42], who considers forbidden transitions as well. The main implications of the above result are as follows:

(i) The location of the absorption maximum is a function of the magnitude of the electric field and all transitions are shifted to lower photon energies by an amount $\delta = \frac{1}{2} MV_d^2 \equiv \frac{1}{2} (m_c + m_v) \frac{c^2 \mathcal{E}_x^2}{B^2}$, with respect to the magnetoabsorption spectrum (see Chapter 5).

Aronov[40] proposed the measurement of this shift, which should yield a value for the sum of the masses of hole and electron. As we saw earlier that the magneto-absorption measurements provide us with the reduced mass μ, the two experiments combined should yield the values of m_c, m_v separately. The order of magnitude of the shift for $M = 10^{-28}$ gm. is

$$\delta \simeq 10^{14}\left(\frac{\mathcal{E}}{B}\right)^{2} \text{sec}^{-1} \simeq 0.3\left(\frac{\mathcal{E}}{B}\right)^{2} \text{eV}$$

where $\mathcal{E} \equiv \mathcal{E}_x$ is in volts/cm. and B is in gauss. The quantity $(\mathcal{E}/B) \ll 1$ for the non-relativistic approximation to hold and thus the shift cannot be very large.

(ii) The selection rule $\Delta n = 0$, valid for direct magneto-absorption case (discussed in Chapter 5) breaks down in the presence of a transverse electric field and the transitions corresponding to $\Delta n = \pm 1, \pm 2, \pm 3, \ldots$ have a finite transition probability. Such transitions will be called <u>electric field induced transitions</u>[43].

It is quite clear that a strong electric field would give rise to a large shift which is easier to observe experimentally. On the other hand, a strong electric field complicates verification of the second aspect of the theory by making very many transitions possible. A weak electric field breaks the selection rule, $\Delta n = 0$ only slightly (see Section 7.3) but does not give rise to a measurable shift. Thus to test the two predictions of the theory we require somewhat opposite experimental conditions. In the next section we compare the theoretically predicted shift with the experimental value observed in strong electric field. The theory for weak electric field is developed in Section 7.3 and

is compared with experiment in Section 7.4.

7.2 Comparison of the Theory with the Experimental Results in Strong Electric Field

Some aspects of the crossed field absorption theory have been confirmed experimentally by Vrehen[41] and by Vrehen and Lax[44] for the case of relatively low electric fields, and by others[45,46] at higher field values. For the present we would consider the experiments involving large electric fields, a discussion of the weak electric field case will be postponed until the next section. The parameter of interest in determining whether we are in the weak or strong field limit is γ. The explanation for this choice is given in Section 12.2. For $M = 10^{-28}$ gm., we have

$$\gamma \simeq 2 \times 10^3 \, \mathcal{E}/B^{3/2}$$

where again B is measured in gauss and $\mathcal{E}$ in volts/cm. When $\gamma \ll 1$, we are in the weak field limit, and $\gamma \gg 1$ implies the strong field limit. This means that for a magnetic field of 10^4 gauss, we are in the weak field limit when $\mathcal{E} \ll 500$ volts/cm and in the strong field limit when $\mathcal{E} \gg 500$ volts/cm.

In the strong fields experiment of Vrehen[45] on Ge, the values of γ were in the range 1.6 to 2.6. In Fig. (7), we have reproduced the curve obtained by Vrehen for, $\eta(\vec{\mathcal{E}} \times \vec{B}) - \eta(0)$ versus the energy of the incident radiation. The experiment was

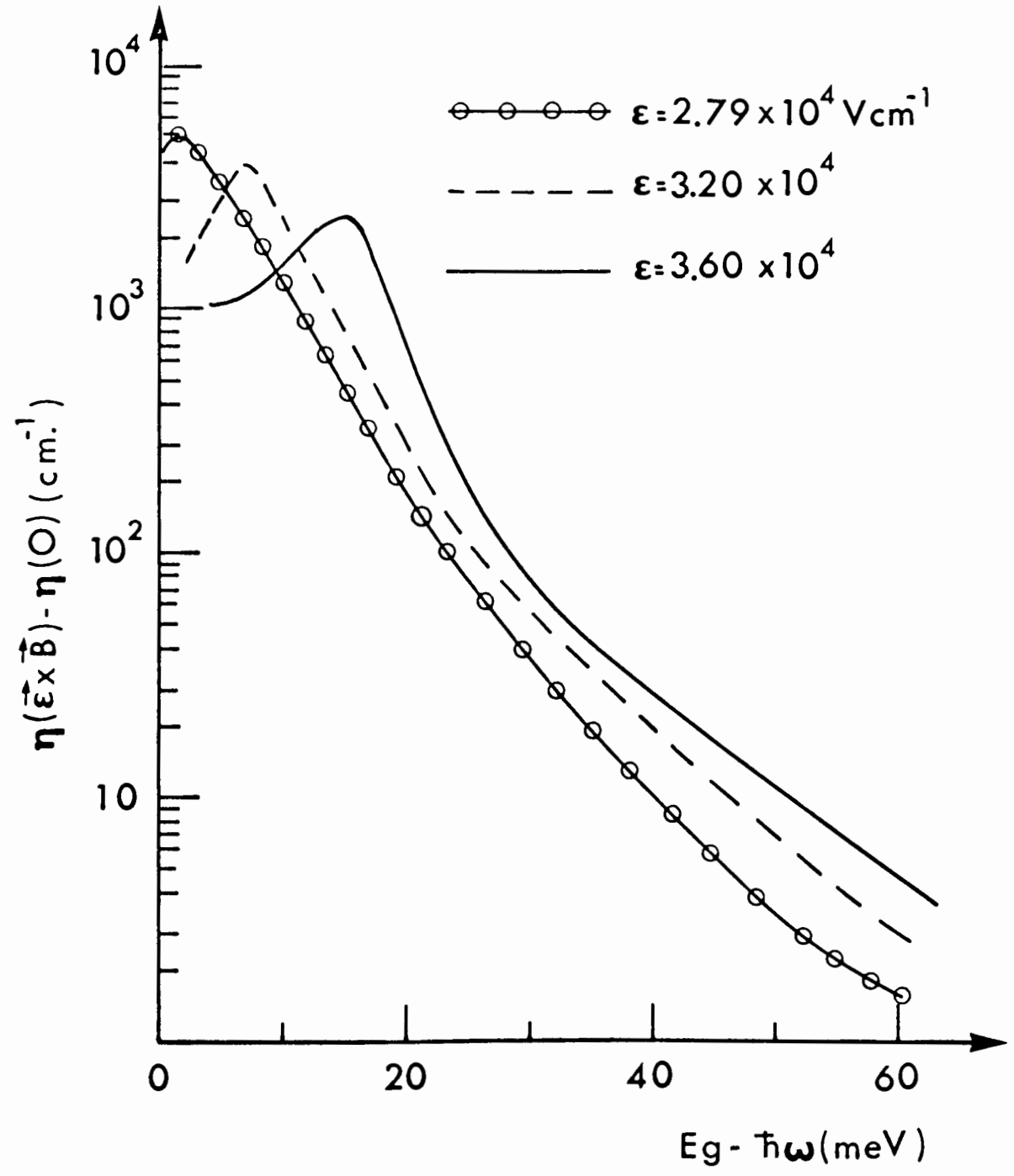

Figure 7. Electric field-induced optical absorption below the direct gap in Ge for crossed electric and magnetic field case for B = 96kG, and for various values of ε (Vrehen(45)).

conducted on a thin sample of germanium at 6° C in the presence of a magnetic field of $\sim 10^5$ gauss and an electric field of $\sim 10^4$ Volts/cm in the crossed electric and magnetic fields configuration. A resonance in the optical absorption, several milli electron volts below the direct band edge in germanium, was observed, which was not present when the electric field was turned off or if it was parallel to the magnetic field.

From equation (7-8) the energy $\hbar\omega$ for the transition between the zeroth Landau levels is given by

$$\hbar\omega = E_g + \frac{1}{2}\hbar\omega_c^* - \frac{1}{2}(m_c + m_v)\frac{c^2\mathcal{E}^2}{B^2} \qquad (7\text{-}9)$$

Thus if $(\hbar\omega - \frac{\hbar\omega_c^*}{2})$ is plotted as a function of $(\mathcal{E}/B)^2$, straight line should result whose slope is related to the value of $(m_c + m_v)$. Vrehen[45] carried out such an analysis, obtaining the value of $\hbar\omega$ from the experimentally determined energy of resonance (Fig. 7) and found that the experimental points lie on a straight line in accordance with equation (7-9) and from the slope he estimated $(m_c + m_v) = (0.074 \pm 0.015)$ m where m is the electron mass. Taking $m_c = 0.036$ m[32] one deduces $m_v = (0.038 \pm 0.015)$ m which is of the order of magnitude of the light hole mass 0.041 m[32]. Thus there is a reasonable agreement between the theory and the experiment.

Thus the shift of the edge in the presence of crossed electric and magnetic fields can be used as a tool for obtaining the sum of effective masses if the sample can stand high electric fields ($\sim 3 \times 10^4$ volts/cm) without considerable heating. Since this is not possible in general, we develop a weak field approximation in the next section and show that the same information can be obtained, in principle at least from a study of the optical absorption above the gap in relatively low electric fields.

7.3 Weak Field Approximation for Optical Absorption in Crossed Electric and Magnetic fields

In the last section it was pointed out that in the presence of crossed electric and magnetic fields, the threshold for absorption shifts to lower photon energies by an amount $\frac{1}{2} MV_d^2$ and from the study of this shift, coupled with the knowledge of the reduced mass, one can obtain the values of m_c, m_v separately. However, to obtain conveniently measurable shifts, fairly high electric fields ($\sim 3 \times 10^4$ V/cm) are needed. High electric fields introduce unpleasant features in the absorption spectroscopy, since the absorption lines are usually broad, even in the zero electric field. In the presence of high electric fields, many more transitions become possible and it becomes more difficult to resolve the lines, and the net effect of the electric field is then to wash out the structure completely. Furthermore, the effect is hard to observe in

high electric fields because of heating and possibly impurity ionization at low temperatures where these experiments are usually performed. Thus it is desirable to work with low electric fields and somehow still obtain the values of m_c, m_v. It is the purpose of this section to show that this is indeed possible.

It will be shown below that for small electric fields, field induced transitions ($\Delta n = \pm k$, $k = 1, 2, \ldots$) have a strength proportional to $\mathcal{E}^{2k}$, so that only $\Delta n = \pm 1$ need be considered. Such field induced transitions can be readily observed experimentally[41]. Since, for these low electric fields, the electric field induced shifts can be neglected, the values of m_c, m_v can then be obtained from the positions of $\Delta n = 0$ and $\Delta n = \pm 1$ transitions.

Vrehen[41] has worked out the weak field approximation in a rather simple way. He started with the exact result (7-6) and for small electric fields i.e. $\gamma << 1$, expanded it in powers of γ^2 and retained terms of order γ^2 and lower. His approach is quite correct but relies on the knowledge of the result (7-6). We present below an alternative method which does not involve the use of the result (7-6), but starts out with equation (7-2). The usefulness of our method will become much more transparent when we employ it to study phonon-assisted transitions in crossed electric and magnetic fields.

In Appendix (D) it is shown that for $\gamma \ll 1$

$$J_{n',n}(a) \simeq \delta_{n',n} + (\gamma)\left\{-\left(\frac{n+1}{2}\right)^{1/2}\delta_{n',n+1} + \left(\frac{n}{2}\right)^{1/2}\delta_{n',n-1}\right\}$$

$$+\left(\frac{\gamma^2}{2}\right)\left\{-\left(n+\frac{1}{2}\right)\delta_{n',n} + \left(\frac{n+2}{2}\right)^{1/2}\left(\frac{n+1}{2}\right)^{1/2}\delta_{n',n+2} + \left(\frac{n}{2}\right)^{1/2}\left(\frac{n-1}{2}\right)^{1/2}\delta_{n',n-2}\right\}$$

Squaring this and retaining terms up to order γ^2 we have

$$J^2_{n',n}(a) \simeq \delta_{n',n}$$

$$+(\gamma^2)\left\{\left(\frac{n+1}{2}\right)\delta_{n',n+1} + \left(\frac{n}{2}\right)\delta_{n',n-1} - \left(n+\frac{1}{2}\right)\delta_{n',n}\right\} \quad (7\text{-}10)$$

Substituting this in (7-2) we get, for the low field limit,

$$\eta(\vec{\mathcal{E}}\times\vec{B}) \simeq \frac{R(\hbar\omega_c^*)}{2\hbar^{1/2}} \sum_{n',n} P_{n,n'}\left(\hbar\omega - E_{n,n'}\right)^{-1/2} \quad (7\text{-}11)$$

where

$$P_{n,n'} = \left\{1 - \left(\frac{2n+1}{2}\right)\gamma^2\right\}\delta_{n',n} + \left\{\left(\frac{n}{2}\right)\gamma^2\right\}\delta_{n',n-1}$$

$$+ \left\{\left(\frac{n+1}{2}\right)\gamma^2\right\}\delta_{n',n+1} \quad (7\text{-}12)$$

and $E_{n,n'}$ is given by (7-8), the sum over n, n' is restricted by the relation (7-3). Thus we see that in the weak field approximation, $P_{n,n'}$ is different from zero only for $\Delta n = n' - n = 0, \pm 1$. The above result agrees with the result obtained by Vrehen[41].

7.4 Results and Discussion

We have numerically plotted the weak field absorption coefficient (7-11) for $\gamma = 0.3$. Two cases involving different ratios of valence to conduction band band masses are considered, namely $\frac{m_v}{m_c} = 1$ (Fig. 8) and $\frac{m_v}{m_c} = 2$ (Fig. 9). Since the electric field induced shift of the band gap is small, the interband absorption starts at $\hbar\omega = E_g + \frac{1}{2}\hbar\omega_c^*$. Whenever $\hbar\omega$ is increased by an amount $\hbar\omega_c^*$, there is resonant absorption because more levels satisfying the $\Delta n = 0$ selection rule become accessible. If there is no breaking of this selection principle the absorption will continue to fall steadily when $\hbar\omega$ is increasing in the range, $E_g + (\ell + \frac{1}{2})\hbar\omega_c^* < \hbar\omega < E_g + (\ell + 3/2)\hbar\omega_c^*$, $\ell = 0, 1, \ldots$ In Figs. (8) and (9), the sudden increase in the absorption signfies the field induced transitions $\Delta n = \pm 1$.

It is clear from Fig. 8 that for equal masses ($m_c = m_v$) the peaks lie at the mid points. For unequal masses (Fig. 9), the peaks due to field induced transitions ($\Delta n = \pm 1$) lie on each side of the $n = 0$ line. Thus we see that the position of the peaks ($\Delta n = \pm 1$) in the range $\hbar\omega_c^*$ depends upon the ratio of the two masses whereas the separation between successive $\Delta n = 0$ lines is $\hbar\omega_c^*$, which involves the reduced mass. Hence it is possible to deduce the values of m_c, m_v separately. The above theory has been supported by experiments[41,44] on germanium.

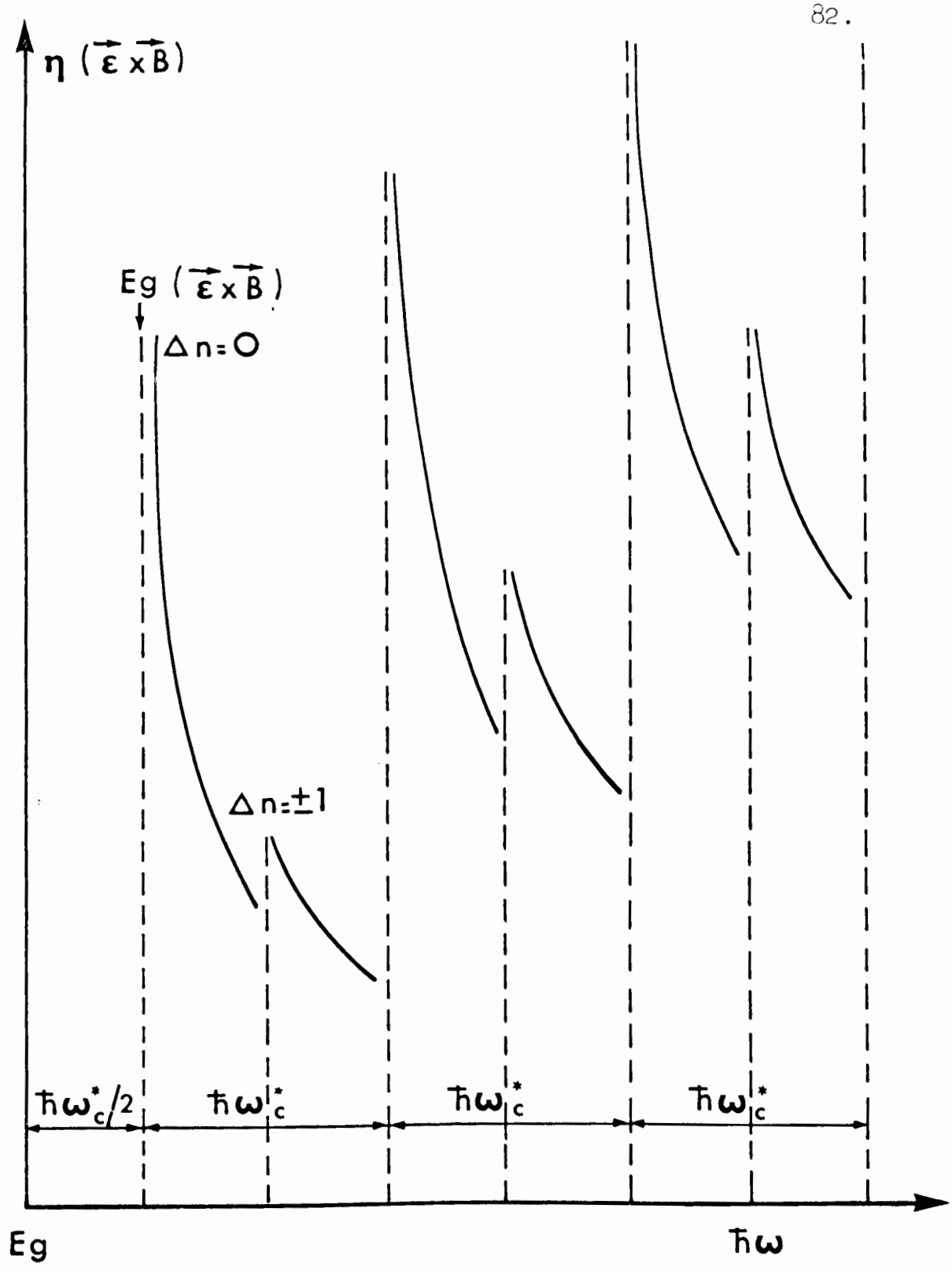

Figure 8. Schematic representation of the crossed fields absorption for the case $m_v/m_c = 1$ and weak electric field ($\gamma = 0.3$). The small peaks are due to field induced transitions ($\Delta n = \pm 1$).

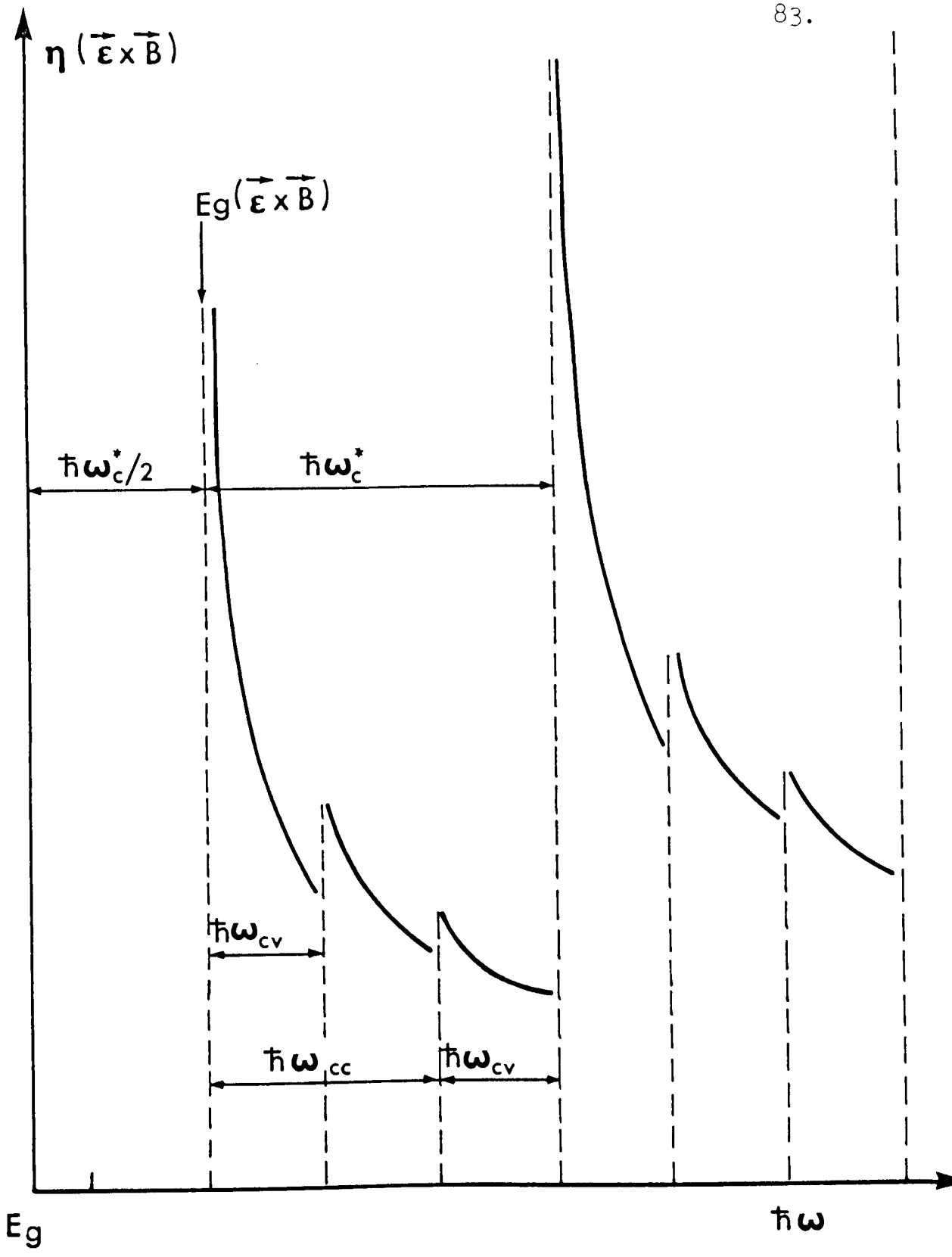

Figure 9. Schematic representation of the crossed fields absorption for the case $m_v/m_c = 2$ and weak electric field ($\gamma = 0.3$). The small peaks are due to field induced transitions ($\Delta n = \pm 1$).

Vrehen[41] has observed some additional peaks due to field induced transitions which were not present in the magneto-absorption spectrum. However further experiments are needed before a quantitative fit between the theory and experiment can be attempted.

CHAPTER 8

ABSORPTION IN PARALLEL ELECTRIC AND MAGNETIC FIELDS

8.1 Derivation of Parallel Field Absorption Coefficient from the General Result

Once again we can start with equation (3-18) and obtain the absorption coefficient in the present field configuration, by setting $\mathcal{E}_x = 0$, which implies that both V_d and 'a' vanish. From Appendix (D), we have then $J_{n',n} = \delta_{n',n}$ and with this equation (3-18) reduces to

$$\eta(\vec{\mathcal{E}} \parallel \vec{B}) = R \frac{\omega^*}{\Theta_F^{1/2}} \left(\frac{\nu^2}{\pi}\right) \sum_n \left| \Lambda \left(\frac{E_n - \hbar\omega}{\hbar\omega_c^*} \right) \right|^2 \qquad (8\text{-}1a)$$

where

$$E_n = E_g(B) + n\hbar\omega_c^* \qquad (8\text{-}1b)$$

The quantum number n takes values, from 0 to Max $\left(\frac{\hbar\omega - E_g(B)}{\hbar\omega_c^*}\right)$ where $E_g(B) = E_g + \frac{1}{2}\hbar\omega_c^*$, as in the magnetoabsorption case. The magnetic field gives rise to Landau level structure and band shift, and the electric field results in tilting the bands and making the phenomenon of photon-assisted tunneling possible. Interband transitions take place between pairs of Landau levels subject to the usual magneto-optical selection rule $\Delta n = 0$. The above result, for the absorption coefficient was first

reported by Reine et al.[47,48]. Recently the same result has been obtained using a different method[49].

The expression (8-1) is valid for photon energies both below and above the direct gap. For $\hbar\omega > E_g$ one obtains the well known magnetoabsorption spectrum, slightly modified by the electric field and this region will not be discussed any further. However, the electric field induces absorption for photon energies less than the direct gap (photon-assisted tunneling), and the effect of a magnetic field on the absorption spectrum, in this region is of some interest. This phenomenon has been called photon-assisted magneto-tunneling in the recent literature[47,48], for obvious reasons. The tunneling process can be easily visualized by looking at the band diagram, (see Fig. 10) where the solid sloping lines represent the conduction and valence bands in the presence of parallel fields and the dotted line shows the position when B = 0. A valence electron of energy E_v tunnels from Z_v to Z_m, absorbs a photon and then tunnels to Z_c. The effect of the magnetic field is to reduce the tunneling by increasing the effective energy gap. We indeed show this, by deriving an expression for the absorption coefficient in the region $\hbar\omega < E_g$, both in the presence and absence of the magnetic field.

If $\hbar\omega < E_g$, then $E_n > \hbar\omega$ and for $\frac{E_n - \hbar\omega}{\hbar\theta_F} >> 1$ we can use

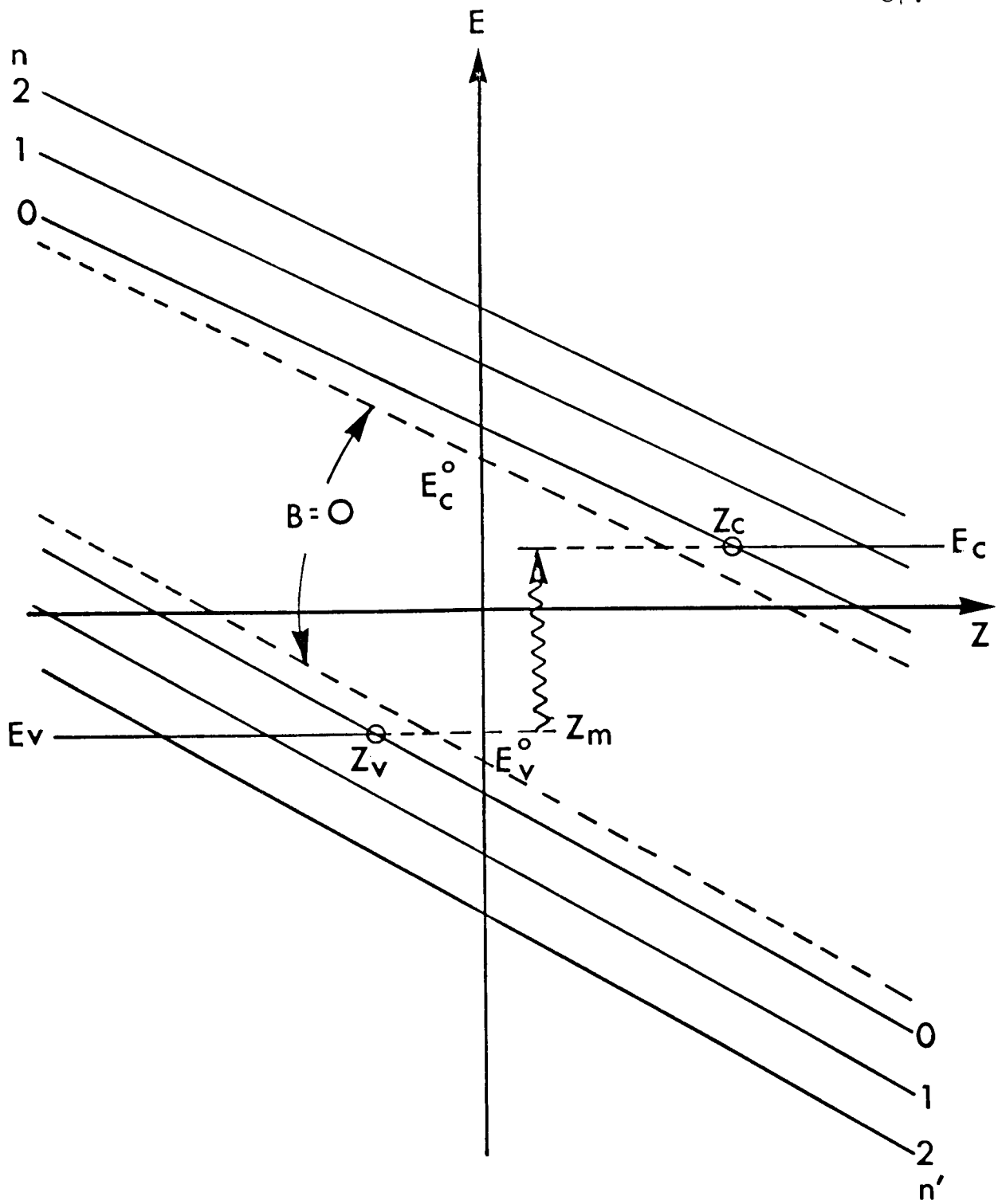

Figure 10. Photon-assisted tunneling in parallel fields. The sloping solid lines represent the conduction and valence band levels quantized by the magnetic field.

the asymptotic approximation (4-3a) for the Airy function, when (8-1) reduces to

$$\eta(\vec{\mathcal{E}}\parallel\vec{B}) = R\,\frac{\omega_c^*}{4}\sum_n\left[\left(\frac{\hbar}{E_n-\hbar\omega}\right)^{1/2}\exp\left\{-\frac{4}{3}\left(\frac{E_n-\hbar\omega}{\hbar\Theta_F}\right)^{3/2}\right\}\right] \tag{8-2}$$

In the limit of a small magnetic field, the sum over n in (8-2) can be replaced by an integral; for B = 0 we get

$$\eta(\mathcal{E}) = R\Theta_F^{1/2}\int_\beta^\infty \frac{1}{4t^{1/2}}\exp\left(-\frac{4}{3}t^{3/2}\right)dt$$

where

$$\beta = \frac{E_g-\hbar\omega}{\hbar\Theta_F} >> 1 \tag{8-3}$$

This integral has been evaluated in Appendix E(i) and we obtain

$$\eta(\mathcal{E}) = R\,\frac{\Theta_F^{3/2}}{8(\omega_g-\omega)}\exp\left\{-\frac{4}{3}\left(\frac{\omega_g-\omega}{\Theta_F}\right)^{3/2}\right\} \tag{8-4}$$

This result for photon-assisted tunneling or Franz-Keldysh effect is the same as we obtained earlier in Chapter 6.

The equations (8-2) and (8-4) both predict an exponential decay of the absorption coefficient into the forbidden gap. The application of a magnetic field parallel to the electric field in the region $\hbar\omega < E_g$ (see equation (8-2)) reduces the absorption compared with the case when electric field is present alone (equation (8-4)).

8.2 Experimental Verification

The optical absorption in the presence of parallel fields in the region $\hbar\omega < E_g$ has recently been investigated experimentally[47,48]. Fig. 11 is an experimental[47] plot of the quantity $\eta(\vec{\mathcal{E}} \parallel \vec{B};\ \hbar\omega < E_g)$ as a function of photon energy below the direct gap, for a fixed $\vec{\mathcal{E}}$, and different values of the magnetic field. It can be seen that the main effect of the magnetic field is to decrease the absorption. This corresponds to the increase in the energy separation between valence and conduction bands with increasing magnetic field. The exponential decrease of absorption with photon energy below the gap, which is characteristic of the Franz-Keldysh effect, is still present even at the highest values of magnetic field applied. This is consistent with equation (8-2).

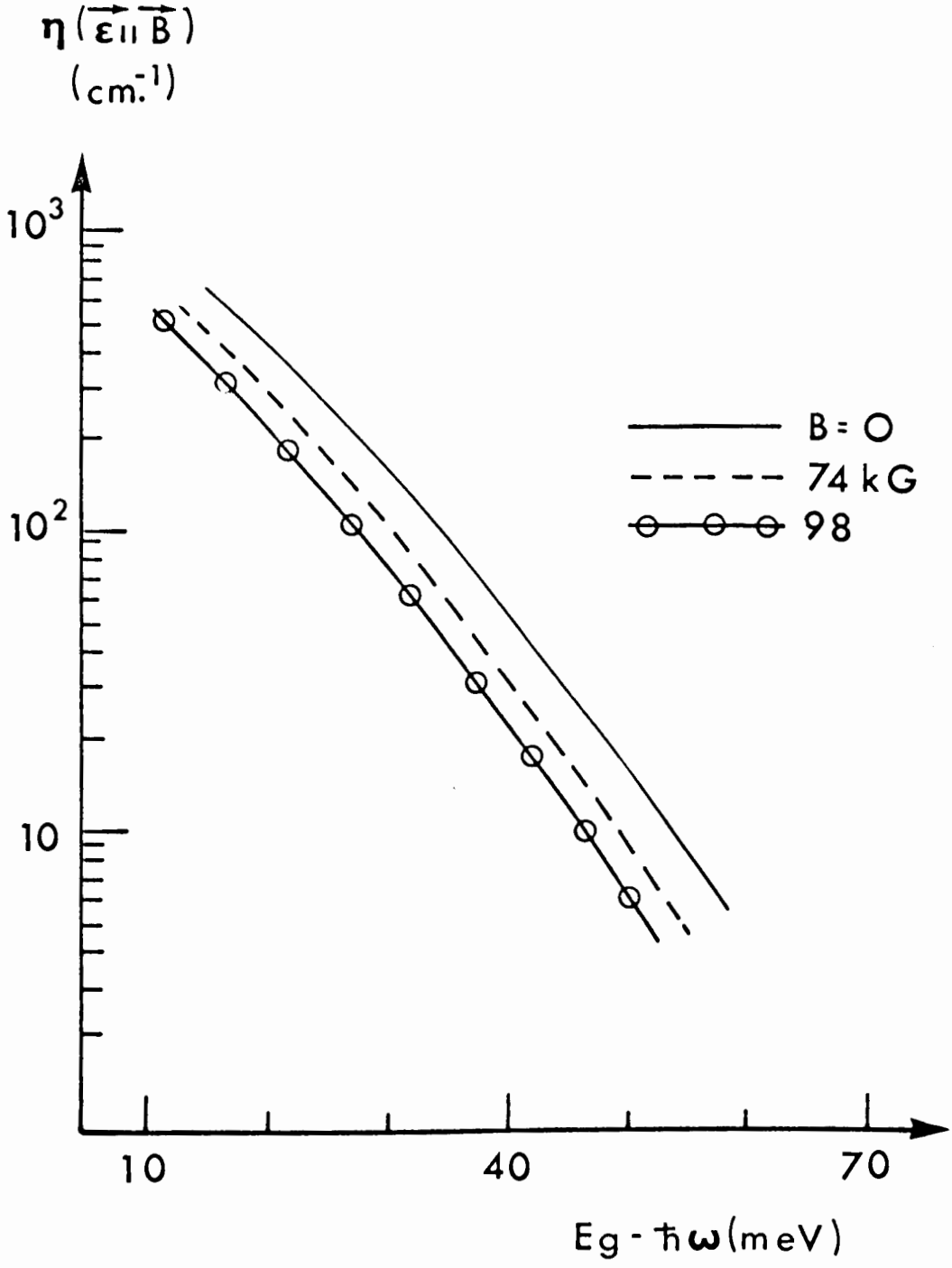

Figure 11. Experimentally determined absorption coefficient of germanium due to an electric field $\mathcal{E} = 2.8 \times 10^4$ V/cm. in the presence of a parallel magnetic field B, as a function of photon energy below the direct gap. (Reine et al.(47))

CHAPTER 9

OPTICAL ABSORPTION BELOW THE BAND GAP IN DIRECT-BAND SEMICONDUCTORS

9.1 Urbach's Law

Until now we were concerned with the absorption of light of frequency ω greater than that corresponding to the direct band gap frequency and our theory predicted vanishing absorption below that frequency in all situations, except in the presence of an electric field which tends to smear the otherwise sharp absorption edge. However, the experimental study of the optical absorption spectra has revealed that nearly all direct gap semiconductors have finite absorption coefficient for photons with energies below that corresponding to the energy gap, even when no external electric field is present. Further in most polar semiconductors, the observed absorption tail for $\hbar\omega < E_g$ is temperature dependent and has the form

$$\eta \propto \exp\left\{\sigma_0\left(\frac{\hbar\omega - E_g}{kT}\right)\right\} \qquad (9\text{-}1)$$

where E_g is the energy gap, kT is the thermal energy, and σ_0 is a numerical parameter which depends on the material and on temperature. Equation (9-1) is known as Urbach's law[2] and has attracted considerable attention[8,9,50-55].

In strongly ionic crystals like alkali halides and II-VI compounds, it is well known that the Urbach tail is associated

with phonon-assisted optical transitions. Several attempts to explain this phenomenon in III-V semiconducting compounds have only resulted in partial success. Below we outline briefly some such attempts.

9.2 Some Attempts to Explain Urbach's Rule

The study of the absorption edge has turned out, perhaps rather surprisingly, to be quite complicated. This is because in the narrow energy range around absorption threshold, various processes like exciton absorption, impurity absorption, internal electric fields due to charged defects[51] and phonon-assisted transitions[6] can all play an important role. The exciton and impurity states usually give rise to a relatively sharp line spectrum, and thus cannot account for the observed exponential edge. The internal electric fields arising from charged defects can in fact smear the band edge and give rise to an exponentially decaying absorption coefficient into the forbidden gap. Thus the Urbach tail may be an internal analog of the Franz-Keldysh effect which was discussed earlier (Chapter 6, equation (6-5)).

In a recent experiment[56] on GaAs, the Urbach tail has been interpreted on the basis of internal electric fields. Although the results seem to be consistent with the hypothesis of internal electric fields, there are several inherent

difficulties with this proposed explanation. First of all, it is quite hard to see why one should expect a temperature dependent absorption coefficient. Secondly, for observing the Franz-Keldysh effect by applying external fields, one needs to apply fields $\sim 10^5$ V/cm. Now if the internal electric fields of such magnitude exist (as is postulated in the above explanation) and give rise to macroscopic effects, there is no reason why these electric fields should not modify the absorption spectrum above the edge. To our knowledge, no one has observed any effect of internal electric fields on optical absorption above the gap. Thus we don't believe that the "internal Franz-Keldysh" mechanism is the correct explanation for Urbach's law but there is no doubt that the internal electric fields due to charged defects will have some effect on the observed absorption edge.

A more commonly accepted mechanism is one involving phonon-assisted transitions. By a phonon-assisted transition we mean a second-order transition through a virtual intermediate state which involves scattering in momentum space by the absorption or emission of a phonon in addition to the usual absorption of an optical photon. In semiconductors like Ge and Si where the absolute extrema in conduction and valence bands are at widely separated points in the Brillouin zone, the phonon-assisted transitions are very well known[57]. In such semiconductors the absorption processes and the corresponding band gap are called "indirect" and absorption is forbidden unless assisted by the

simultaneous emission or absorption of one or more phonons of wave vector comparable to the difference between the wave vectors at the two band extrema.

We are interested in direct band gap semiconductors, where the extrema are at or very near the same point in the Brillouin zone e.g. InSb and InAs. The possible existence of phonon-assisted transitions in direct band semiconductors was first suggested by Dumke[6]. It was subsequently shown that absorption processes assisted by phonons of small or zero wave vector are in fact allowed for a direct gap.[58,59,60] InSb[7,61] and InAs[60] displayed absorption below the band gap which was consistent with the idea of phonon-assisted transitions in direct gap semiconductors.

It is now clear how one can use this concept to explain Urbach's law in direct gap semiconductors. If we consider only second order processes involving the absorption of a single (optical) phonon, the model predicts a threshold of absorption which is lower than the threshold for direct transitions by an amount equal to one phonon energy. Since the probability of absorbing a phonon depends upon temperature through Bose-Einstein factor, the optical absorption coefficient for phonon-assisted transitions is expected to be temperature dependent. The absorption coefficient for one phonon processes was calculated by Dumke[6] and we will discuss Dumke's result in

detail in the next chapter. Higher order phonon processes extend the threshold to even lower energies and it has been shown[8,9] that one indeed obtains an exponential edge if higher order phonon processes are included. We will have occasion to discuss this in Chapter 13.

Apart from the fact that phonon-assisted transitions can provide some insight towards an understanding of Urbach's law, there is some intrinsic interest in these studies. For example, we will see in Chapters 11, 12 that the study of phonon-assisted transitions in the presence of external static fields can give useful information about the effective masses. We will restrict ourselves to allowed phonon-assisted transitions in direct band semiconductors in the framework of effective mass approximation (E.M.A.)[11].

CHAPTER 10

PHONON-ASSISTED OPTICAL ABSORPTION IN DIRECT-BAND SEMICONDUCTORS

10.1 Model of the Phonon-Assisted Transition Process

It was pointed out in the last chapter that phonon-assisted transitions in direct-band semiconductors can shift the threshold for optical absorption to lower photon energies and thus modify the absorption edge. In this chapter we will compute the absorption coefficient for such transitions using second-order time dependent perturbation theory. Most results in this chapter are not new[6], however, we derive them from a somewhat different point of view, providing a useful introduction to the theory of phonon-assisted transitions. Also the physical and mathematical assumptions of this chapter will provide a basis for extending the theory to include external static fields.

Consider a direct-gap semiconductors whose valence-band maximum and conduction-band minimum are at the centre of the Brillouin zone ($\vec{k} = 0$). Below the threshold for direct transitions, the dominant electron transition will be a second-order process involving the absorption of a single optical phonon of energy $k\theta$ and the absorption spectrum may be calculated using second-order perturbation theory as was first done by Dumke[6]. Higher phonon processes make a negligible contribution in the energy range where second-order processes are allowed if the electron-phonon interaction is not too strong. This will be

shown quantitatively in Chapter 13.

The two types of second-order transitions which contribute to the above absorption are shown in Fig. 12. In case (a) an electron initially in a state i absorbs a photon of energy $\hbar\omega$, makes a virtual transition to an intermediate state j in the conduction band, and subsequently arrives in the final state f via the electron-phonon interaction. In case (b) an electron is optically excited from e to f followed by the transition of the electron at i to the hole at e. In either case, energy is conserved only in the overall process so that $E_f - E_i = \hbar\omega + k\theta$. The energy conservation principle need not be fulfilled in the intermediate state because of the uncertainty principle. The absorption therefore occurs via two groups of intermediate states lying near the bottom of the conduction and near the top of the valence band respectively. It is sufficient to consider only processes of type (a), the calculation for type (b) processes proceeds in exactly identical fashion and does not change the shape of the absorption spectrum in any important way. For example if the electron-phonon interaction in the two bands are different, type (b) processes would simply alter the scale. Thus we will only discuss processes of type (a)

The phonons of interest have small wave number and only phonons of small wave number having a significant energy are those associated with the optical modes. Furthermore in ionic

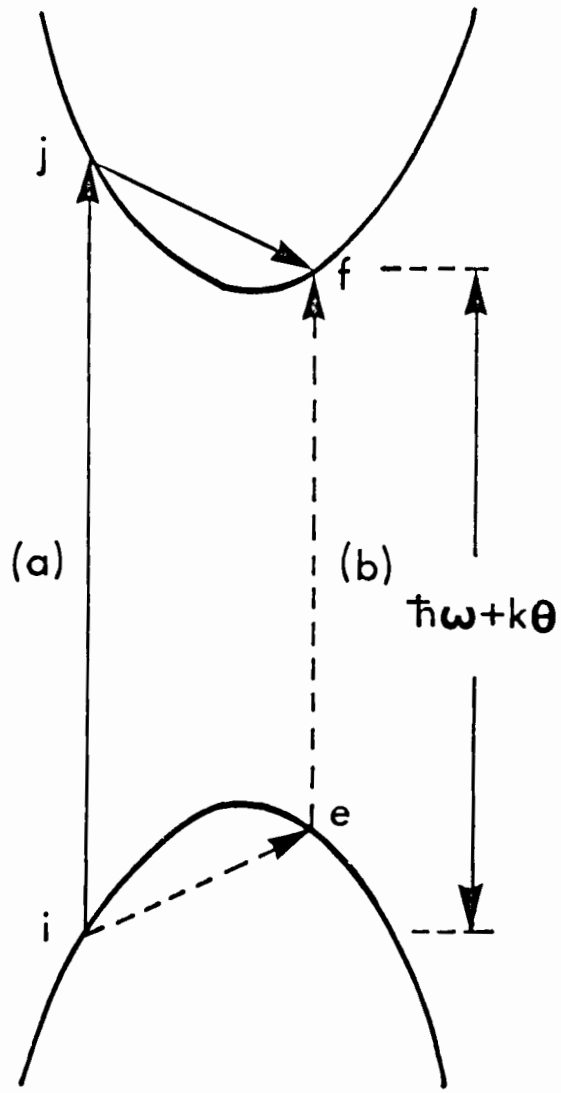

Figure 12. Energy diagram showing two different types of phonon-assisted optical transitions.

crystals in which we are interested the electrons interact strongly only with the longitudinal optical phonons. For the wavelengths of interest these phonons have essentially a constant energy $k\theta$. Although indirect transitions may occur which involve acoustic mode phonons, at long wavelengths these phonons have too little energy to take part in indirect transitions. The effect of higher bands can be neglected because uncertainty in energy is large for such virtual transitions.

10.2 Calculation of the Absorption Coefficient

In order to calculate the absorption coefficient we need to know the eigenvalues and eigenfunctions for electrons in conduction band and valence band. It was shown in Chapter 2 that the wave function for the electrons in the band α is given according to E.M.A.

$$\psi_{\alpha\mu}(\vec{r}) = u_{\alpha o}(\vec{r})\, F_{\alpha\mu}(\vec{r}) \quad , \quad \alpha = (c \text{ or } v) \qquad (10\text{-}1)$$

where $u_{\alpha o}(\vec{r})$ is the periodic part of the Bloch function of band α at $\vec{k} = 0$ and μ, the quantum number characterizing a state in band α. The wave function given by (10-1) is sufficient to calculate allowed transitions (see Chapter 3) in which we are interested. For the field free situation, the quantum number μ

is simply the propagation vector $\vec{k}$ and we have

$$F_{c\vec{k}'}(\vec{r}) = \frac{1}{\sqrt{V}} \exp(i\vec{k}''\cdot\vec{r})$$
$$F_{v\vec{k}}(\vec{r}) = \frac{1}{\sqrt{V}} \exp(i\vec{k}\cdot\vec{r}) \qquad (10\text{-}2)$$

For parabolic energy bands of opposite parity, the corresponding energy eigenvalues are

$$E_c(\vec{k}') = E_c^0 + \alpha_c \frac{\hbar^2 k'^2}{2m}$$
and $$E_v(\vec{k}) = E_v^0 - \alpha_v \frac{\hbar^2 k^2}{2m} \qquad (10\text{-}3)$$

where $E_c^0 - E_v^0 = E_g$ is the energy gap; m is the free electron mass and α_c, α_v are the ratios of m to the conduction and valence band effective masses respectively. The absorption coefficient for phonon-assisted transitions in second order perturbation theory is (see Chapter 1),

$$\eta_\theta(\omega) = \frac{4\pi n_0}{cN\hbar V} \sum_{\vec{k},\vec{k}''} |M_{cv}|^2 \, \delta(E_c(\vec{k}') - E_v(\vec{k}) - \hbar\omega \pm \hbar\omega_q) \qquad (10\text{-}4)$$

with

$$M_{cv} = \sum_{\vec{k}''} \frac{\langle c\vec{k}', f-1|H_2|f, c\vec{k}''\rangle\langle c\vec{k}'', N-1|H_1|N, v\vec{k}\rangle}{E_c(\vec{k}'') - E_v(\vec{k}) - \hbar\omega} \qquad (10\text{-}5)$$

where H_1 and H_2 are the Hamiltonians for the electron-photon and electron-phonon interactions respectively, N is the photon-number state and f is the phonon-number state. The matrix elements involving photon-interaction were worked out in detail in Chapter 3 where for allowed transitions we obtained (see equation (3-8))

$$\langle c\vec{k}'', N-1|H_1|N, v\vec{k}\rangle = -\frac{e}{m}\sqrt{\frac{2\pi\hbar N}{\omega n_o^2}}\left(\vec{p}_{cv}\cdot\hat{\xi}\right)\int_V F^*_{c\vec{k}''}\, F_{v\vec{k}}\; d\vec{r}$$

Substituting from (10-2) the expressions for the envelope functions and completing the integral we have

$$\langle c\vec{k}'', N-1|H_1|N, v\vec{k}\rangle = -\frac{e}{m}\sqrt{\frac{2\pi\hbar N}{\omega n_o^2}}\left(\vec{p}_{cv}\cdot\hat{\xi}\right)\delta_{\vec{k}'',\vec{k}} \qquad (10\text{-}6)$$

With the help of (10-5) and (10-6), the expression for the absorption coefficient becomes

$$\eta_\theta(\omega) = \frac{2(2\pi)^2 e^2}{c m^2 \omega n_o V}\left|\left(\vec{p}_{cv}\cdot\hat{\xi}\right)\right|^2 \times \sum_{\vec{k},\vec{k}'}\left|H_{\vec{k}'\vec{k}}\right|^2 \frac{\delta\left(E_g+\epsilon_v(\vec{k})+\epsilon_c(\vec{k}')-\hbar\omega-k\theta\right)}{\left[E_g+\left(1+\frac{\alpha_c}{\alpha_v}\right)\epsilon_v(\vec{k})-\hbar\omega\right]^2} \qquad (10\text{-}7)$$

where

$$\epsilon_v(\vec{k}) = \alpha_v \frac{\hbar^2 k^2}{2m_v}$$

and (10-8)

$$\epsilon_c(\vec{k}') = \alpha_c \frac{\hbar^2 k'^2}{2m_c}$$

and $H_{\vec{k}',\vec{k}}$ is the electron-phonon interaction matrix element. In evaluating equation (10-7), it is necessary to know the form of the electron-phonon interaction. Two cases may be distinguished: (a) optical phonon scattering in nonpolar materials or scattering by transverse phonons in polar materials, and (b) scattering by longitudingal optical phonons in ionic materials. In case (a), the electron-phonon matrix element is essentially independent of $\vec{k}$ and $\vec{k}'$ and we may put

$$\left|H_{\vec{k}'\vec{k}}\right|^2 = \frac{1}{V} |\beta|^2 \left[e^{\Theta/T} - 1\right]^{-1} \qquad (10\text{-}9)$$

In case (b), the magnitude of the electron-phonon interaction depends strongly on the phonon wave vector, $\vec{q}$, and diverges for $\vec{q} \to 0$. If electron screening effects are included, the matrix element again approaches a constant value for $\vec{q}$ wave vectors smaller than the reciprocal of the screening length. Throughout this presentation we shall assume the form of $H_{\vec{k}',\vec{k}}$ given by equation (10-9). Dumke[6] has shown that this assumption is in excellent agreement with the experiments on weakly ionic materials such as InSb. Further the summations over $\vec{k}$ and $\vec{k}'$ in equation

(10-7) can be replaced by integrations through the density of state factors, namely

$$\sum_{\vec{k}} \longrightarrow \frac{V}{4\pi^2}\left(\frac{2m}{\alpha_v \hbar^2}\right)^{3/2} \int_0^\infty \epsilon_v^{1/2}(\vec{k}')\, d\epsilon_v(\vec{k}') \qquad (10\text{-}10)$$

and similarly for the conduction band

$$\sum_{\vec{k}'} \longrightarrow \frac{V}{4\pi^2}\left(\frac{2m}{\alpha_c \hbar^2}\right)^{3/2} \int_0^\infty \epsilon_c^{1/2}(\vec{k}')\, d\epsilon_c(\vec{k}') \qquad (10\text{-}11)$$

Substituting (10-9), (10-10) and (10-11) in (10-7) we get

$$\eta_\theta(\omega) = \frac{A}{(e^{\theta/T}-1)}\left(\frac{1}{\pi}\right)\int_0^\infty \epsilon_c^{1/2}(\vec{k}')\, d\epsilon_c(\vec{k}') \times \int_0^\infty \frac{\epsilon_v^{1/2}(\vec{k})\,\delta\left(E_g+\epsilon_c(\vec{k}')+\epsilon_v(\vec{k})-\hbar\omega-k\theta\right)}{\left[\epsilon_v(\vec{k})+\frac{E_g-\hbar\omega}{r}\right]^2}\, d\epsilon_v(\vec{k}) \qquad (10\text{-}12)$$

where

$$A = \left(\frac{4}{\pi}\right)\frac{e^2 m |\beta|^2 |(\vec{p}_{cv}\cdot\vec{\xi})|^2}{c\hbar^5 n_o E_g (\alpha_c\alpha_v)^{1/2} r^2} \qquad (10\text{-}13)$$

and

$$r = 1 + \frac{\alpha_c}{\alpha_v}$$

In the expression for A, we took $\omega \simeq E_g/\hbar$. The average scattering probability is proportional to the number of phonons in each vibrational mode through the Bose-Einstein factor $(e^{\theta/T} - 1)^{-1}$. Introducing

$$\hbar\omega + k\theta - E_g \equiv \Delta \,, \qquad \frac{E_g - \hbar\omega}{r} \equiv d > 0 \tag{10-14}$$

and carrying out the integration over $\epsilon_v(\vec{k})$ with the help of the delta function in (10-12), we find

$$\eta_\theta^{(o)} = \frac{A}{(e^{\theta/T} - 1)} \left(\frac{1}{\pi}\right) \int_0^\Delta dx \, \frac{[x\Delta - x^2]^{1/2}}{[x + d]^2}$$

Notice that this integral vanishes if $\Delta = 0$. For positive non-vanishing values of Δ and d, the integral can be readily completed to obtain

$$\eta_\theta^{(o)} = \frac{A}{(e^{\theta/T} - 1)} \left[\frac{1}{2} \frac{2d + \Delta}{\sqrt{[d(d+\Delta)]}} - 1\right] \text{ for } \Delta > 0$$
$$= 0 \qquad \text{for } \Delta \leq 0 \tag{10-15}$$

Thus there is no absorption until $\hbar\omega + k\theta > E_g$. The absorption coefficient is zero at $\hbar\omega + k\theta = E_g$ because the joint density of

states in the valence and conduction bands vanishes at the edges of three-dimensional energy bands. Since 'd' is a positive quantity for phonon-assisted transitions under consideration, the magnitude of the absorption coefficient for $\Delta > 0$ is always real.

We have plotted the absorption coefficient (10-15) as a function of the incident photon energy. Two cases involving different ratios of conduction to valence band masses are considered, namely $\alpha_c/\alpha_v = 1$ and $\alpha_c/\alpha_v = 2$ (Fig. 13). The absorption coefficient starts out with the value zero at $\hbar\omega = E_g - k\theta$ and increases smoothly as $\hbar\omega$ is varied in the range $E_g - k\theta < \hbar\omega < E_g$. If higher order processes were included the cut-off would shift to lower photon energies and some absorption would persist for $\hbar\omega \leq E_g - k\theta$. The infrared absorption data on InSb[7] has been analysed by Dumke[6] with the help of the above theory. The agreement is found to be quantitative if in our theoretical expression (10-15) we choose $\theta = 290°$ K and $\alpha_c/\alpha_v = 5$. Experimentally the magnitude of the indirect absorption in InSb closely follows an $(e^{\theta/T} - 1)^{-1}$ law, reflecting its dependence on the number of optical phonons.

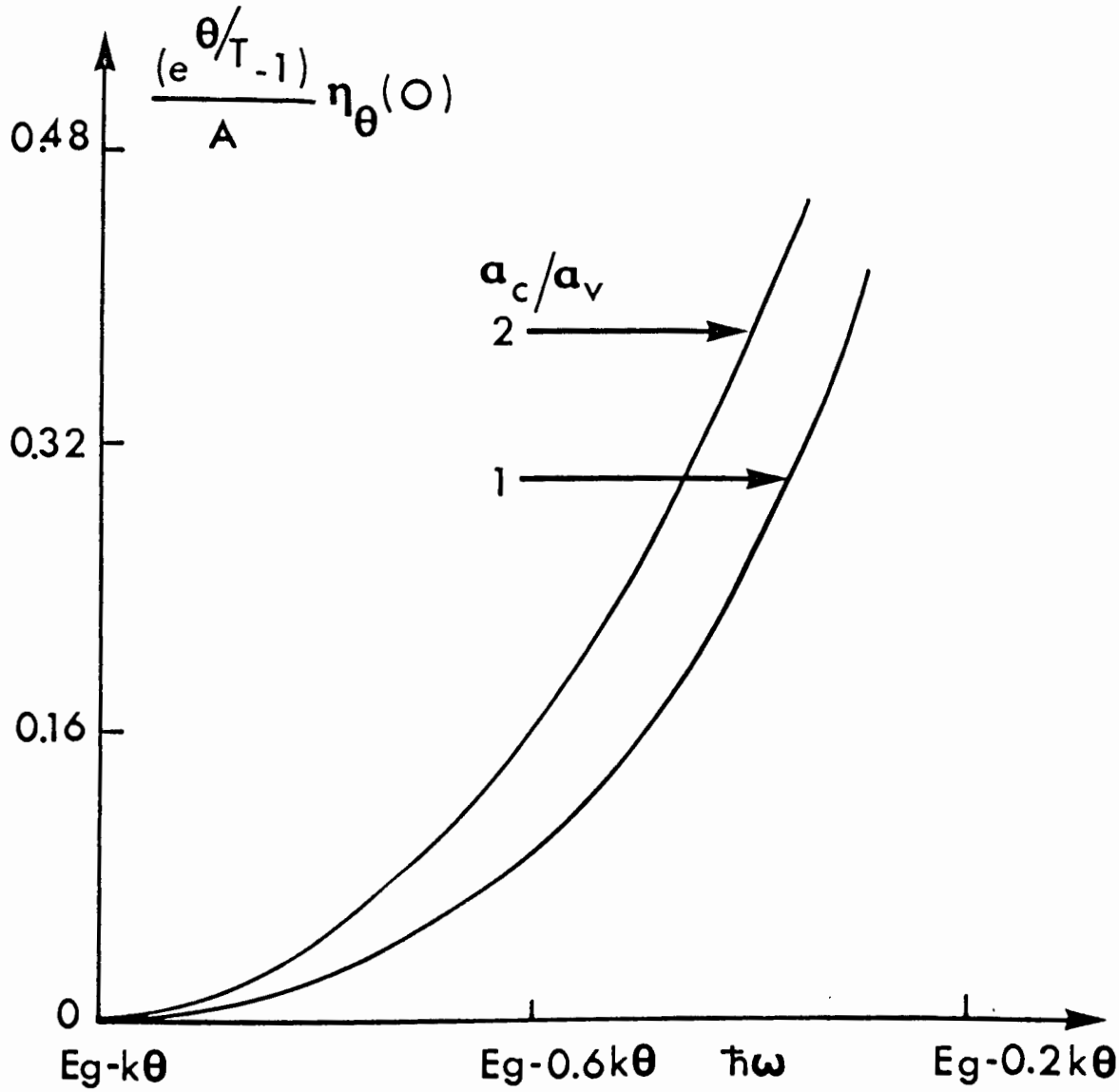

Figure 13. Phonon-assisted absorption spectrum as a function of photon energy for two different values of α_c/α_v.

CHAPTER 11

PHONON-ASSISTED MAGNETOABSORPTION IN DIRECT BAND SEMICONDUCTORS

11.1 Calculation of the Magnetoabsorption Coefficient

In this chapter we extend the calculations of the previous chapter to study the effect of the magnetic field on phonon-assisted transitions. Once again we consider a semiconductor whose valence and conduction bands are 'simple', i.e. the bands are nondegenerate, have their extrema at $\vec{k} = 0$, and the dependence of energy on crystal momentum, $\hbar\vec{k}$, is spherically symmetric and quadratic. In the framework of effective mass approximation (E.M.A.), the wave function for the electrons in band α is (see Chapter 2)

$$\psi_{\alpha\mu}(\vec{r}) = u_{\alpha 0}(\vec{r})\, F_{\alpha\mu}(\vec{r}) \tag{11-1}$$

If the magnetic field is directed parallel to the Z-axis, then μ stands for a set of quantum numbers (n, k_y, k_z) and we have from equation (2-39)

$$\begin{aligned} F_{c\mu'}(\vec{r}) &= \frac{1}{\sqrt{L_y L_z}}\, \exp i\left(k'_y y + k'_z z\right)\, \Phi_{n'}\left(x - \lambda^2 k'_y\right), \\ F_{v\mu}(\vec{r}) &= \frac{1}{\sqrt{L_y L_z}}\, \exp i\left(k_y y + k_z z\right)\, \Phi_{n}\left(x - \lambda^2 k_y\right) \end{aligned} \tag{11-2}$$

where n, the Landau magnetic quantum number, is a positive

integer or zero and $\lambda = \sqrt{\frac{c\hbar}{eB}}$ is the magnetic length.

The energy levels of the charge carriers are given by (see equation (2-40))

$$E_c(n', k_z) = E_c^0 + \alpha_c\left(n' + \tfrac{1}{2}\right)\hbar\omega_c + \frac{\hbar^2 k_z^2}{2m_c}$$
$$E_v(n, k_z) = E_v^0 - \alpha_v\left(n + \tfrac{1}{2}\right)\hbar\omega_c - \frac{\hbar^2 k_z^2}{2m_v} \qquad (11\text{-}3)$$

We notice that the energies of the carriers are quantized in the plane perpendicular to the magnetic field but remain quasi-continuous in the direction of the field, thus forming a series of 'one-dimensional sub-bands' (Fig. 1) Chapter 5. The minimum of the lowest sub-band of the conduction band occurs at an energy $\frac{1}{2}\alpha_c\hbar\omega_c$ above the energy band minimum in zero field and the maximum of the highest sub-band in the valence band occurs at an energy $\frac{1}{2}\alpha_v\hbar\omega_c$ below the valence band maximum in zero field, thus increasing the band gap by $\frac{1}{2}(\alpha_c + \alpha_v)\hbar\omega_c \equiv \frac{1}{2}\hbar\omega_c^*$ (Fig. 1).

The Landau levels are highly degenerate with respect to the choice of the 'orbit centre', $x_o = \lambda^2 k_y$. (The degenerate states differ from one another in the value of the third quantum number k_y, not appearing in the energy expressions). This degeneracy can be estimated[25] by considering the system to be

contained in a box of sides L_x, L_y, L_z. The number of possible values of k_y in a small interval Δk_y is

$$L_y \frac{\Delta k_y}{2\pi} \tag{11-4}$$

The maximum value of k_y is determined by the requirement that x_o, the orbit centre lies inside the box i.e.

$$-\frac{L_x}{2} \leq x_o \leq \frac{L_x}{2}$$

So, substituting for x_o, we get

$$-\frac{L_x}{2\lambda^2} \leq k_y \leq \frac{L_x}{2\lambda^2}$$

The number of states in a single Landau level is then using (11-4)

$$L_y \frac{\Delta k_y}{2\pi} = \frac{L_x L_y}{2\pi\lambda^2} \tag{11-5}$$

One frequently encounters statements in the literature that the degeneracy per unit area of the sample transverse to the magnetic field is given by $\frac{1}{2\pi\lambda^2}$. The meaning of this statement is quite transparent from equation (11-5).

Possessing the wave functions and the energy eigenvalues, the magnetoabsorption coefficient for phonon-assisted transitions can be computed in a standard fashion (see Chapter 1)

$$\eta_{\theta}(B) = \frac{4\pi n_0}{cNnV} \sum_{\mu,\mu'} |M_{cv}|^2 \, \delta\left(E_c(n',k_z') - E_v(n,k_z) - \hbar\omega - k\theta\right) \quad (11\text{-}6)$$

where

$$M_{cv} = \sum_{n''} \frac{\langle c\mu', f-1|H_2|f, c\mu''\rangle \langle c\mu'', N-1|H_1|N, v\mu\rangle}{E_c(n'', k_z'') - E_v(n,k_z) - \hbar\omega} \quad (11\text{-}7)$$

In Chapter 3 equation (3-8) it was found that for allowed transitions the matrix element is given by

$$\langle c\mu'', N-1|H_1|N, v\mu\rangle = -\frac{e}{m}\sqrt{\frac{2\pi\hbar N}{\omega n_0}}\left(\vec{p}_{cv}\cdot\hat{\epsilon}\right) I_{\mu''\mu}$$

and the overlap integral for the present case from (11-2) is

$$I_{\mu''\mu} = \frac{1}{L_y}\int_{-L_y/2}^{L_y/2} dy \; e^{i(k_y - k_y'')y} \times \frac{1}{L_z}\int_{-L_z/2}^{L_z/2} dz \; e^{i(k_z - k_z'')z}$$
$$\times \int_{-\infty}^{\infty} dx \; \Phi_{n''}(x - \lambda^2 k_y'') \, \Phi_n(x - \lambda^2 k_y)$$
$$= \delta_{k_y'', k_y} \, \delta_{k_z'', k_z} \, \delta_{n'', n}$$

Notice that the electron-photon interaction does not change the magnetic quantum number n. Substituting this value for the overlap integral above, we obtain

$$\langle c\mu'', N-1 \,|\, H_1 \,|\, N, v\mu \rangle = -\frac{e}{m}\sqrt{\frac{2\pi\hbar N}{\omega n_0^2}}\,(\vec{p}_{cv}\cdot\hat{\xi})\,\delta_{\mu'',\mu} \qquad (11\text{-}8)$$

The delta function in (11-8) enables us to complete the summation over intermediate states in (11-7) and the expression for the absorption becomes

$$\eta_\theta(B) = \frac{2(2\pi)^2 e^2 |(\vec{p}_{cv}\cdot\hat{\xi})|^2}{c m^2 n_0 \omega V} \times \sum_{\mu,\mu'} |H_{\mu'\mu}|^2 \frac{\delta\left(E_g(B) + \epsilon_v(n,k_z) + \epsilon_c(n',k_z') - \hbar\omega - k\theta\right)}{\left[E_g(B) + \left(1+\frac{\alpha_c}{\alpha_v}\right)\epsilon_v(n,k_z) - \hbar\omega\right]^2} \qquad (11\text{-}9)$$

where

$$E_g(B) = E_g + \frac{1}{2}(\alpha_c + \alpha_v)\hbar\omega_c \qquad (11\text{-}10)$$

and

$$\epsilon_v(n,k_z) = \alpha_v\left\{\frac{\hbar^2 k_z^2}{2m} + n\hbar\omega_c\right\},$$
$$\epsilon_c(n',k_z') = \alpha_c\left\{\frac{\hbar^2 k_z'^2}{2m} + n'\hbar\omega_c\right\} \qquad (11\text{-}11)$$

Following the discussion in the last chapter, we approximate the electron-phonon interaction by a constant namely

$$|H_{\mu'\mu}|^2 = \frac{1}{V} |\beta|^2 \left[e^{\beta/1} - 1 \right]^{-1} \qquad (11\text{-}12)$$

To carry out the summations over k_y, k_y', k_z, k_z' in equation (11-9) it is convenient to convert them into integrations through the density of state factors. While calculating the density of states, the degeneracy (11-5) of each state is taken into account and we have

$$\sum_{k_y, k_z}' \longrightarrow \frac{V}{4\pi^2} \left(\frac{2m}{\alpha_v \hbar^2} \right)^{3/2} \frac{(\alpha_v \hbar \omega_c)}{2} \times \int_0^\infty \frac{d\epsilon_v(n, k_z)}{\left[\epsilon_v(n, k_z) - n \alpha_v \hbar \omega_c \right]^{1/2}} \qquad (11\text{-}13)$$

and

$$\sum_{k_y', k_z'} \longrightarrow \frac{V}{4\pi^2} \left(\frac{2m}{\alpha_c \hbar^2} \right)^{3/2} \frac{(\alpha_c \hbar \omega_c)}{2} \times \int_0^\infty \frac{d\epsilon_c(n', k_z')}{\left[\epsilon_c(n', k_z') - n' \alpha_c \hbar \omega_c \right]^{1/2}} \qquad (11\text{-}14)$$

Substituting (11-12), (11-13) and (11-14) in (11-9) we get

$$\eta_\theta(B) = \frac{A}{(e^{\theta/T}-1)} \frac{(\alpha_c' \alpha_v')}{4\pi} \times \sum_{n,n'} \left[\int_0^\infty \frac{d\epsilon_v(n,k_z)}{\{\epsilon_v(n,k_z)+\Delta(B)\}^2 \{\epsilon_v(n,k_z)-a_n\}^{1/2}} \times \int_0^\infty \frac{d\epsilon_c(n',k_z') \, \delta(\epsilon_v(n,k_z)+\epsilon_c(n',k_z')-\Delta(\omega))}{\{\epsilon_c(n',k_z')-a_{n'}\}^{1/2}} \right] \quad (11\text{-}15)$$

where A and r are as defined in (10-13),

$$\begin{aligned} \hbar\omega + k\theta - E_g(B) &= \Delta(\omega), \\ \frac{E_g(B)-\hbar\omega}{r} &= \Delta(B) > 0, \\ \alpha_c \hbar\omega_c &= \alpha_c', \quad \alpha_v \hbar\omega_v = \alpha_v', \\ n'\alpha_c' &= a_{n'}, \quad n\alpha_v' = a_n, \end{aligned} \quad (11\text{-}16)$$

and carrying out the integration over ϵ_c (for fixed n,n') with the help of the delta function, we obtain

$$\eta_\theta(B) = \frac{A}{(e^{\theta/T}-1)} \frac{(\alpha_c' \alpha_v')}{4\pi} \times \sum_{n,n'} \int_{a_v}^{\Delta(B)-a_{n'}} \frac{d\epsilon_v(n,k_z)}{[\epsilon_v(n,k_z)+\Delta(B)]^2 [\epsilon_v(n,k_z)-a_n]^{1/2} [\Delta(B)-a_{n'}-\epsilon_v(n,k_z)]^{1/2}}$$

The above integral vanishes if $\Delta(B) = a_n + a_{n'}$. For $\Delta(B) > a_n + a_{n'}$, The integral can be evaluated by standard methods and the final expression for the absorption coefficient is given by

$$\eta_\theta(B) = \frac{A}{(e^{\theta/T} - 1)} \frac{(\alpha_c' \alpha_v')}{8} \times \sum_{n,n'} \left[\frac{2d(B) + \Delta(B) + a_n - a_{n'}}{\left\{ \left(d(B) + a_n \right) \left(d(B) + \Delta(B) - a_{n'} \right) \right\}^{3/2}} \right] \tag{11-17}$$

with the restriction $a_n + a_{n'} < \Delta(B)$. This restriction implies that there is no absorption until

$$\hbar\omega + k\theta > E_g(B)$$

Thus $E_g(B)$ can be interpreted as the effective energy gap in the presence of a magnetic field. The summation is over all non-negative integers n, n' consistent with the above restriction and the usual magnetoabsorption selection rule $\Delta n = 0$ is not obeyed. Thus we would expect the phonon-assisted magnetoabsorption spectrum to display the structure of the valence and conduction bands separately. The result (11-17) was first reported by Batra and Haering[63], the details of the calculations and other implications have since then been published[10].

11.2 The Zero Field Limit

In the limit of zero magnetic field the summations over n, n' in equation (11-17) can be replaced by integrations through the conversions

$$\alpha_c' \sum_{n'} \longrightarrow \int dy \quad , \quad a_{n'} \longrightarrow y$$

and

$$\alpha_v' \sum_{n} \longrightarrow \int dx \quad , \quad a_n \longrightarrow x$$

where x and y are restricted by the condition $x + y < \Delta$ and we have

$$\gamma_\theta(0) = \frac{A}{(e^{\theta/T}-1)} \left(\frac{1}{8}\right) \int_0^\Delta dy \int_0^{\Delta-y} dx \, \frac{2(d+\Delta+x-y)}{[(d+x)(d+\Delta-y)]^{3/2}}$$

$$= \frac{A}{(e^{\theta/T}-1)} \left(\frac{1}{8}\right) \left[\int_0^\Delta \frac{dy}{(d+\Delta-y)^{3/2}} \int_0^{\Delta-y} \frac{dx}{(d+x)^{1/2}} \right.$$

$$\left. + \int_0^\Delta \frac{dy}{(d+\Delta-y)^{1/2}} \int_0^{\Delta-y} \frac{dx}{(d+x)^{3/2}} \right]$$

The integrals involved are elementary and the final expression can be immediately written down

$$\eta_\theta(0) = \frac{A}{(e^{\theta/T} - 1)} \left[\frac{1}{2} \frac{2\lambda + \Delta}{\sqrt{\lambda(\lambda + \Delta)}} - 1 \right], \quad \Delta > 0 \qquad (11\text{-}18)$$

This limiting result agrees with the result obtained in the last chapter (see equation (10-15)).

11.3 Results and Discussion

We have numerically plotted the absorption coefficient for nonzero and zero values of the magnetic field, using equations (11-17) and (11-18) respectively. Three cases involving different ratios of conduction to valence band masses are considered, namely $\alpha_c/\alpha_v = 1$ (Fig. 14), $\alpha_c/\alpha_v = 2$ (Fig. 16), and $\alpha_v = 0$ (Fig. 18). For all these cases the zero magnetic field absorption coefficient $\eta_\theta(0)$ starts out with the value zero at $\hbar\omega = E_g - k\theta$ and increases smoothly as $\hbar\omega$ is varied in the range $E_g - k\theta < \hbar\omega < E_g$.

In the presence of the magnetic field, the energy gap of the material increases (equation (11-10)) and the absorption remains zero so long as $\hbar\omega \leq E_g(B) - k\theta$. At $\hbar\omega$ slightly greater than $E_g(B) - k\theta$, $\eta_\theta(B)$ suddenly rises to a value higher than the

corresponding value of $\eta_\theta(0)$ at that point. As $\hbar\omega$ is varied in the range $E_g(B) - k\theta < \hbar\omega < E_g(B)$, photons can be absorbed by carriers in low-lying Landau levels in the valence band and can be promoted to Landau levels situated at higher energies in the conduction band. Whenever an additional Landau level of the conduction band or valence band is permitted by energy conservation to take part in the absorption process, $\eta_\theta(B)$ jumps discontinuously from a value below $\eta_\theta(0)$ to a value above $\eta_\theta(0)$. Usually $\alpha'_{c,v}$ $(= \alpha_{c,v}\ \hbar\omega_c)$ is of the order 0.1 $k\theta$ or 0.2 $k\theta$ and one would see several steps in the range $E_g(B) - k\theta < \hbar\omega < E_g(B)$. (In fact we will show that the necessary condition to see phonon-assisted magnetoabsorption is that $\alpha_{c,v}\hbar\omega_c < k\theta$.) We have also plotted the difference $[\eta_\theta(B) - \eta_\theta(0)] \equiv \Delta\eta_\theta(B)$ for the three cases discussed above (Figs. 15, 17, and 19).

It is to be noted that the absorption curves in Figs. 14 - 19 display the Landau level spectrum of the valence and conduction bands separately. This is in contradistinction to normal direct interband absorption, which only involves the reduced mass for the two bands because of the selection rule $\Delta n = 0$. Thus if we extend the usual magneto-optics experiments to the region below the direct gap, the conduction band and valence band masses can be determined individually. In the next section we suggest the experimental conditions for studying the phonon-assisted magnetoabsorption.

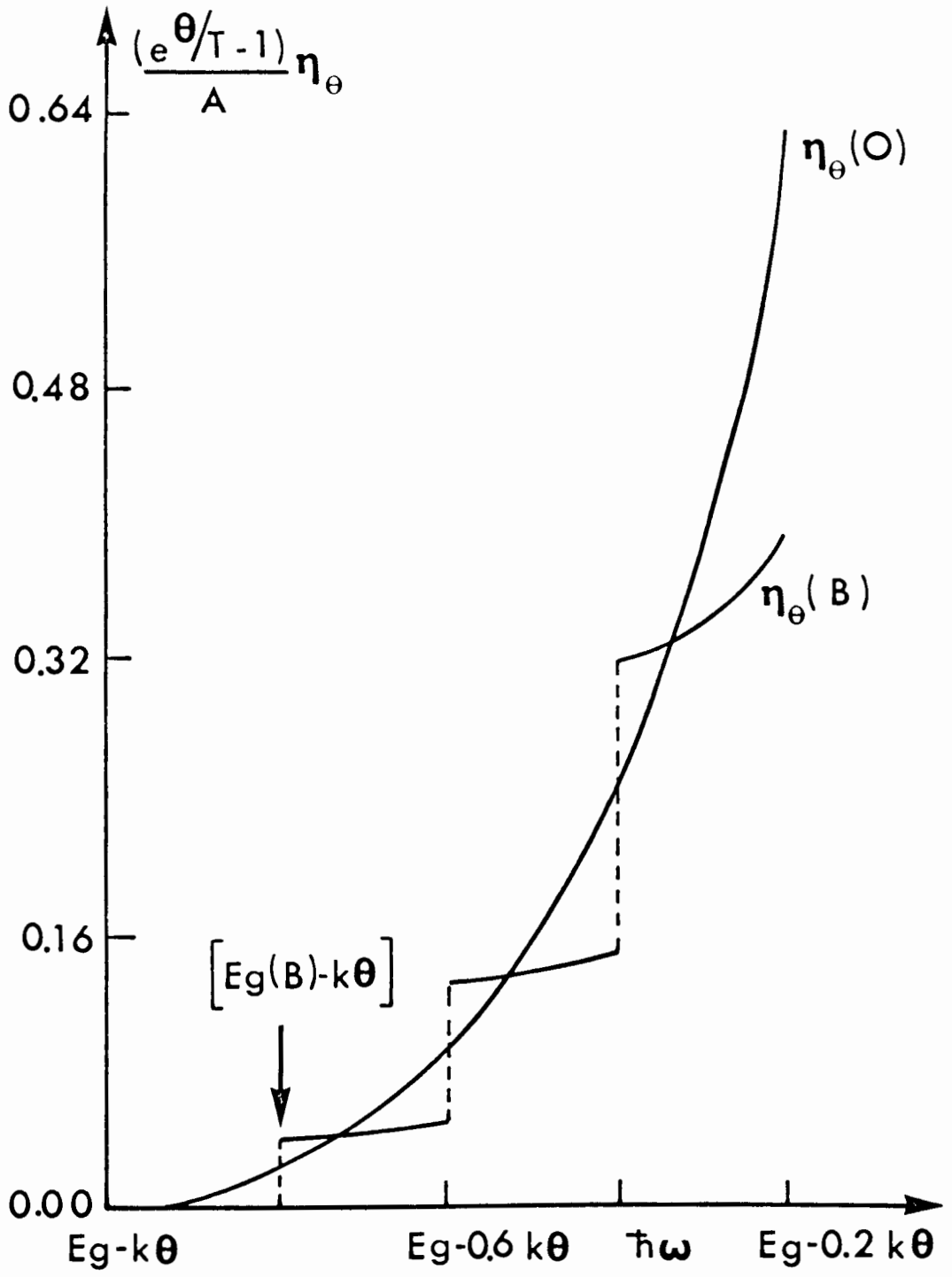

Figure 14. Interband absorption spectrum for B = 0 and B ≠ 0 as a function of photon energy for the case $\alpha_c/\alpha_v = 1$ and $E_g(B) = E_g + 0.2\ k\theta$.

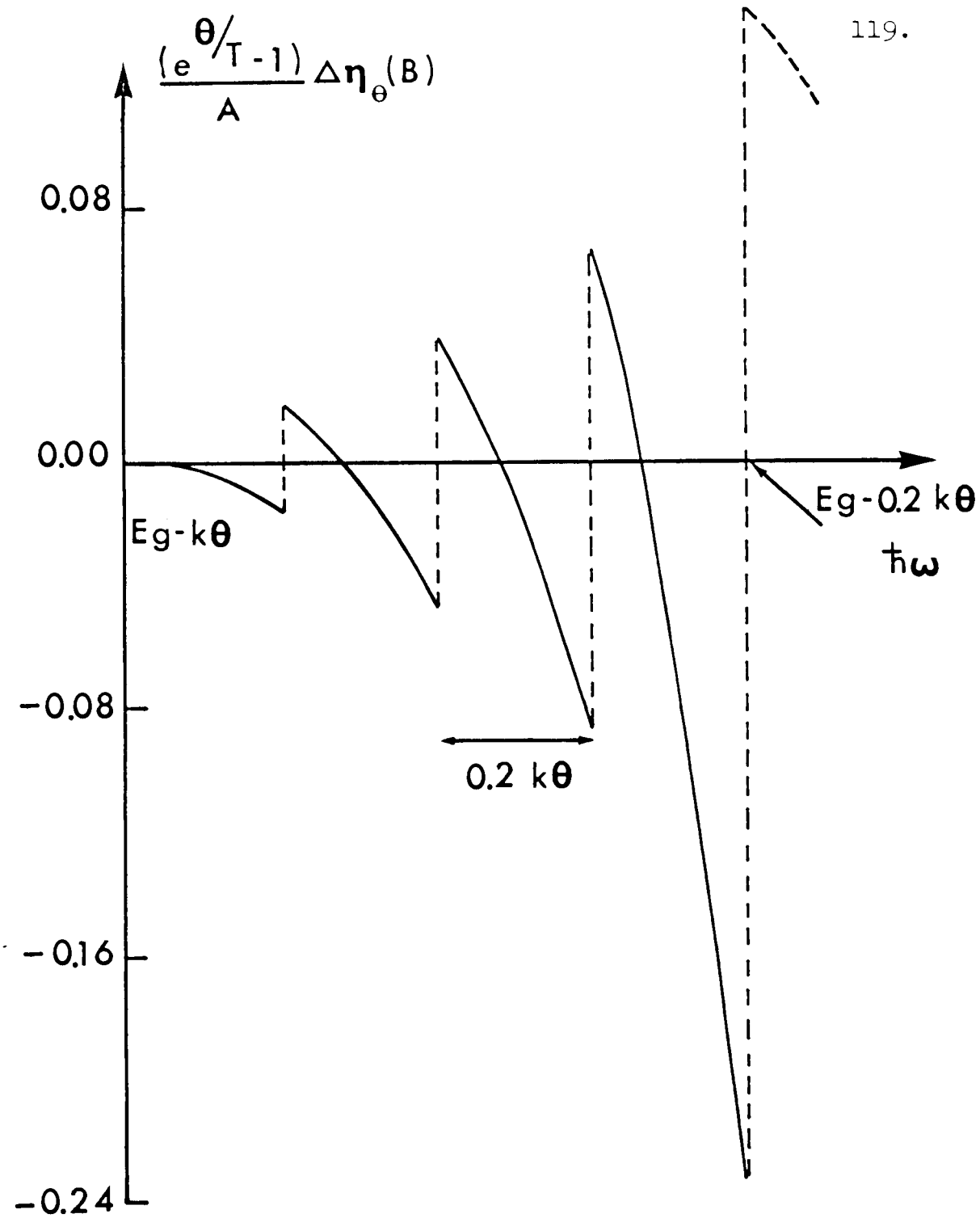

Figure 15. Difference of absorption coefficients $[\eta_\theta(B) - \eta_\theta(0)] \equiv \Delta\eta_\theta(B)$ as a function of photon energy for the case $\alpha_c/\alpha_v = 1$.

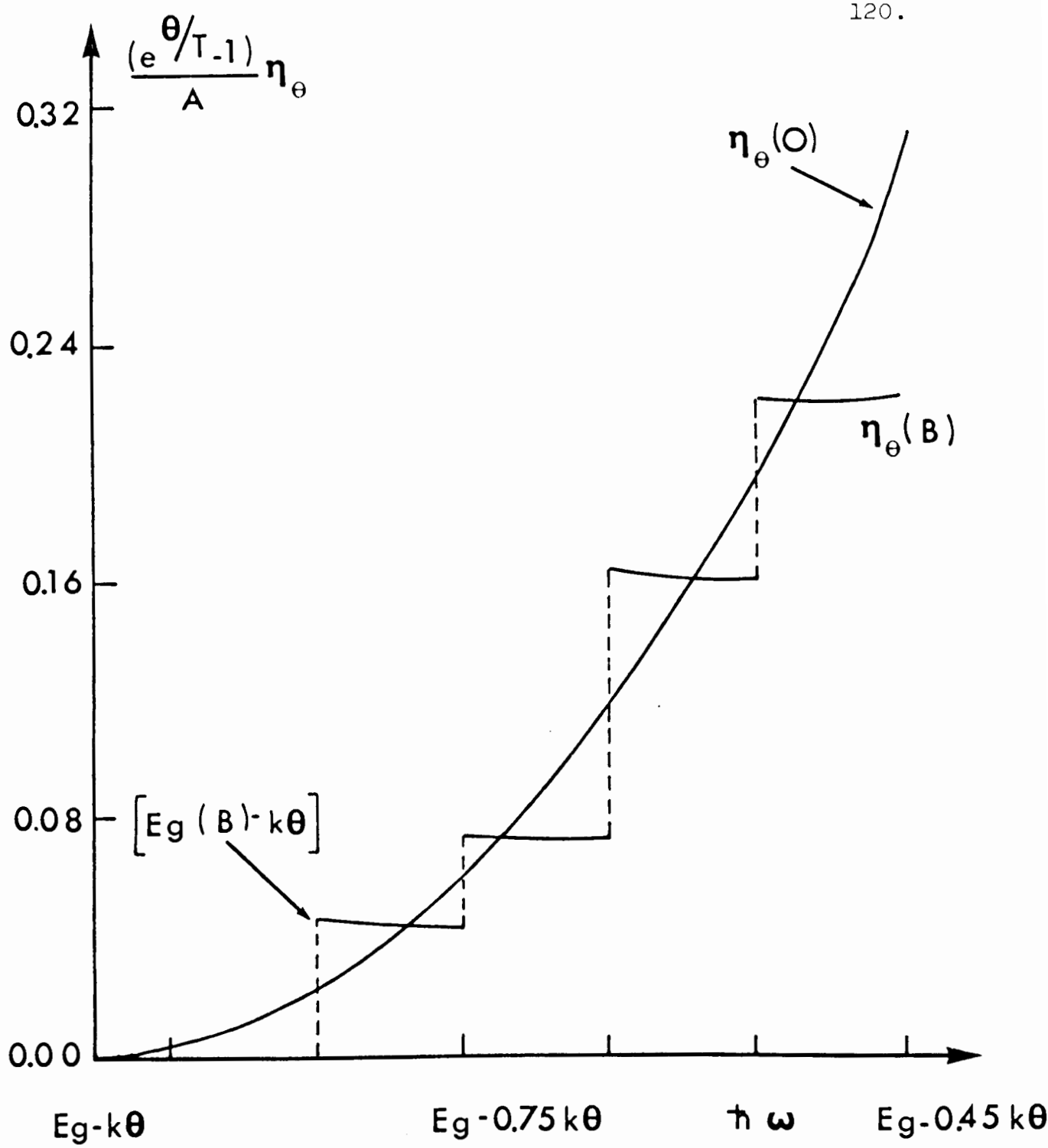

Figure 16. Interband absorption spectrum for B = 0 and B ≠ 0 as a function of photon energy for the case $\alpha_c/\alpha_v = 2$ and $E_g(B) = E_g + 0.15\ k\theta$.

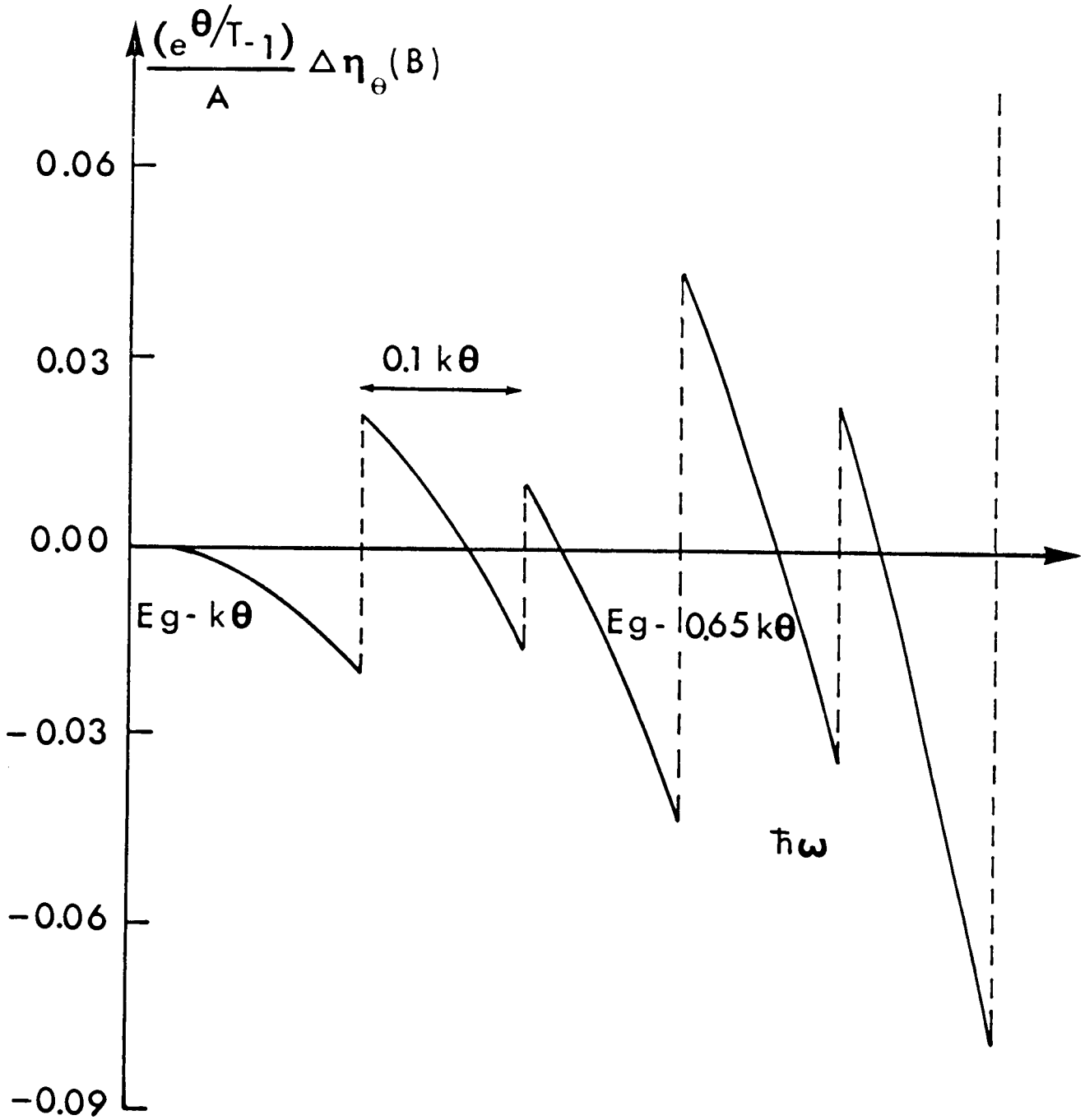

Figure 17. Difference of absorption coefficients $[\eta_\theta(B) - \eta_\theta(0)] \equiv \Delta\eta_\theta(B)$ as a function of photon energy for the case $\alpha_c/\alpha_v = 2$.

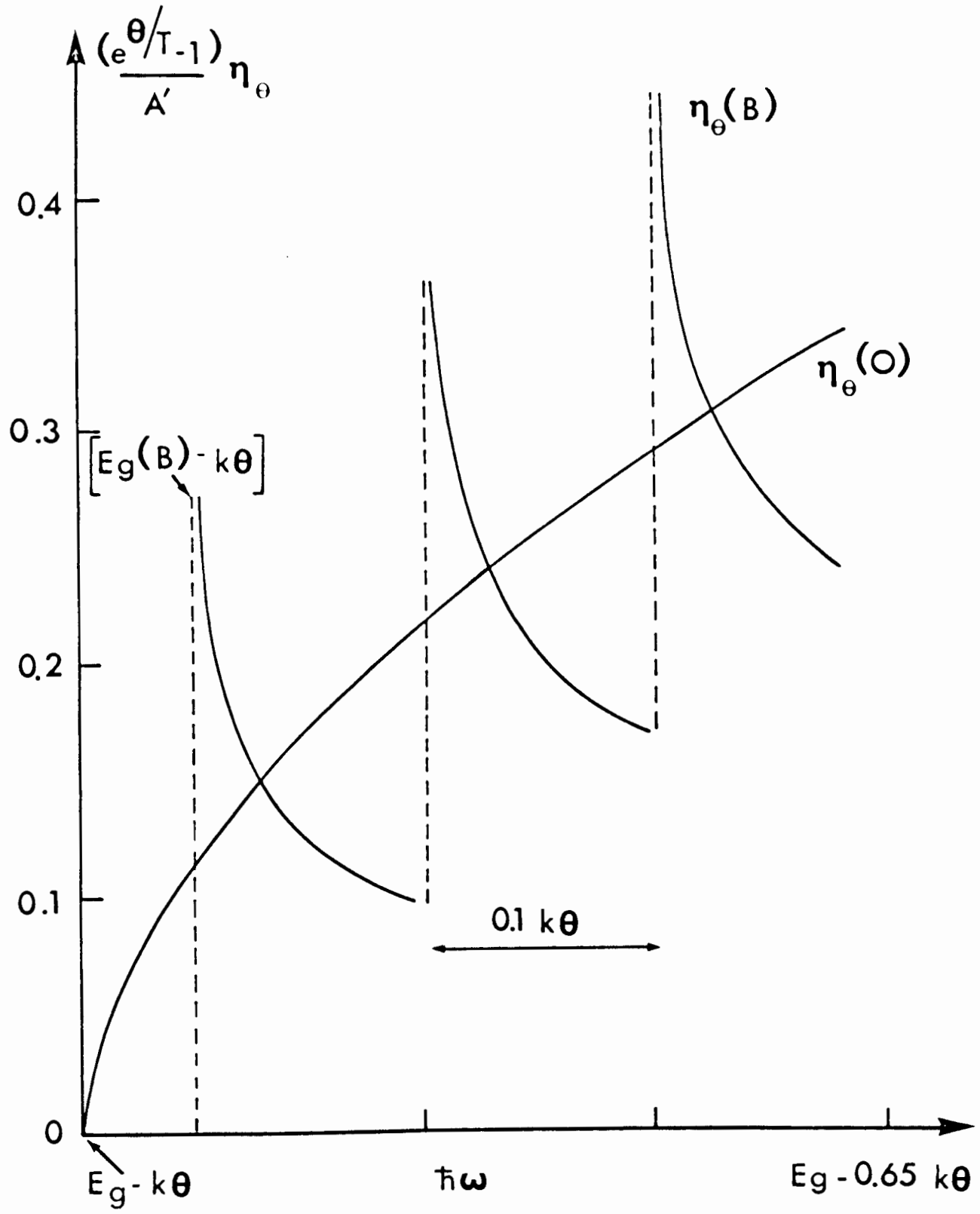

Figure 18. Interband absorption spectrum for B = 0 and B ≠ 0 as a function of photon energy for $\alpha_v \to 0$, E_g (B) = $E_g + 0.05\ k\theta$. $A' = A(\alpha_v/\alpha_c)^{3/2}\ r^2$, where A is given by equation (10.13).

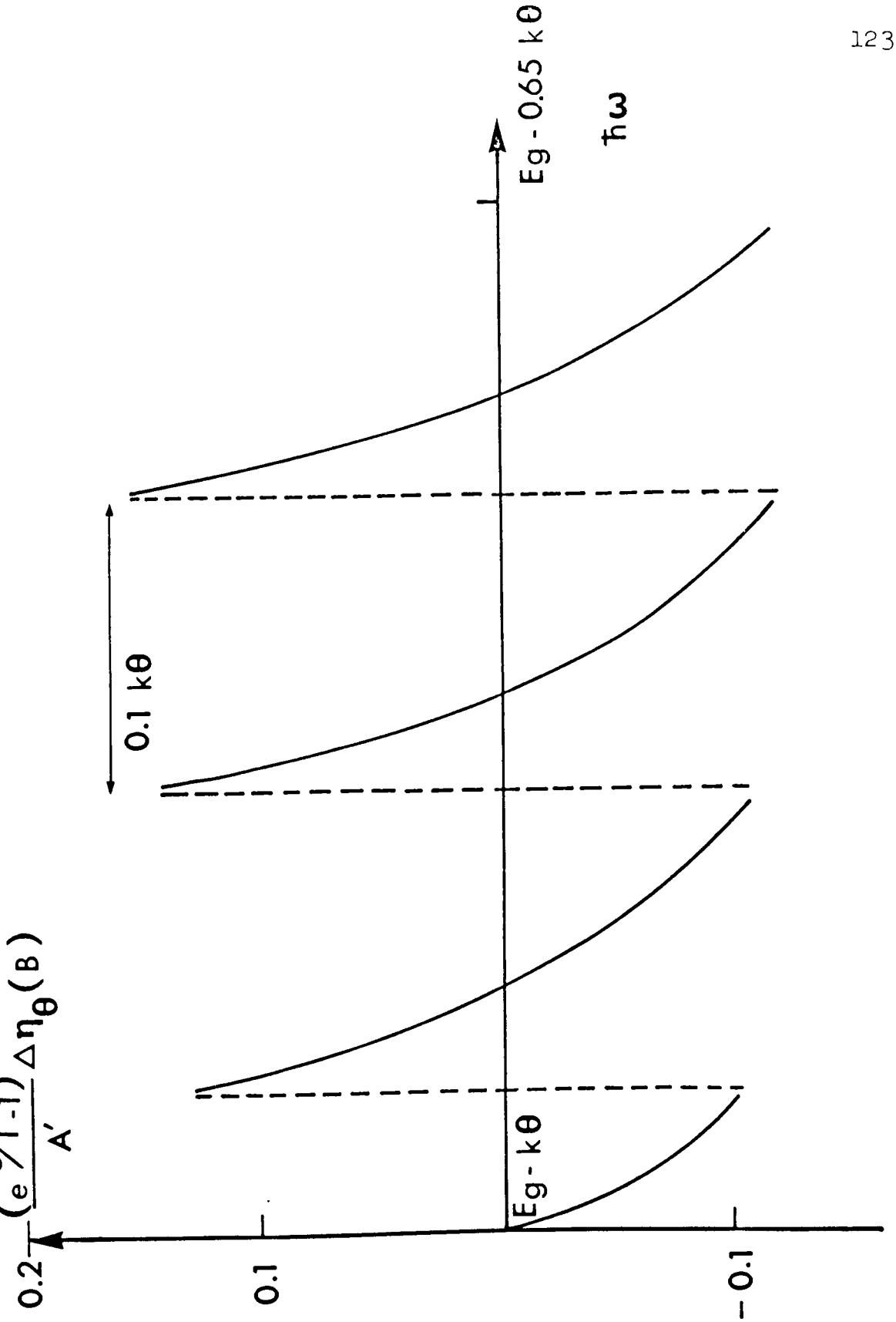

Figure 19. Difference of the absorption coefficients $[\eta_\theta(B) - \eta_\theta(0)] \equiv \Delta\eta_\theta(B)$ as a function of photon energy for $\alpha_v \to 0$.

11.4 Numerical Estimates and Practical Considerations

In order to study the magnetoabsorption spectrum discussed above, the semiconductor chosen must have a direct band gap because we worked out the theory corresponding to this case. A necessary condition for observing well defined structure is that the spacing between the Landau levels be greater than the broadening of the levels and therefore the product of the cyclotron frequency (involving the effective mass for the band under consideration) and the scattering time (τ) must be greater than unity in each band. If this condition holds only for one band, the structure of the other band will not be resolved. Below, we restrict the discussion to the conduction band, similar considerations are also valid for the valence band.

The use of low temperatures to increase τ should clearly be advantageous for observing detailed structure. However, we have shown that $\eta_{\theta}(B)$ is proportional to the number of phonons present $[e^{\theta/T} - 1]^{-1}$ and hence decreases quickly at temperatures below the Debye temperature , resulting in a negligibly small absorption at low temperatures. Hence, it is necessary that the condition $\alpha_c \omega_c \tau \equiv \omega_{cc} \tau > 1$ be satisfied at temperatures where a significant absorption below the energy gap is observed. A small effective mass and a large magnetic field will, of course, help to achieve this condition. However, the magnetic field must

not be so large that $\alpha_c \hbar\omega_c \sim k\theta$, since no oscillations will be observed for fields larger than this value. The maximum number of oscillations that may be seen is $k\theta/\alpha_c \hbar\omega_c$.

Materials which exhibit normal interband magneto-optical oscillations above the band gap and an Urbach absorption tail below the band gap are potential candidates to display phonon-assisted magnetoabsorption below the band gap. InSb and GaAs are in this category and their relevant properties along with the suggested experimental conditions are listed in the Table I. It appears that both substances should display the structure predicted[10] in this chapter.

TABLE I

Properties of InSb and GaAs

Property	InSb	GaAs
Energy bands	Direct gap[64]	Direct gap[65]
$m_c \equiv \frac{m}{\alpha_c}$	$0.013m$[66]	$0.078m$[67]
$k\theta$	0.024 eV[68]	0.036 eV[69]
τ (From mobility data)	5×10^{-13} sec. at 300° K[70]	4×10^{-13} sec. at 300° K[71]
$\alpha_c\omega_c \equiv \omega_{cc}$	1.3×10^{13} sec.$^{-1}$ at $B = 10^4$ G	1.1×10^{13} sec.$^{-1}$ at $B = 5 \times 10^4$ G
$\alpha_c\omega_c\tau \equiv \omega_{cc}\tau$	~ 7 at 300° K and $B = 10^4$ G	~ 5 at 300° K and $B = 5 \times 10^4$ G
$k\theta/\alpha_c\hbar\omega_c \equiv \frac{k\theta}{\omega_{cc}\tau}$	~ 3 at $B = 10^4$ G	~ 5 at $B = 5 \times 10^4$ G

CHAPTER 12

PHONON-ASSISTED ABSORPTION IN CROSSED ELECTRIC AND MAGNETIC FIELDS IN DIRECT-BAND SEMICONDUCTORS

12.1 Calculation of the Absorption Coefficient

The analysis in the presence of crossed electric and magnetic fields proceeds in a manner very similar to the magnetoabsorption case in principle, but the actual computation is enormously tedious. Some additional assumptions will be required and the weak electric field approximation will be invoked. The validity conditions and the experimental implications of such an approximation will be thoroughly discussed.

When an electric field $\vec{\mathcal{E}} = (\mathcal{E}, 0, 0)$ and a magnetic field $\vec{B} = (0, 0, B)$ are present the wave function for the electrons in band α is given by (see Chapter 2)

$$\psi_{\alpha\mu}(\vec{r}) = u_{\alpha 0}(\vec{r})\, F_{\alpha\mu}(\vec{r}) \qquad (12\text{-}1)$$

where $u_{\alpha 0}(\vec{r})$ is the periodic part of the Bloch function of band α at $\vec{k} = 0$ and the envelope functions for the conduction band and the valence bands are,

$$F_{\alpha\mu'}(\vec{r}) = \frac{1}{\sqrt{L_y L_z}}\, e^{i(k_y' y + k_z' z)}\, \Phi_{n'}\left(x - \lambda^2 k_y' - \frac{V_{\alpha}}{\omega_{c\alpha}}\right) \qquad (12\text{-}2a)$$

and

$$F_{v\mu}(\vec{r}) = \frac{1}{\sqrt{L_y L_z}} e^{i(k_y y + k_z z)} \Phi_n\left(x - x' k_y + \frac{V_d}{\omega_c}\right) \qquad (12\text{-}2b)$$

respectively. Here $V_d = \frac{c\mathcal{E}_x}{B}$ is the drift speed in crossed electric and magnetic fields and μ denotes a set of quantum numbers (n, k_y, k_z). The corresponding energy eigenvalues of the carriers are

$$E_c(\mu') = E_c^0 + \left(n' + \frac{1}{2}\right)\hbar\omega_c + \alpha_c \frac{\hbar^2 k_z^2}{2m} - \frac{1}{2} m V_d^2 - \hbar k_y V_d$$

$$E_v(\mu) = E_v^0 - \left(n + \frac{1}{2}\right)\hbar\omega_v - \alpha_v \frac{\hbar^2 k_z^2}{2m} + \frac{1}{2} m V_d^2 - \hbar k_y V_d \qquad (12\text{-}3)$$

The absorption coefficient is given by (Chapter 1)

$$\gamma_\theta(\vec{\mathcal{E}} \times \vec{B}) = \frac{4\pi n_0}{cN\hbar V} \sum_{\mu,\mu'} |M_{cv}|^2 \delta\left(E_c(\mu') - E_v(\mu) - \hbar\omega - k\theta\right) \qquad (12\text{-}4)$$

where

$$M_{cv} = \sum_{\mu''} \frac{\langle c\mu', N-1 | H_2 | f, c\mu''\rangle \langle c\mu'', N-1 | H_1 | N, v\mu\rangle}{E_c(\mu'') - E_v(\mu) - \hbar\omega} \qquad (12\text{-}5)$$

The electron-photon interaction matrix element is given by (see Chapter 3)

$$\langle \mu'', N-1 | H_1 | N, \nu\mu \rangle = -\frac{e}{m} \sqrt{\frac{2\pi\hbar N}{\omega n_0^2}} \left(\quad \right) I_{\mu''\mu}$$

where for the present case the envelope functions are given by (12-2) and the overlap integral is then

$$I_{\mu''\mu} = \int_V \Gamma^*_{\mu''}(\vec{r}) F_{\nu\mu}(\vec{r}) \, d\tau$$

$$= \frac{1}{L_y} \int_{-L_y/2}^{L_y/2} dy \, e^{i(k_y - k_y'')y} \cdot \frac{1}{L_z} \int_{-L_z/2}^{L_z/2} \quad$$

$$\times \int_{-\infty}^{\infty} \Phi_{n''}\left(x - \lambda^2 k_y'' - \frac{v_1}{\omega_c}\right) \Phi_n\left(x - \lambda^2 k_y + \frac{v_1}{\omega_c}\right) dx$$

$$= \delta_{k_y'', k_y} \delta_{k_z'', k_z} \int_{-\infty}^{\infty} \Phi_{n''}(x) \Phi\left(x + \frac{v_1}{\omega_c}, \frac{v_1}{\omega_c}\right) dx$$

$$= \delta_{k_y'', k_y} \delta_{k_z'', k_z} J_{n'', n}(\alpha)$$

where

$$J_{n'', n}(\alpha) = \int_{-\infty}^{\infty} \Phi_{n''}(x) \Phi_n(x + \alpha) \, dx \qquad (12\text{-}6)$$

and

$$a = \frac{V_1}{\quad} + \frac{V_1}{\quad} \equiv \frac{M\lambda}{\hbar} V_1$$

Hence

$$\langle c\mu'', N-1 | H_1 | N, \nu\mu \rangle = -\frac{e}{m} \sqrt{\frac{2\pi\hbar N}{\omega V}} \; (\vec{\varepsilon}\cdot\hat{\xi}) \, \delta_{k'', k+\kappa} \, \delta_{\mu'', \mu k} \, J_{\mu'', \mu}(\omega) \qquad (12\text{-}7)$$

Substituting (12-7) in (12-5) and simplifying we obtain

$$|M_{\nu}|^2 = \frac{2\pi\hbar N}{(e^{\theta/T} - 1)} \; |P|^2 \, |(\vec{\varepsilon}\cdot\hat{\xi})|^2$$

$$\left| \sum_{n''} \frac{J_{n'', n}(\omega)}{\left[E_g(\vec{\varepsilon}\times\vec{P}) + \alpha_c \left(\frac{\hbar^2 k^2}{2m} + n''\hbar\omega_0 \right) + \alpha_v \left(\frac{\hbar^2 k^2}{2m} + n\hbar\omega_0 - \hbar\omega \right) \right]} \right|^2$$

where we replaced electron-phonon interaction matrix elements by a constant and

$$E_g(\vec{\varepsilon}\times\vec{P}) \equiv E_g + \frac{1}{2}(\alpha_c + \alpha_v)\hbar\omega_0 - \frac{1}{2} M V_1^2 \qquad (12\text{-}8)$$

If we set

$$E_g(\vec{\mathcal{E}}\times\vec{B}) + \alpha_c \frac{\hbar^2 k_z}{m} + \alpha_v \left\{ \frac{\hbar^2 k_z}{m} \right. \qquad (12\text{-}9)$$

then

$$|M_{cv}|^2 = \frac{\pi N |H|^2 |(\vec{k}_v \cdot \vec{\mathcal{E}})|^2}{(\epsilon - 1)\, n^2 \omega m^2 V} \qquad (12\text{-}10)$$

where

$$S = \sum_{n''} \left[\frac{J_{n'',n}(a)}{\{n + n''\alpha_c'\}} \right] \qquad (12\text{-}11)$$

We cannot proceed any further until the summation over n" is completed. If we substitute the closed form of $J_{n'',n}(a)$ (see Appendix (C)) in (12-11), it is impossible to sum the resulting expression over all values of n". Thus it is necessary to introduce some approximation which would enable us to simplify (12-11). It is at this stage that we specialize to the weak electric field case. The d.c. field will be called weak when the dimensionless parameter $\frac{a}{\lambda}(\equiv \gamma) \ll 1$. The validity of this criterion is discussed in Section 12.2. In the remaining portion of this chapter we restrict ourselves to the case $\gamma \ll 1$.

When $\gamma \ll 1$, a power series expansion for $J_{n'',n}(a)$ gives (see Appendix (D))

$$J_{n'',n}(a) \simeq \delta_{n'',n} + (\gamma)\left\{\left(\frac{n+1}{2}\right)^{1/2}\delta_{n'',n+1} + \left(\frac{n}{2}\right)^{1/2}\delta_{n'',n-1}\right\}$$
$$+\left(\frac{\gamma^2}{2}\right)\left\{(n+\tfrac{1}{2})\,\delta_{n'',n} + \left(\frac{n+1}{2}\right)^{1/2}\left(\frac{n+2}{2}\right)^{1/2}\delta_{n'',n+2}\right. \qquad (12\text{-}12)$$
$$\left. + \left(\frac{n}{2}\right)^{1/2}\left(\frac{n-1}{2}\right)^{1/2}\delta_{n'',n-2}\right\} + O(\gamma^3)$$

Substituting (12-12) in (12-11) we get

$$S \simeq \frac{1}{D + n\alpha'_c} + (\gamma)\left\{-\frac{\left(\frac{n+1}{2}\right)^{1/2}}{D+(n+1)\alpha'_c} + \frac{\left(\frac{n}{2}\right)^{1/2}}{D+(n-1)\alpha'_c}\right\}$$
$$+\left(\frac{\gamma^2}{2}\right)\left\{-\frac{(n+1)}{D+n\alpha'_c} + \frac{\left(\frac{n+2}{2}\right)^{1/2}\left(\frac{n+1}{2}\right)^{1/2}}{D+(n+2)\alpha'_c}\right.$$
$$\left. + \frac{\left(\frac{n}{2}\right)\left(\frac{n+1}{2}\right)^{1/2}}{D+(n-1)\alpha'_c}\right\} + O(\gamma^3)$$

Squaring this and retaining terms up to order γ^2, we obtain

$$|S|^2 \simeq \frac{1}{\{D + n\alpha_c'\}^2} + (\gamma)\left[\frac{1}{(D+n\alpha_c')}\left\{-\frac{\sqrt{2(n+1)}}{(D+(n+1)\alpha_c')}+\frac{\sqrt{2n}}{(D+(n-1)\alpha_c')}\right\}\right]$$

$$+\left(\frac{\gamma^2}{2}\right)\left[\frac{(n+1)}{\{D+(n+1)\alpha_c'\}^2}+\frac{(n)}{\{D+(n-1)\alpha_c'\}^2}\right. \qquad (12\text{-}13)$$

$$-\frac{2\sqrt{n(n+1)}}{\{D+(n+1)\alpha_c'\}\{D+(n-1)\alpha_c'\}}-\frac{(n+1)}{\{D+n\alpha_c'\}^2}$$

$$\left.+\frac{1}{(D+n\alpha_c')}\left\{\frac{\sqrt{(n+2)(n+1)}}{(D+(n+2)\alpha_c')}+\frac{\sqrt{n(n-1)}}{(D+(n-2)\alpha_c')}\right\}\right]$$

Replacing D by the complete expression (12-9) and then substituting the above value of $|S|^2$ in (12-10) we get

$$|M_{cv}|^2 = \frac{2\pi\hbar N e^2 |I|^2 |(\vec{P}_{cv}\cdot\hat{\xi})|^2}{(e^{\hbar\omega/kT}-1)\, m^2\omega\, n_0^2 V r^2}\left[\frac{1}{t^2}\right.$$

$$+(\gamma)\left\{-\frac{\sqrt{2(n+1)}}{t(t+\hbar\Omega_c)}+\frac{\sqrt{2n}}{t(t-\hbar\Omega_c)}\right\}$$

$$+\left(\frac{\gamma^2}{2}\right)\left\{\frac{(n+1)}{(t+\hbar\Omega_c)^2}+\frac{(n)}{(t-\hbar\Omega_c)^2}\right.$$

$$-\frac{2\sqrt{(n)(n+1)}}{(t+\hbar\Omega_c)(t-\hbar\Omega_c)}-\frac{(n+1)}{t^2}$$

$$\left.+\frac{\sqrt{(n+2)(n+1)}}{t(t+2\hbar\Omega_c)}+\frac{\sqrt{(n)(n-1)}}{t(t-2\hbar\Omega_c)}\right]$$

$$\equiv \frac{2\pi\hbar N e^2 |I|^2 |(\vec{P}_{cv}\cdot\hat{\xi})|^2}{(e^{\hbar\omega/kT}-1)\, m^2\omega\, n_0^2 V r^2}\left[\int(\epsilon_v)\right] \qquad (12\text{-}14)$$

where

$$\epsilon_v(n,k_z) = \alpha_v\left\{\frac{\hbar^2 k_z^2}{2m} + n\hbar\omega_c\right\},$$

$$\epsilon_c(n',k_z') = \alpha_c\left\{\frac{\hbar^2 k_z'^2}{2m} + n'\hbar\omega_c\right\},$$

$$\Delta(\vec{\mathcal{E}}\times\vec{B}) = \frac{E_g(\vec{\mathcal{E}}\times\vec{B}) - \hbar\omega}{\gamma} > 0 \qquad (12\text{-}15)$$

$$t = \epsilon_v(n,k_z) + \Delta(\vec{\mathcal{E}}\times\vec{B}),$$

$$\frac{\alpha_c'}{\gamma} = \frac{eB}{Mc} = \hbar\Omega_c$$

Substituting (12-14) in (12-4) and replacing the summations over k_y, k_y', k_z, k_z' in (12-4) by integrations, and taking into account the density of state factors (see equations (11-13) and (11-14)) we find

$$\eta_\theta(\vec{\mathcal{E}}\times\vec{B}) = \frac{A}{(e^{\theta/T}-1)}\cdot\frac{(\alpha_c'\alpha_v')}{4\pi} \times \sum_{n,n'}\left[\int_0^\infty \frac{f(\epsilon_v)\,d\epsilon_v(n,k_z)}{\{\epsilon_v(n,k_z) - a_n\}^{1/2}} \times \int_0^\infty \frac{d\epsilon_c(n',k_z')\,\delta\left(\epsilon_v(n,k_z) + \epsilon_c(n',k_z') - \Delta(\vec{\mathcal{E}}\times\vec{B})\right)}{\{\epsilon_c(n',k_z') - a_{n'}\}^{1/2}}\right] \qquad (12\text{-}16)$$

where we set

$$\hbar\omega + k\dot{x} - F_y(\vec{\varepsilon}\times\vec{B}) \equiv \Delta\,(\vec{\varepsilon}\times\vec{B}),$$

$$n'\alpha_{n'} = a_{n'}\,, \quad n\alpha_n = a_n\,, \tag{12-17}$$

other symbols have been defined previously. Our next task is to complete the many integrals involved in equation (12-16). This is a rather straight forward but a very long process. In order to save us a great deal of writing we set

$$P \equiv \beta(\vec{\varepsilon}\times\vec{B}) + a_n\,,$$

$$Q \equiv \alpha(\vec{\varepsilon}\times\vec{B}) + \Delta(\vec{\varepsilon}\times\vec{B}) - a_{n'} \tag{12-18}$$

In terms of P, and Q, the final expression for the absorption coefficient becomes

$$\eta_{\theta}(\vec{\mathcal{E}}\times\vec{B}) = \frac{A}{(e^{2\gamma_T}-1)}\cdot\frac{(\alpha_c'\alpha_v')}{\delta}\sum_{n\,n'}\Bigg[\Bigg\{\frac{P+Q}{(PQ)^{3/2}}\Bigg\}$$

$$+(\gamma)\Bigg\{\frac{\sqrt{\delta(n+1)}}{\hbar\Omega_c}\left(\frac{1}{(P+\hbar\Omega_c)^{1/2}(Q+\hbar\Omega_c)^{1/2}}-\frac{1}{(PQ)^{1/2}}\right)$$

$$+\frac{\sqrt{\delta n}}{\hbar\Omega_c}\left(\frac{1}{(P-\hbar\Omega_c)^{1/2}(Q-\hbar\Omega_c)^{1/2}}-\frac{1}{(PQ)^{1/2}}\right)\Bigg\}$$

$$+(\gamma^2)\Bigg\{\frac{(n+1)}{2}\left(\frac{P+Q+2\hbar\Omega_c}{(P+\hbar\Omega_c)^{3/2}(Q+\hbar\Omega_c)^{3/2}}\right) \qquad (12\text{-}19)$$

$$+\frac{(n)}{2}\left(\frac{P+Q-2\hbar\Omega_c}{(P-\hbar\Omega_c)^{3/2}(Q-\hbar\Omega_c)^{3/2}}\right)-\frac{(2n+1)}{2}\left(\frac{P+Q}{(PQ)^{3/2}}\right)$$

$$+\frac{\sqrt{(n)(n+1)}}{\hbar\Omega_c}\left(\frac{1}{(P+\hbar\Omega_c)^{1/2}(Q+\hbar\Omega_c)^{1/2}}-\frac{1}{(P-\hbar\Omega_c)^{1/2}(Q-\hbar\Omega_c)^{1/2}}\right)$$

$$+\frac{\sqrt{(n+2)(n+1)}}{2\hbar\Omega_c}\left(\frac{1}{(PQ)^{1/2}}-\frac{1}{(P+2\hbar\Omega_c)^{1/2}(Q+2\hbar\Omega_c)^{1/2}}\right)$$

$$+\frac{\sqrt{(n)(n-1)}}{2\hbar\Omega_c}\left(\frac{1}{(P-2\hbar\Omega_c)^{1/2}(Q-2\hbar\Omega_c)^{1/2}}-\frac{1}{(PQ)^{1/2}}\right)\Bigg\}\Bigg]$$

with the restriction $a_n + a_{n'} < \Delta(\vec{\mathcal{E}}\times\vec{B})$. This restriction implies that there is no absorption until

$$\hbar\omega + k\theta > E_g(\vec{\mathcal{E}}\times\vec{B})$$

Thus $E_g(\vec{\mathcal{E}}\times\vec{B})$ acts as the threshold for absorption in the presence of crossed electric and magnetic fields. The effect of the electric field is to reduce the threshold for absorption.

If in equation (12-19) we retain only the zeroth order term in the expansion parameter γ, the absorption coefficient to this order is

$$\eta_0^{(0)}(\vec{\mathcal{E}}\times\vec{B}) = \frac{A}{(e^{\beta/T}-1)}\cdot\frac{(\alpha_c'\alpha_v')}{8} \times \sum_{n,n'}{}' \left[\frac{\rho\,\mathcal{I}(\vec{\mathcal{E}}\times\vec{B}) + \Delta(\vec{\mathcal{E}}\times\vec{B}) + \alpha_{n'} - \hbar\omega}{\{(\alpha(\vec{\mathcal{E}}\times\vec{B}) + \alpha_n)(\alpha(\vec{\mathcal{E}}\times\vec{B}) + \Delta(\vec{\mathcal{E}}\times\vec{B}) - \alpha_{n'})\}^{3/2}} \right] \tag{12-20}$$

On comparing this with the phonon-assisted magnetoabsorption case (equation (11-17)) we find that the only effect of the electric field is to replace $E_g(B) \rightarrow E_g(\vec{\mathcal{E}} \times \vec{B})$. Hence if the electric field is very weak such that the zeroth order term is most dominant, the full effect of the electric field is to shift the threshold of absorption to slightly longer wavelengths. The whole structure will shift to the left without altering the magnitude of the magnetoabsorption effect. Notice that the magnetoabsorption coefficient is readily reproduced from (12-20) if we let $\mathcal{E} \rightarrow 0$.

Higher order terms in γ tend to break the selection rule $\Delta n = 0$ and make the transitions $\Delta n = \pm 1, \pm 2, \ldots$ possible. However this will only change the magnitude of the phonon-assisted magnetoabsorption and is not expected to produce any additional structure, because electron-phonon interaction does not obey the $\Delta n = 0$ selection rule anyway (see Fig. 20). Such an effect of the electric field can be fruitfully exploited in

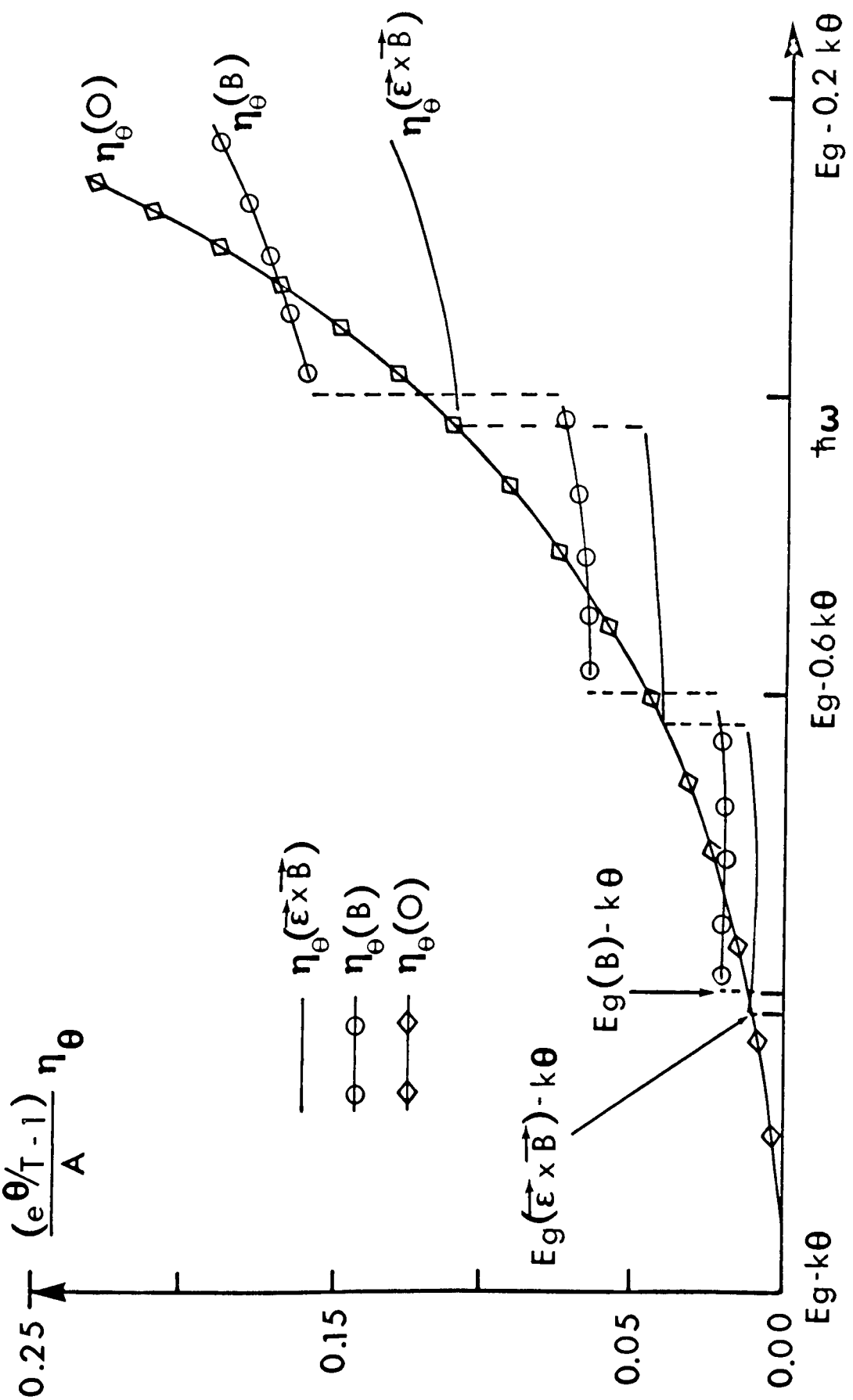

Figure 20. Interband absorption spectrum $\eta_\theta(\vec{\varepsilon}\times\vec{B})$, $\eta_\theta(B)$ and $\eta_\theta(O)$ as a function of photon energy for the case $\alpha_c = \alpha_v$ and $\gamma = 0.4$.

identifying the magnetoabsorption structure because an application of the electric field shifts the magnetic structure. In Fig. 20 we have numerically plotted the absorption coefficient, in the presence of crossed electric fields (equation (12-19)), magnetic field alone (equation (11-17)) and no field at all (equation (11-18)), for the case $\alpha_c/\alpha_v = 1$. As stated above $\eta_\theta(\vec{\mathcal{E}} \times \vec{B})$ is indeed shifted to the left (lower enegy) and the magnitude is different from $\eta_\theta(B)$. As the structure is very similar to $\eta_\theta(B)$, we do not draw any more figures here and one can refer back to the previous chapter to visualize $\eta_\theta(\vec{\mathcal{E}} \times \vec{B})$ curves for other ratios of α_c and α_v. The experimental considerations and the choice of material etc. discussed in the last chapter are also valid here.

12.2 Weak Electric Field Criterion

It was stated above that the d.c. electric field will be considered weak if the condition $\gamma \ll 1$ is satisfied. Since we can write

$$\gamma = \frac{e\mathcal{E}\lambda}{\hbar\Omega_c} \qquad (12\text{-}21)$$

the condition $\gamma < 1$ physically implies that the energy picked up by the carriers, over a distance of magnetic length $\lambda = (\frac{c\hbar}{eB})^{\frac{1}{2}}$ from the electric field should be small compared with the splitting of the levels. (Recall that $\Omega_c = \frac{eB}{Mc}$). Thus it appears

that γ is a reasonable parameter to choose. Let us see what electric fields are implied by the low electric field limit. We know that

$$\lambda = 2.5 \times 10^{-1} \frac{1}{B^{1/2}} \quad (\text{cm})$$

where B is measured in gauss. If $\mathcal{E}$ is measured in volts/cm., we can write

$$\gamma = \frac{eM}{\hbar} \cdot \frac{\mathcal{E}}{B^{3/2}} \cdot 2.5 \times 10^{-1}$$

Choosing $M \approx 10^{-28}$ gm. We obtain

$$\gamma \simeq 1 \times 10^{3} \frac{\mathcal{E}}{B^{3/2}}$$

For a magnetic field of 10^4 gauss, we are in the weak field limit when $\mathcal{E} << 500$ volts/cm. Thus to observe the effects predicted in this chapter, one should not exceed the 500 volts/cm limit. However, small effective masses and higher magnetic fields will permit still higher electric fields, which would eventually be limited by the current density that a given sample can tolerate.

CHAPTER 13

HIGHER-ORDER PHONON PROCESSES AND VALIDITY RANGE OF THE PERTURBATION THEORY

13.1 Introduction

It was shown in Chapter 10 using perturbation theory that the processes involving the absorption of one longitudinal optical phonon of energy k_θ produce an absorption coefficient which is non-zero to one phonon energy below the edge. A process involving n phonons would extend the threshold of absorption to $n(k_\theta)$ below the edge, but would not readily lend itself to a perturbation treatment. Thus to investigate the absorption in the region many phonons below the edge it is essential to use a non-perturbative treatment which contains the electron-phonon interaction to all orders. This calculation has recently been carried out by Dunn[8] and his result for the absorption coefficient contains energy and temperature dependences which are in agreement with Urbach's law (see equation (9-1)). No such calculations exist in the presence of external fields due to mathematical complications.

In the previous three chapters, we calculated the absorption coefficient for one-phonon processes in the energy interval, $E_g - k_\theta < \hbar\omega < E_g$ in the absence and presence of external static fields using perturbation theory but did not take into account many-phonon processes. Since in a real

crystal higher-order phonon processes are always present, it is not obvious as to why the perturbation theory should be applicable even for photon energies $\hbar\omega$ in the interval $(E_g - k\theta, E_g)$. In this chapter we wish to show that for weak electron-phonon coupling constant such as in InSb, the perturbative and non-perturbative calculations give identical results in the energy range $E_g - k\theta < \hbar\omega < E_g$ and the contribution of the higher order processes can be neglected in this interval. This will be done by comparing the numerical values of the absorption coefficient in the absence of external fields obtained by perturbation theory with the values obtained through a non-perturbational method in the region $E_g - k\theta < \hbar\omega < E_g$ for different values of the electron-phonon interaction coupling constant[62].

In the next section we state the theoretical expressions for the absorption coefficient calculated by two different prescriptions. The first method is a perturbative one which takes into account only one-phonon processes, the second being a non-perturbative method takes into account many-phonon processes. The actual numerical comparison is carried out in Section 13.3. We find that for the (weak) interaction involved in InSb the two methods give essentially the same results in the energy interval $E_g - k\theta < \hbar\omega < E_g$. For stronger interactions the perturbation results are nowhere applicable.

13.2 Expressions for Absorption Coefficient

It has been shown by Dunn[8] using a non-perturbative method that the phonon-assisted optical absorption coefficient which contains the electron-phonon interaction to all orders is given by

$$\eta_{\theta}^{N.P.}(\omega) = D\int_{0}^{\infty} dy\; y^{1/2}\; Im\left[\frac{1}{y\left(1+\frac{m_c}{m_v}\right)+E_g-\hbar\omega+\sum(y+\mu_c-\hbar\omega)}\right] \qquad (13\text{-}1)$$

where m_c, m_v are effective masses and μ_c, μ_v are origins for measuring energies of conduction and valence bands such that the forbidden gap $E_g = \mu_c + \mu_v$. In deriving (13-1) the group of intermediate states lying near the top of valence-band have been considered (see Chapter 10 where such states have been called type (b)). The superscript N.P. on η indicates that it is the non-perturbative result. The constant D is given by

$$D = \left(\frac{1}{\pi}\right)\frac{e^2\left|(\vec{p}_{cv}\cdot\hat{\varepsilon}_g)\right|^2(2m_c)^{3/2}}{c\hbar^5 n_o E_g m^2} \qquad (13\text{-}2)$$

and the self energy $\sum$ according to Dunn[8] is

$$\sum(E) \simeq \frac{\beta^2 (2m_v^3)^{1/2}}{n_o} \Big[(1+F)\left(E + \hbar\omega + \mu_v + \sum(E+\hbar\omega)\right)^{1/2} + (F)\left(E - k\theta + \mu_v + \sum(E-k\theta)\right)^{1/2} - (1+F)\,\mathrm{Re}\left(k\theta + \sum(k\theta + \mu_v)\right)^{1/2} - (F)\,\mathrm{Re}\left(-k\theta + \sum(-k\theta - \mu_v)\right)^{1/2} \Big] \quad (13\text{-}3)$$

where $F = 1/(e^{\theta/T} - 1)$, is the Bose-Einstein factor, β^2 determines the strength of the electron-phonon interaction, n_o is the refractive index, $\vec{p}_{cv}$ is interband matrix element and $\hat{\xi}$ stands for the unit polarization vector of the photon. It has been assumed in writing (13-1) and (13-3) that $\hbar\omega \sim E_g >> kT$ and $E \sim \mu_v >> kT$.

It is convenient to rewrite equation (13-1) in terms of a dimensionless parameter, ρ and we obtain

$$\eta_\theta^{N.P.}(\omega) = Q \int_0^\infty \mathrm{Im}\left[\frac{1}{x\left(1+\frac{m_c}{m_v}\right) + \rho + \sum(x+\rho)}\right] \quad (13\text{-}4)$$

where

$$\xi = \Gamma (k\theta)^{1/2} ,$$

$$\rho = \frac{E_g - \hbar\omega}{k\theta} \quad \text{and} \tag{13-5}$$

$$\Gamma (E/k\theta) = \frac{1}{(k\theta)} \sum (E - E_v)$$

The perturbation expression for the absorption coefficient was obtained in Chapter 10, equation (10-15), by considering the group of intermediate states near the bottom of the conduction band (type(a) intermediate states). The results valid for type (b) intermediate states can be obtained from (10-15) by interchanging $\alpha_c \longleftrightarrow \alpha_v$ (or $m_c \longleftrightarrow m_v$) and thus we obtain

$$\gamma_\theta^{R}(\omega) = \left(\frac{4}{\pi}\right) \cdot \frac{e^2 m \beta^2 |(\vec{k}_{cv} \cdot \hat{\xi})|^2}{c \hbar^2 n_0 E_g (\alpha_c \alpha_v)^{3/2} (1+\rho)^{1/2} (e^{\rho\theta} - 1)}$$

$$\times \left[\frac{1}{2} \cdot \frac{2(E_g - \hbar\omega)}{\left(1 + \frac{\alpha_v}{\alpha_c}\right)} + \hbar\omega + k\theta - E_g \Big/ \left\{ \left(\frac{E_g - \hbar\omega}{1 + \frac{\alpha_v}{\alpha_c}} \right) \left(\frac{E_g - \hbar\omega}{1 + \frac{\alpha_v}{\alpha_c}} + \hbar\omega + k\theta - E_g \right) \right\}^{1/2} - 1 \right] \tag{13-6}$$

In the notation of the present chapter, we can write (13-6) in the form

$$\eta_\theta^{P.}(\omega) = Q\,G_1\,\frac{\pi}{\left(1+\frac{m_c}{m_v}\right)^2}\,F \times \left[\frac{1}{2}\,\frac{\frac{2\rho}{\left(1+\frac{m_c}{m_v}\right)}+(1-\rho)}{\left\{\left(\frac{\rho}{1+\frac{m_c}{m_v}}\right)\left(\frac{\rho}{1+\frac{m_c}{m_v}}+1-\rho\right)\right\}^{1/2}}-1\right] \tag{13-7}$$

where the coupling constant

$$G_1 = \frac{\beta^2}{2\pi}\left(\frac{2m_v^3}{k\Theta}\right)^{1/2} \tag{13-8}$$

It can be shown quite easily that in the limit $G \to 0$, equation (13-4) reduces to equation (13-7) and the perturbative and non-perturbative results are identical. However in any real material where the Urbach tail is seen experimentally, the coupling constant is not zero and then the two results may differ considerably. In the following section we compare (13-4) and (13-7) for different values of G, choosing InSb as an example.

13.3 Comparison of $\eta_\theta^{N.P.}(\omega)$ and $\eta_\theta^{P.}(\omega)$ for Different Values of G

We have numerically evaluated the values of $\eta_\theta^{N.P.}(\omega)$ and $\eta_\theta^{P.}(\omega)$ for $\theta = T = 290°$ K, $m_c/m_v = \frac{1}{20}$ (which is very nearly the situation in InSb) for different values of the coupling constant

G. For InSb, the value of G lies in the range 0.01 to 0.03. This has been estimated from the experimental data[6] for the absorption coefficient, the $\vec{k} \cdot \vec{p}$ theory has been used to estimate the interband matrix elements[72]. For ease of comparison we have plotted the quantity η_θ/QG vs $\hbar\omega$. This gives just one curve for $\eta_\theta^{P.}$ since $\eta_\theta^{P.}/QG$ is independent of G (see equation (13-77)) whereas $\eta_\theta^{N.P.}/QG$ depends on the value chosen for G. We see from Fig. 21, that for realistic values of coupling constant for InSb, the perturbative results and non-perturbative results are hardly distinguishable.

In Fig. 22 the quantity

$$\left\{ \frac{\eta_\theta^{N.P.}(\omega) - \eta_\theta^{P.}(\omega)}{\eta_\theta^{N.P.}(\hbar\omega = E_g - 0.1\, k\theta)} \right\} \times 100$$

has been plotted as a function of $\hbar\omega$ for different values of G. This quantity is a measure of the percentage difference between the two results normalized in terms of the non-perturbative value of the absorption coefficient at $\hbar\omega = E_g - 0.1\, k\theta$. For $G < 0.06$ the difference between the two results is negligible and we have not shown the corresponding curve. For $G \geq 0.06$ the difference between $\eta_\theta^{N.P.}$ and $\eta_\theta^{P.}$ becomes much more apparent and for $G \sim 0.1$ the two results differ by 15% at some points. The perturbative result goes to zero at $\hbar\omega = E_g - k\theta$ and the non-perturbative result drops to about 1% of its initial value even for $G = 0.2$ which is ten times larger than the value of G

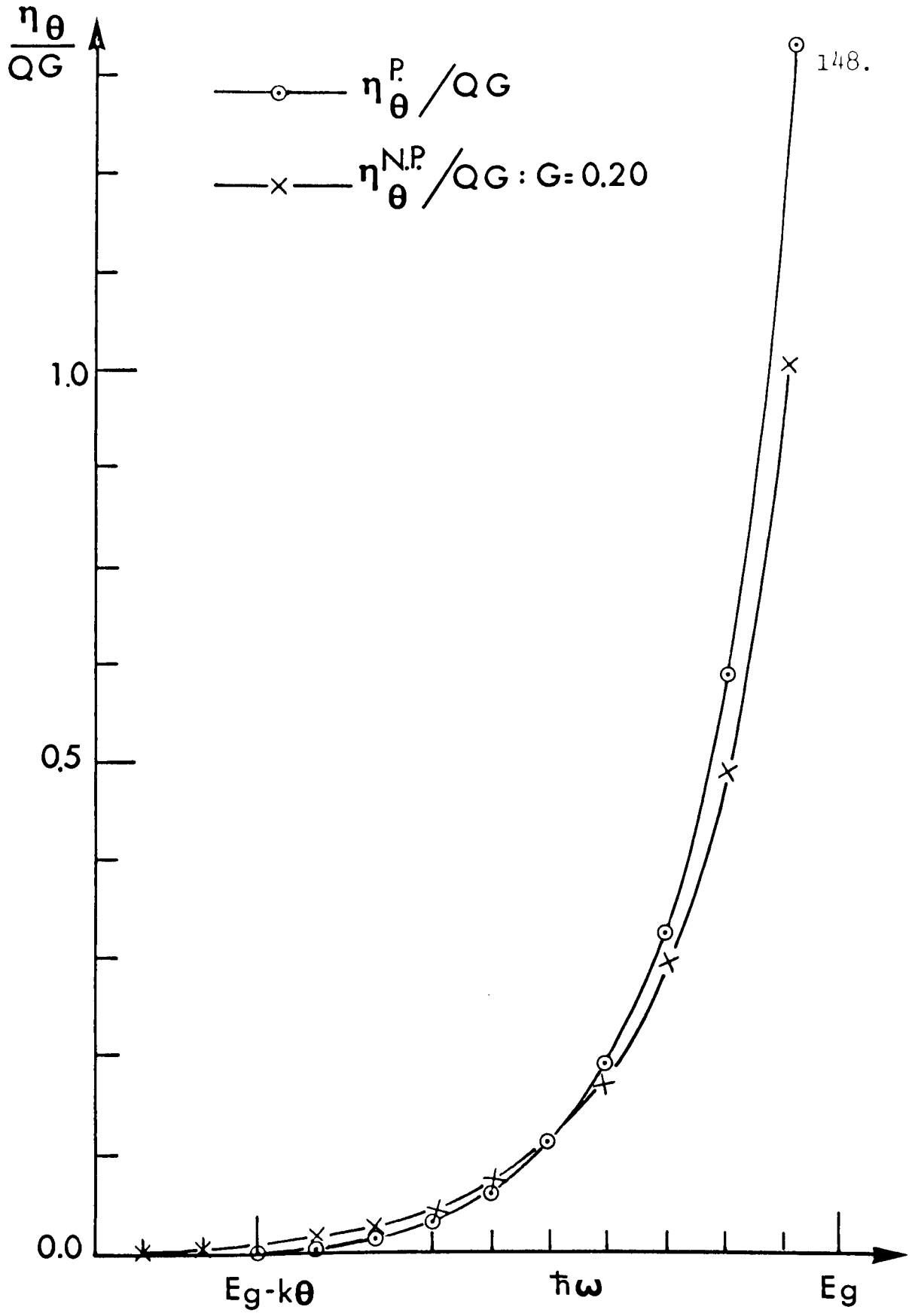

Figure 21. Absorption spectrum calculated using perturbative and non-perturbative techniques as a function of photon energy for different values of G. For $G \leq 0.05$, the two approaches give identical results.

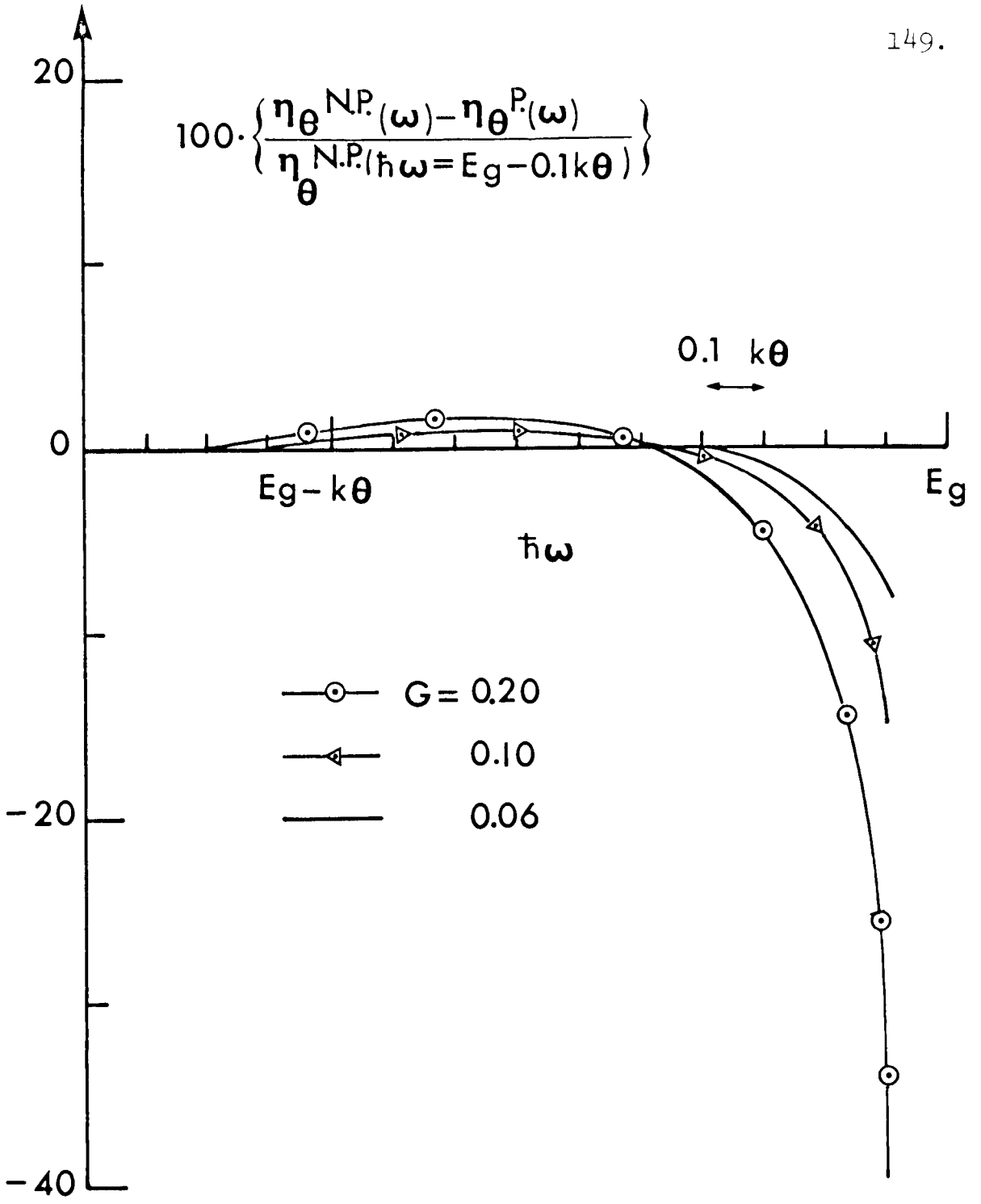

Figure 22. Percentage difference between non-perturbative and perturbative values of the absorption coefficient normalized in terms of the value of $\eta_\theta^{N.P.}$ at $\hbar\omega = E_g - 0.1\ k_\theta$, as a function of $\hbar\omega$ for different values of G.

for InSb. Thus the perturbation theory is strictly valid in the energy range $E_g - k\theta < \hbar\omega < E_g$.

13.4 Conclusion

It has been shown that for values of the electron-phonon interaction coupling constant $G \leq 0.05$ the perturbative and non-perturbative results are in excellent agreement with each other and we are justified in ignoring higher-order processes in Chapters 10, 11 and 12. For InSb, $G \approx 0.02$ and we would expect that other weakly ionic compounds also fall into the above range. However the experimental data for absorption below the gap is not available for many such compounds and without this we cannot make reliable estimates of G. Strongly ionic materials like alkali halides may show considerable deviation due to large coupling constants involved. Such conclusions have been arrived at earlier in the literature by us.[62]

CHAPTER 14

DISCUSSION AND CONCLUSION

During the entire presentation we calculated the absorption coefficient for direct allowed transitions and for phonon-assisted transitions in the framework of Effective Mass Approximation. A table of the cases discussed, along with the reasons for not discussing certain fields configurations is shown below.

TABLE II - Summary

External Static Fields Present	Absorption Coefficient for Direct Allowed Transitions	Absorption Coefficient for Phonon-Assisted Transitions
NO Fields	Chapter 4	Chapter 10
$\vec{B}$	Chapter 5	Chapter 11
$\vec{\mathcal{E}}$	Chapter 6	Due to smearing of the edge this case is experimentally uninteresting, so not discussed.
$\vec{\mathcal{E}} \times \vec{B}$	Chapter 7	Chapter 12
$\vec{\mathcal{E}} \times \vec{B}$ (weak $\vec{\mathcal{E}}$)	Chapter 7	Chapter 12
$\vec{\mathcal{E}} \parallel \vec{B}$	Chapter 8	Experimentally uninteresting (see $\vec{\mathcal{E}}$ field case).
$\vec{\mathcal{E}}$ and $\vec{B}$ (arbitrary orentation)	Chapter 3	Mathematically involved, not illuminating.

The phonon-assisted transitions are responsible for finite absorption coefficient for $\hbar\omega < E_g$ and give rise to the Urbach tail in the absorption spectrum. The expression for the absorption coefficient for the phonon-assisted transitions involving many phonons in the absence of external fields has been reported in the literature. The calculation involving more than one phonon in the presence of external fields is extremely difficult and has not been attempted. In our presentation we included only one phonon-processes in the presence of external static fields, but showed rigorously that the effect of higher-order phonon processes is ngligible in this region of the absorption spectrum, provided the electron-phonon interaction is not too strong.

We have shown that the effect of a magnetic field on phonon-assisted transitions in the energy range $E_g - k\theta < \hbar\omega < E_g$ is to make the absorption oscillatory in nature. In contrast to the normal interband absorption coefficient, the phonon-assisted magnetoabsorption spectrum reflects the Landau level structure of valence-band and conduction-band separately. The application of a small electric field shifts the magneto-absorption structure and can assist in identifying it. Such effects may be observable in InSb and GaAs at room temperature by applying magnetic field $\sim 10^5$ gauss and an electric field $\sim$ 500 volts/cm. We have also predicted the existence of magnetic surface states in semiconductors and have discussed the

experimental conditions under which these may be detected.

The structure in the optical absorption coefficient (not involving phonons) due to external fields has been tested experimentally and has provided us with quantitative data for the band parameters of solids. The structure in the phonon-assisted absorption coefficient due to the effects of external fields, predicted by us, has not been so far confirmed experimentally. It is hoped that such experiments would be conducted in near future and would lead to a slightly better understanding of the band structure of solids.

APPENDICES

APPENDIX A

EFFECTIVE MASS APPROXIMATION WAVE FUNCTIONS IN EXTERNAL FIELDS

Let us start with Schrödinger equation for a particle of mass m, charge 'e', in a periodic potential $V_p(\vec{r})$, a constant magnetic field of magnitude B in a Landau gauge, $\vec{A}_o = (-By, 0, 0)$, and another perturbation $U(\vec{r})$ due to a constant electric field:

$$\left[\frac{1}{2m}\left(\vec{P} - \frac{e}{c}A_o(\vec{r})\right)^2 + V_p(\vec{r}) + U(\vec{r})\right]\psi(\vec{r}) = E\,\psi(\vec{r}) \qquad \text{(A-1)}$$

In the special gauge, the Hamiltonian of equation (A-1) can be written as follows

$$H = H^{(o)} + \left(\frac{\hbar s}{m}\right) y\, p_x + \left(\frac{\hbar^2 s^2}{2m}\right) y^2 + U(\vec{r}) \qquad \text{(A-2)}$$

where $s = \frac{eB}{c\hbar}$ and $H^{(o)}$ is the Hamiltonian of the electron in the periodic potential (Bloch Hamiltonian). The eigenfunctions of $H^{(o)}$ are the Bloch functions $\Phi_{\alpha\vec{k}}$ and the corresponding eigenvalues are $E_\alpha(\vec{k})$, α labelling the band and $\vec{k}$ wandering through the first Brillouin zone of the crystal. Thus possessing,

$$H^{(o)}\,\Phi_{\alpha\vec{k}} = E_\alpha(\vec{k})\,\Phi_{\alpha\vec{k}} \qquad \text{(A-3)}$$

we want to solve for wave function ψ, in external field, from the Schrödinger equation

$$H\psi = E\psi \tag{A-4}$$

In order to proceed further, it is necessary to choose some complete set of functions in which to expand ψ. Here we use the Kohn-Luttinger[11] representation and accordingly choose for the complete set the wave functions,

$$|\alpha, \vec{k}\rangle = e^{i\vec{k}\cdot\vec{r}} u_{\alpha 0}(\vec{r}) \tag{A-5}$$

where $u_{\alpha 0}(\vec{r})$ is the Bloch function at the band edge which has been chosen for convenience at $\vec{k} = 0$. An expansion in terms of the functions (A-5) may be made in the form

$$\psi_\alpha(\vec{r}) = \sum_{\alpha'} \int d\vec{k}' A_{\alpha\alpha'}(\vec{k}') u_{\alpha' 0}(\vec{r}) e^{i\vec{k}'\cdot\vec{r}} \tag{A-6}$$

Substituting this back into the original equation (A-4), one can immediately derive[11] the equation

$$\sum_{\alpha'} \int d\vec{k}' \langle \alpha, \vec{k} | H | \alpha', \vec{k}' \rangle A_{\alpha\alpha'}(\vec{k}') = E A_{\alpha}(\vec{k}) \tag{A-7}$$

where

$$\langle \alpha, \vec{k} | H | \alpha', \vec{k}' \rangle = \Big[\Big\{ \Big(E_\alpha^\circ + \frac{\hbar^2 k^2}{2m} \Big) \delta(\vec{k}-\vec{k}') + \frac{\hbar^2 k_x s}{m} \frac{1}{i} \frac{\partial \delta(\vec{k}-\vec{k}')}{\partial k_y'} - \frac{\hbar^2 s^2}{2m} \frac{\partial^2 \delta(\vec{k}'-\vec{k})}{\partial k_y'^2} \Big\} \delta_{\alpha,\alpha'} + \frac{1}{m} \Big\{ \hbar k_j \, p^j_{\alpha\alpha'} \, \delta(\vec{k}-\vec{k}') + \hbar s \, | \, \frac{1}{i} \frac{\partial \delta(k'-k)}{\partial} \Big\} + \langle \alpha, \vec{k} \, | \, U(\vec{r}) \, | \, \alpha', \vec{k}' \rangle \Big] \tag{A-8}$$

In the last expression, E_α° is the energy at the bottom of band α and

$$p^j_{\alpha\alpha'} = \frac{(2\pi)^3}{\Omega} \int_\Omega u^*_{\alpha_0}(\vec{r}) \Big(\frac{\hbar}{i} \nabla_j \Big) u_{\alpha'_0}(\vec{r}) \, d\vec{r} \tag{A-9}$$

where Ω is the volume of a unit cell and the integration is over a unit cell.

The equation (A-7) is not yet of the desired form, since it still contains terms involving $\vec{p}_{\alpha\alpha'}$, which represent a coupling between bands. (The requirement, that the fractional change of the perturbation potential $U(\vec{r})$ be small over the dimension of a unit cell, makes U diagonal[11] in the band index.)

The nondiagonal terms are proportional to either k or s. In either case these are small because k^{-1} and $\lambda = \sqrt{\frac{c\hbar}{eB}}$ are much larger than the interatomic spacing when $k \sim 0$ close to the band edge and $B \sim 10^4 - 10^5$ gauss. Now in the effective mass theory one works correctly up to order k^2 only, so by making a suitable transformation A, can be made diagonal to first order in k and $\frac{eB}{c\hbar}$ and the cross terms neglected. This transformation is given by[11]

$$A_{\alpha\alpha'}(\vec{k}') = \sum_{\gamma} \int d\vec{k}\; e^{[\langle \alpha', \vec{k}' | S | \gamma, \vec{k} \rangle]} B_{\gamma\alpha}(\vec{k}) \qquad \text{(A-10)}$$

The operator S is chosen such that the equations for the $B_{\gamma\alpha}(\vec{k})$ contain no interband elements. This, along with the assumption that we are considering wave function for electrons in band α only, implies that

$$B_{\gamma\alpha}(\vec{k}) = B_{\alpha\alpha}(\vec{k})\, \delta_{\gamma\alpha} \qquad \text{(A-11)}$$

Substituting (A-11) in (A-10) we get

$$A_{\alpha\alpha'}(\vec{k}') = \int d\vec{k}\; e^{[\langle \alpha', \vec{k}' | S | \alpha, \vec{k} \rangle]} B_{\alpha\alpha}(\vec{k}) \qquad \text{(A-12)}$$

where[11]

$$\langle \alpha', \vec{k}' | S | \alpha, \vec{k} \rangle = - \frac{\hbar (1 - \delta_{\alpha',\alpha})}{m [E^0_{\alpha'} - E^0_{\alpha}]} \times \left[\vec{k}' \cdot \vec{p}_{\alpha'\alpha} \delta(\vec{k}' - \vec{k}) - \frac{ieB}{c\hbar} p^x_{\alpha'\alpha} \frac{\partial \delta(\vec{k} - \vec{k}')}{\partial k_y} \right] \tag{A-13}$$

To first order in S,

$$\exp\left[\langle \alpha', \vec{k}' | S | \alpha, \vec{k} \rangle\right] \simeq \delta_{\alpha',\alpha} \delta(\vec{k}' - \vec{k}) + \langle \alpha', \vec{k}' | S | \alpha, \vec{k} \rangle$$

and hence, the equation (A-12) becomes, using (A-13)

$$A_{\alpha\alpha'}(\vec{k}') = \delta_{\alpha',\alpha} B_{\alpha\alpha}(\vec{k}') - \frac{\hbar (1 - \delta_{\alpha',\alpha})}{m [E^0_{\alpha'} - E^0_{\alpha}]} \times \left[\vec{k}' \cdot \vec{p}_{\alpha'\alpha} B_{\alpha\alpha}(\vec{k}') - \left(\frac{ieB}{c\hbar} p^x_{\alpha'\alpha} \right) \int d\vec{k} \, B_{\alpha\alpha}(\vec{k}) \frac{\partial \delta(\vec{k} - \vec{k}')}{\partial k_y} \right] \tag{A-14}$$

The integral over $\vec{k}$ in the last expression can be carried out by partial integration to obtain

$$\iint dk_x \, dk_z \, \delta(k_x - k'_x) \delta(k_z - k'_z) \int dk_y \, B_{\alpha\alpha}(\vec{k}) \frac{\partial}{\partial k_y} \delta(k_y - k'_y)$$

$$= - \frac{\partial B_{\alpha\alpha}(\vec{k}')}{\partial k'_y}$$

Thus equation (A-14) becomes

$$A_{\alpha\alpha'}(\vec{k}') = \delta_{\alpha'\alpha} B_{\alpha\alpha}(\vec{k}') + \frac{(1-\delta_{\alpha'\alpha})}{m(E_\alpha^0 - E_{\alpha'}^0)} \left\{ \vec{p} \cdot \vec{p}_{\alpha'\alpha} B_{\alpha\alpha}(k') + \frac{ieB}{c} p_{\alpha'\alpha}^x \frac{\partial B_{\alpha\alpha}(\vec{k}')}{\partial k_y'} \right\} \qquad \text{(A-15)}$$

where $\vec{p} = -i\hbar\vec{\nabla}$. Now we substitute this equation in (A-6) to obtain

$$\psi_\alpha(\vec{r}) = \int d\vec{k}' B_{\alpha\alpha}(\vec{k}') e^{i\vec{k}\cdot\vec{r}} u_{\alpha'}(\vec{r}) + \left[\sum_{\alpha' \neq \alpha} \frac{u_{\alpha'0}(\vec{r})}{m(E_\alpha^0 - E_{\alpha'}^0)} \left\{ \int d\vec{k}' B_{\alpha\alpha}(\vec{k}') e^{i\vec{k}'\cdot\vec{r}} \vec{p}_{\alpha'\alpha} \cdot \vec{p} + \left(\frac{ieb}{c} p_{\alpha'\alpha}^x \right) \int d\vec{k}' \frac{\partial B_{\alpha\alpha}(\vec{k}')}{\partial k_y} e^{i\vec{k}'\cdot\vec{r}} \right\} \right] \qquad \text{(A-16)}$$

Carrying out the partial integration and then transforming back to coordinate space through the following relation

$$F_\alpha(\vec{r}) = \int d\vec{k}' B_{\alpha\alpha}(\vec{k}') e^{i\vec{k}'\cdot\vec{r}} , \qquad \text{(A-17)}$$

when equation (A-16) becomes

$$\psi_\alpha(\vec{r}) = u_{\alpha_0}(\vec{r})\, F_\alpha(\vec{r}) + \sum_{\alpha' \neq \alpha} \frac{u_{\alpha' 0}(\vec{r})\, F_\alpha(\vec{r})}{m(E^0_\alpha - E^0_{\alpha'})} \left\{ \vec{p}_{\alpha'\alpha} \cdot \vec{p} - \frac{e}{c} (-i\hbar) \vec{A}_{\alpha'\alpha} \right\}$$

or

$$\psi_\alpha(\vec{r}) = \left[u_{\alpha_0}(\vec{r}) + \sum_{\alpha' \neq \alpha} u_{\alpha' 0}(\vec{r}) \frac{\vec{p}_{\alpha'\alpha} \cdot \vec{\Pi}}{m(E^0_\alpha - E^0_{\alpha'})} \right] F_\alpha(\vec{r}) \quad \text{(A-18)}$$

where

$$\vec{\Pi} = \vec{p} - \frac{e}{c} \vec{A}_0$$

$F_\alpha(\vec{r})$ can be shown[11] to be the solution of the differential equation

$$\left[E_\alpha\left(\left(\frac{1}{i} \vec{\nabla} \right) - \left(\frac{e}{c\hbar} \right) \vec{A}_0 \right) + U(\vec{r}) \right] F_\alpha(\vec{r}) = E F_\alpha(\vec{r}) \quad \text{(A-19)}$$

where $E_\alpha \left[\left(\frac{1}{i} \vec{\nabla} \right) - \left(\frac{e}{c\hbar} \right) \vec{A}_0 \right]$ is an expression that is obtained by expanding $E_\alpha(\vec{k})$, the Bloch energy, up to quadratic terms, replacing $\vec{k}$ by $(1/i)\ \vec{\nabla} - \left(\frac{e}{c\hbar} \right) \vec{A}_0$. In the main text, the symbol $\vec{\pi}$ has been used for compactness. Equation (A-19) is called the

effective mass equation. It is important to point out that the results obtained are gauge-independent.

APPENDIX B

FORBIDDEN TRANSITIONS

We wish to evaluate the matrix elements of the operator $\vec{\pi} \cdot\cdot \hat{\xi}$ using the E.M.A. wave functions (3-1). In the gauge $A_o(\vec{r}) = \frac{1}{2}(\vec{B} \times \vec{r})$, we have

$$\vec{\pi} \cdot \hat{\xi} = \vec{p} \cdot \hat{\xi} + \frac{e}{2c} \vec{\pi} \cdot (\hat{\xi} \times \vec{r}) \qquad \text{(B-1)}$$

Then the matrix element we wish to evaluate is

$$\langle \psi_{c\mu'} | \vec{\pi} \cdot \hat{\xi} | \psi_{v\mu} \rangle = \langle \psi_{c\mu'} | \vec{p} \cdot \hat{\xi} | \psi_{v\mu} \rangle + \frac{e}{2c} \langle \psi_{c\mu'} | \vec{\pi} \cdot (\hat{\xi} \times \vec{r}) | \psi_{v\mu} \rangle \qquad \text{(B-2)}$$

The first term on the right-hand side involves a differential operator, and the second term contains a multiplicative one. The first term, using (3-1) becomes

$$\begin{aligned} \langle \psi_{c\mu'} | \vec{p} \cdot \hat{\xi} | \psi_{v\mu} \rangle &= \langle u_{co} F_{c\mu'} | \vec{p} \cdot \hat{\xi} | u_{vo} F_{v\mu} \rangle \\ &+ \sum_{\beta \neq v} \vec{R}_{\beta v} \cdot \langle u_{co} F_{c\mu'} | \vec{p} \cdot \hat{\xi} | u_{\beta o} \vec{\pi} F_{v\mu} \rangle \\ &- \sum_{\beta \neq c} \vec{R}_{c\beta} \cdot \langle u_{\beta o} \vec{\pi} F_{c\mu'} | \vec{p} \cdot \hat{\xi} | u_{vo} F_{v\mu} \rangle \end{aligned} \qquad \text{(B-3)}$$

where

$$\vec{R}_{\alpha'\alpha} = \frac{\vec{p}_{\alpha'\alpha}}{m [E^o_\alpha - E^o_{\alpha'}]} = -\vec{R}^*_{\alpha\alpha'} \qquad \text{(B-4)}$$

Now

$$\langle u_{co} F_{c\mu'} | \vec{p}\cdot\hat{\xi} | u_{vo} F_{v\mu} \rangle = \langle u_{co} F_{c\mu'} | F_{v\mu} \vec{p}\cdot\hat{\xi}\, u_{vo} \rangle + \langle u_{co} F_{c\mu'} | u_{vo} \vec{p}\cdot\hat{\xi}\, F_{v\mu} \rangle$$

$$\simeq (u_{co} | \vec{p}\cdot\hat{\xi} | u_{vo}) \langle F_{c\mu'} | F_{v\mu} \rangle + (u_{co} | 1 | u_{vo}) \langle F_{c\mu'} | \vec{p}\cdot\hat{\xi} | F_{v\mu} \rangle$$

where the notation (2-16) has been used and the factors of $(2\pi)^3$ have been omitted in accordance with our normalization convention. The second term in the last expression vanishes due to the condition (2-11) and we finally obtain

$$\langle u_{co} F_{c\mu'} | \vec{p}\cdot\hat{\xi} | u_{vo} F_{v\mu} \rangle \simeq (\vec{p}_{cv}\cdot\hat{\xi}) \langle F_{c\mu'} | F_{v\mu} \rangle \qquad \text{(B-5)}$$

Similarly

$$\langle u_{co} F_{c\mu'} | \vec{p}\cdot\hat{\xi} | u_{p o} \vec{\pi} F_{v\mu} \rangle \simeq (\vec{p}_{cp}\cdot\hat{\xi}) \langle F_{c\mu'} | \vec{\pi} | F_{v\mu} \rangle + \delta_{cp} \langle F_{c\mu'} | \vec{p}\cdot\hat{\xi}\, \vec{\pi} | F_{v\mu} \rangle \qquad \text{(B-6)}$$

and

$$\langle u_{p o} \vec{\pi} F_{c\mu'} | \vec{p}\cdot\hat{\xi} | u_{vo} F_{v\mu} \rangle \simeq (\vec{p}_{\beta v}\cdot\hat{\xi}) \langle F_{c\mu'} | \vec{\pi} | F_{v\mu} \rangle + \delta_{\beta v} \langle F_{c\mu'} | \vec{\pi}\, \vec{p}\cdot\hat{\xi} | F_{v\mu} \rangle \qquad \text{(B-7)}$$

where, the hermiticity of $\vec{\pi}$ has been used. The order of $\vec{\pi}$ and $\vec{p}$ is important, since these operators do not commute. Using equations (B-4) through (B-7), the equation (B-3) can be transformed into

$$\begin{aligned} \langle \psi_{c\mu'} | \vec{p}\cdot\hat{\xi} | \psi_{v\mu} \rangle = & (\vec{p}_{cv}\cdot\hat{\xi}) \langle F_{c\mu'} | F_{v\mu} \rangle \\ & + \vec{T}_{cv}\cdot \langle F_{c\mu'} | \vec{\pi} | F_{v\mu} \rangle \\ & + \frac{\vec{p}_{cv}\cdot}{m E_g} \langle F_{c\mu'} | [\vec{\pi}, \vec{p}\cdot\hat{\xi}] | F_{v\mu} \rangle \end{aligned} \qquad \text{(B-8)}$$

where (since $\vec{p}_{\beta\beta} = 0$)

$$\vec{T}_{cv} = \frac{1}{m} \sum_{\beta \neq c,v} \left\{ \frac{\vec{p}_{\beta v} (\vec{p}_{c\beta}\cdot\hat{\xi})}{E_v^o - E_\beta^o} + \frac{\vec{p}_{c\beta} (\vec{p}_{\beta v}\cdot\hat{\xi})}{E_c^o - E_\beta^o} \right\}, \qquad \text{(B-9)}$$

$$E_g = E_c^o - E_v^o \quad , \qquad [a, b] = ab - ba$$

In order to simplify the third term of equation (B-8), we need to know the commutator $[\pi_j, p_i]$ which can be evaluated as follows:

$$\vec{\pi} = \vec{p} - \frac{e}{c}\vec{A}_o$$

With the special gauge $\vec{A}_o = \frac{1}{2}(\vec{B} \times \vec{r})$

$$\pi_j = p_j - \frac{e}{2c}(\vec{B}\times\vec{r})_j$$

Introducing the Levi-Civita antisymmetric symbol

$$\epsilon_{jlm} = \begin{cases} 1 & \text{if } jlm \quad 123, 231, 312 \\ -1 & \text{if } jlm \quad 321, 213, 132 \\ 0 & \text{otherwise} \end{cases} \qquad \text{(B-10)}$$

we can write, using the summation convention

$$\Pi_j = p_j - \frac{e}{2c} \epsilon_{jlm} B_l r_m \qquad \text{(B-11)}$$

Thus

$$\begin{aligned} [\Pi_j, p_i] &= \left[p_j - \frac{e}{2c} \epsilon_{jlm} B_l r_m, p_i \right] \\ &= [p_j, p_i] - \frac{e}{2c} \epsilon_{jlm} B_l [r_m, p_i] \\ &= -\frac{e}{2c} \epsilon_{jlm} B_l i\hbar \delta_{mi} \\ &= -\frac{i\hbar e}{2c} \epsilon_{jli} B_l \end{aligned} \qquad \text{(B-12)}$$

The desired term

$$\begin{aligned} \frac{p_{cv}^j \mathcal{E}_i}{m E_g} \langle F_{cu'} | [\Pi_j, p_i] | F_{vu} \rangle &= \frac{i e \hbar B_l}{2mc E_g} \left\{ -\epsilon_{jli} p_{cv}^j \mathcal{E}_i \right\} \langle F_{cu'} | F_{vu} \rangle \\ &= -\frac{i\hbar \vec{\omega}_c}{2E_g} \cdot (\hat{\mathcal{E}} \times \vec{p}_{cv}) \langle F_{cu'} | F_{vu} \rangle \end{aligned} \qquad \text{(B-13)}$$

Hence (B-8) can now be written as

$$\langle \psi_{c\mu'} | \vec{\pi}\cdot\hat{\xi} | \psi_{v\mu} \rangle = \Big[\Big\{ (\vec{p}_{cv}\cdot\hat{\xi}) - \frac{i\hbar\omega_c}{2E_g}\cdot(\hat{\xi}\times\vec{p}_{cv}) \Big\} \langle F_{c\mu'} | F_{v\mu} \rangle + \vec{T}_{cv}\cdot\langle F_{c\mu'} | \vec{\pi} | F_{v\mu} \rangle \Big] \qquad \text{(B-14)}$$

Next consider the second term of B-2), where we evaluate elements of a mulitiplicative operator. As before

$$\langle u_{c0} F_{c\mu'} | \vec{B}\cdot(\hat{\xi}\times\vec{r}) | u_{v0} F_{v\mu} \rangle \simeq 0 \qquad (c \neq v) \,,$$

$$\langle u_{c0} F_{c\mu'} | \vec{B}\cdot(\hat{\xi}\times\vec{r}) | u_{\beta 0}\vec{\pi} F_{\nu\mu} \rangle \simeq \delta_{c,\beta} \langle F_{c\mu'} | \vec{B}\cdot(\hat{\xi}\times\vec{r})\vec{\pi} | F_{v\mu} \rangle \,,$$

$$\langle u_{\beta 0}\vec{\pi} F_{c\mu'} | \vec{B}\cdot(\hat{\xi}\times\vec{r}) | u_{v0} F_{v\mu} \rangle \simeq \delta_{\beta,v} \langle F_{c\mu'} | \vec{\pi}(\hat{\xi}\times\vec{r})\cdot\vec{B} | F_{v\mu} \rangle$$

Hence

$$\frac{e}{2c}\langle \psi_{c\mu'} | \vec{B}\cdot(\hat{\xi}\times\vec{r}) | \psi_{v\mu} \rangle = \frac{e\, p^{j}_{cv} B_i}{2mc\, E_g} \langle F_{c\mu'} | [\pi_j, (\hat{\xi}\times\vec{r})_\ell] | F_{v\mu} \rangle$$

$$= \frac{e\, p^{j}_{cv} B_\ell \epsilon_{\ell mn} \xi_m}{2mc\, E_g} \langle F_{c\mu'} | [\pi_j, r_n] | F_{v\mu} \rangle$$

$$= -\frac{i\hbar\vec{\omega}_c}{2E_g}\cdot(\hat{\xi}\times\vec{p}_{cv}) \langle F_{c\mu'} | F_{v\mu} \rangle \qquad \text{(B-15)}$$

Finally

$$\langle \psi_{c\mu'} | \vec{\pi}\cdot\hat{\xi} | \psi_{v\mu} \rangle = \Big[\Big\{ (\vec{p}_{cv}\cdot\hat{\xi}) + \frac{i\hbar\vec{\omega}_c}{E_g}\cdot(\vec{p}_{cv}\times\hat{\xi}) \Big\} \times \langle F_{c\mu'} | F_{v\mu} \rangle + \vec{T}_{cv}\cdot\langle F_{c\mu'} | \vec{\pi} | F_{v\mu} \rangle \Big] \qquad \text{(B-16)}$$

For B = 10^4 Gauss, $\frac{\hbar\omega_c}{E_g} \sim 10^{-4}$ if E_g = 1 eV. Thus the term involving $\frac{\hbar\omega_c}{E_g}$ differs from 1 by 10^{-3} - 10^{-4} for most semiconductors and hence is negligible in absorption process. Thus it is sufficient to write

$$\langle \psi_{c\mu'} | \vec{\pi}\cdot\hat{\xi} | \psi_{v\mu} \rangle \simeq (\vec{p}_{cv}\cdot\hat{\xi}) \langle F_{c\mu'} | F_{v\mu} \rangle + \vec{r}_{cv}\cdot \langle F_{c\mu'} | \vec{\pi} | F_{v\mu} \rangle \qquad \text{(B-17)}$$

For $\vec{p}_{cv} \neq 0$ and $\vec{r}_{cv} = 0$, we have the case of <u>allowed</u> transitions. Throughout the main text, we only considered such transitions.

When $\vec{p}_{cv} = 0$ and $\vec{r}_{cv} \neq 0$ we have the case of <u>forbidden</u> transitions. The absorption coefficient η_F, for forbidden transitions can be calculated by a method very similar to the one used for allowed transitions, (see Chapter 3). In the absence of magnetic field,

$$\eta_F(\omega) = \frac{2e^2\hbar^2}{3n_o m^2 c\omega} |\vec{r}_{cv}|^2 \left(\frac{2\mu}{\hbar^2}\right)^{5/2} [\hbar\omega - E_g]^{3/2} \qquad \text{(B-18)}$$

Notice that, this has quite a different energy dependence and is easy to distinguish from allowed transitions. For calculations, involving the effect of a magnetic field, the reader is referred to the literature.[23,73]

APPENDIX C

THE TWO-CENTRE OVERLAP INTEGRAL (A CLOSED FORM)

We wish to evaluate

$$J_{n',n}(a) = \int_{-\infty}^{\infty} \Phi_{n'}(x)\ \Phi_{n}(x-a)\ dx \qquad \text{(C-1)}$$

where 'a' is a real constant and

$$\Phi_n(x) = \frac{1}{\sqrt{2^n\, n!\, \pi^{1/2}\, \lambda}}\ e^{-(\xi^2/2)}\ H_n(\xi), \quad \left(\xi = \frac{x}{\lambda}\right) \qquad \text{(C-2)}$$

is the nth level (n = 0, 1, 2, ...) simple harmonic oscillator wavefunction normalized in x and centred about x = 0. The parameter ξ is a dimensionless number since $\lambda = (\frac{c\hbar}{eB})^{\frac{1}{2}}$ is the magnetic length, and $H_n(\xi)$ is the Hermite polynomial defined by[15,74]

$$H_n(\xi) = (-1)^n\ e^{\xi^2}\ \frac{d^n}{d\xi^n}\left(e^{-\xi^2}\right)$$

and has for its generating function

$$\exp\left(-\xi^2 + 2s\xi\right) = \sum_{n=0}^{\infty} \frac{H_n(\xi)}{n!}\ s^n \qquad \text{(C-3)}$$

From (C-1), (C-2) and (C-3) we get

$$\sum_{n',n=0}^{\infty} \left[\left(2^{n+n'}\pi\right)^{1/2} J_{n',n}(a) \frac{t^n}{\sqrt{n!}} \frac{s^{n'}}{\sqrt{n'!}} \right]$$

$$= \int_{-\infty}^{\infty} d\xi \, \exp\left\{ -s^2 + 2s\xi - t^2 + 2t(\xi + \gamma) - \xi^2 - \xi\gamma - \frac{\gamma^2}{2} \right\}$$

where $\gamma = \frac{a}{\lambda}$ is a dimensionless quantity. Completing the square on ξ in the exponent of the right-hand side we get

$$\sum_{n',n=0}^{\infty} \left[\left(2^{n+n'}\pi\right)^{1/2} J_{n',n}(a) \frac{t^n s^{n'}}{\sqrt{n!\,n'!}} \right]$$

$$= \exp\left[-\frac{1}{4}\gamma^2 + \gamma s + \gamma t - \gamma s + st \right] \times \int_{-\infty}^{\infty} d\xi \, \exp\left[-\left\{ \xi - \left(s + t - \frac{\gamma}{2}\right) \right\}^2 \right]$$

The integral on the right-hand side is, by change of variables, equal to $\int_{-\infty}^{\infty} e^{-u^2} du = \sqrt{\pi}$, and expanding the terms containing s, t we get

$$\sum_{n',n=0}^{\infty} J_{n',n}(a) \frac{\left(2^{n+n'}\right)^{1/2}}{\sqrt{n!\,n'!}} t^n s^{n'} = \exp\left(-\frac{1}{4}\gamma^2\right)$$

$$\times \left[\sum_{p=0}^{\infty} \frac{(2st)^p}{p!} \right] \left[\sum_{q=0}^{\infty} \frac{(\gamma t)^q}{q!} \right] \left[\sum_{r=0}^{\infty} \frac{(-1)^r (\gamma s)^r}{r!} \right]$$

Equating the terms of order $t^n s^{n'}$ on both sides we get

$$J_{n',n}(a) = \frac{\sqrt{n!\,n'!}}{\left(2^{n+n'}\right)^{1/2}} e^{-(\gamma^2/4)} \sum_{\ell=0}^{\min\{n',n\}} \frac{2^\ell (\gamma)^{n-\ell} (-\gamma)^{n'-\ell}}{\ell!\,(n-\ell)!\,(n'-\ell)!}$$

or

$$J_{n',n}(a) = \frac{e^{-(\gamma^2/4)}}{(2^{n+n'} n!\, n'!)^{1/2}} \sum_{\ell=0}^{\min\{n',n\}} \frac{(-1)^{n'-\ell}\, n!\, n'!\, 2^{\ell}\, \gamma^{n+n'-2\ell}}{\ell!\,(n-\ell)!\,(n'-\ell)!} \qquad \text{(C-4)}$$

This is the form in which it is sometimes used. For $n \geq n'$

$$J_{n',n}(a) = \frac{\sqrt{n!\, n'!}}{(2^{n+n'})^{1/2}}\, e^{-(\gamma^2/4)}\, \gamma^{n-n'}\, 2^{n'} \sum_{\ell=0}^{n'} \frac{(-\gamma^2/2)^{n'-\ell}}{\ell!\,(n-\ell)!\,(n'-\ell)!}$$

Letting $n' - \ell = u$ in the sum we obtain

$$J_{n',n}(a) = e^{-(\gamma^2/4)} \left(\frac{\gamma}{\sqrt{2}}\right)^{n-n'} \left(\frac{n'!}{n!}\right)^{1/2} \left[(n!) \sum_{u=0}^{n'} \frac{(-\gamma^2/2)^{u}}{u!\,(n'-u)!\,(n-n'+u)!}\right]$$

or

$$J_{n',n}(a) = \left(\frac{n'!}{n!}\right)^{1/2} \left(\frac{\gamma}{\sqrt{2}}\right)^{n-n'} e^{-(\gamma^2/4)}\, L_{n'}^{n-n'}\left(\frac{\gamma^2}{2}\right), \quad n \geq n' \qquad \text{(C-5)}$$

where $L^{p}_{q}(x)$ is the associated Laguerre polynomial defined by [74]

$$L^{p}_{q}(x) = (p+q)! \sum_{u=0}^{q} \frac{(-x)^{u}}{u!\,(q-u)!\,(p+u)!} \qquad \text{(C-6)}$$

where $p > -1$, q and u are integers though p need not be in which case gamma functions are used where necessary. To obtain

the Laguerre polynomial occuring in (C-4), make the identifications $n' = q$, $n = p + q$. By following a very similar method we have for the case $n' \geq n$

$$J_{n',n}(\alpha) = \left(\frac{n!}{n'!}\right)^{1/2} \left(-\frac{\gamma}{\sqrt{2}}\right)^{n'-n} e^{-(\gamma^2/4)} L_n^{n'-n}\left(\frac{\gamma^2}{2}\right) \quad , \quad n' \geq n \qquad \text{(C-7)}$$

For $n = n'$, both (C-5) and (C-7) give the same result.

APPENDIX D

THE TWO-CENTRE OVERLAP INTEGRAL (A POWER SERIES EXPANSION)

We wish to derive a power series expansion for $J_{n',n}(a)$, for small values of real constant 'a'. The overlap integral was defined in Appendix (C) in terms of the harmonic oscillator wave functions. For the purposes of making a Taylor series expansion, we introduce two dimensionless quantities

$$\gamma = \frac{a}{\lambda} \quad , \quad \xi = \frac{x}{\lambda}$$

in terms of which

$$J_{n',n}(a) = \int_{-\infty}^{\infty} \Phi_{n'}(\xi) \, \Phi_{n}(\xi + \gamma) \, d\xi \qquad \text{(D-1)}$$

where

$$\Phi_{n}(\xi) = \frac{1}{\sqrt{2^{n} \, n! \, \pi^{1/2}}} \; e^{-(\xi^2/2)} \; H_{n}(\xi) \qquad \text{(D-2)}$$

satisfies the orthonormality condition

$$\int_{-\infty}^{\infty} \Phi_{n'}(\xi) \, \Phi_{n}(\xi) \, d\xi = \delta_{n',n} \qquad \text{(D-3)}$$

For $\gamma \ll 1$

$$\Phi_n(\xi+\gamma) \simeq \Phi_n(\xi) + \gamma \frac{d\Phi_n(\xi)}{d\xi} + \frac{\gamma^2}{2!}\frac{d^2\Phi_n}{d\xi^2} + \cdots$$

$$= \Phi_n(\xi) + (\cdot)\left\{-\xi\,\Phi_n(\xi) + \frac{e^{-\xi^2/2}}{\sqrt{2^n n!\,\pi^{1/2}}} H_n'(\xi)\right\}$$

$$+ \left(\frac{\gamma^2}{2}\right)\left\{(\xi^2-1)\,\Phi_n(\xi) - \frac{2\xi\, e^{-\xi^2/2}}{\sqrt{2^n n!\,\pi^{1/2}}} H_n'(\xi) + \frac{e^{-\xi^2/2}}{\sqrt{2^n n!\,\pi^{1/2}}} H_n''(\xi)\right\} + O(\gamma^3) \qquad \text{(D-4)}$$

the prime over, $H_n(\xi)$, denotes differenciation with respect to its argument. Substitute (D-4) into (D-1) and split the integral into three parts, then

$$J_{n',n}(\gamma) \simeq J^{(0)}_{n',n} + J^{(1)}_{n',n} + J^{(2)}_{n',n} \qquad \text{(D-5)}$$

where

$$J^{(0)}_{n',n} = \int_{-\infty}^{\infty} \Phi_{n'}(\xi)\,\Phi_n(\xi)\,d\xi \,, \qquad \text{(D-6)}$$

$$J^{(1)}_{n',n} = (-\gamma)\int_{-\infty}^{\infty} \xi\,\Phi_{n'}(\xi)\,\Phi_n(\xi)\,d\xi + \left(\frac{\gamma}{\sqrt{2^n n!\,\pi^{1/2}}}\right)\int_{-\infty}^{\infty} e^{-\xi^2/2}\,\Phi_{n'}(\xi)\,H_n'(\xi)\,d\xi \,. \qquad \text{(D-7)}$$

and

$$J^{(2)}_{n',n} = \left(-\frac{\gamma^2}{2}\right)\int_{-\infty}^{\infty} \Phi_{n'}(\xi)\,\Phi_n(\xi)\,d\xi + \left(\frac{\gamma^2}{2}\right)\int_{-\infty}^{\infty} \xi^2\,\Phi_{n'}(\xi)\,\Phi_n(\xi)\,d\xi$$

$$-\left(\frac{\gamma^2}{2\sqrt{2^n n!\,\pi^{1/2}}}\right)\int_{-\infty}^{\infty} \xi\, e^{-\xi^2/2}\,\Phi_{n'}(\xi)\,H_n'(\xi)\,d\xi \qquad \text{(D-8)}$$

$$+\left(\frac{\gamma^2}{2\sqrt{2^n n!\,\pi^{1/2}}}\right)\int_{-\infty}^{\infty} e^{-\xi^2/2}\,\Phi_{n'}(\xi)\,H_n''(\xi)\,d\xi$$

In order to carry out the various integrations involved above, we need to know a few properties of Hermite polynomials and the integrals involving them. For convenience we list some useful properties of Hermite polynomials below[15].

$$\text{For} \quad n > 0\,, \quad H_n'(\xi) = 2n\,H_{n-1}(\xi) \quad ; \quad H_0'(\xi) = 0 \qquad \text{(D-9)}$$

For $n > 1$,

$$H_n''(\xi) = 4n\,\xi\,H_{n-1}(\xi) - 2n\,H_n(\xi)$$

and (D-10)

$$H_0''(\xi) = H_1''(\xi) = 0$$

Further

$$\int_{-\infty}^{\infty} e^{-\xi^2} H_n(\xi)\,H_m(\xi)\,d\xi = \left(2^n n!\,\pi^{1/2}\right)\delta_{m,n}\,, \qquad \text{(D-11)}$$

$$\int_{-\infty}^{\infty} e^{-\xi^2} \xi\, H_n(\xi)\, H_m(\xi)\, d\xi = \left\{ 2^n (n+1)!\, \pi^{1/2} \right\} \delta_{m,n+1} + \left\{ 2^{n-1} (n)!\, \pi^{1/2} \right\} \delta_{m,n-1} \qquad \text{(D-12)}$$

and

$$\int_{-\infty}^{\infty} e^{-\xi^2} \xi^2\, H_n(\xi)\, H_m(\xi)\, d\xi = \left\{ 2^n (n+2)!\, \pi^{1/2} \right\} \delta_{m,n+2} + \left\{ 2^{n-2} (n)!\, \pi^{1/2} \right\} \delta_{m,n-2} + \left\{ 2^n \left(n+\tfrac{1}{2}\right) \pi^{1/2} \right\} \delta_{m,n} \qquad \text{(D-13)}$$

We now proceed to evaluate (D-6), (D-7) and (D-8) using the above properties. Integral (D-6) can be completed immediately using the orthonormality condition (D-3) and we get

$$J^{(0)}_{n',n} = \delta_{n',n} \qquad \text{(D-14)}$$

Next, from (D-7) and (D-2) we have

$$J^{(1)}_{n',n} = \left(- \frac{\gamma}{\sqrt{2^{n+n'} n!\, n'!\, \pi}} \right) \left[\int_{-\infty}^{\infty} e^{-\xi^2} \xi\, H_n(\xi)\, H_{n'}(\xi)\, d\xi - (2n) \int_{-\infty}^{\infty} e^{-\xi^2} H_{n-1}(\xi)\, H_{n'}(\xi)\, d\xi \right]$$

where in the second integral above, we employed the relation (D-9). The integrals can now be completed by using (D-11) and (D-12) and we finally obtain

$$J^{(1)}_{n',n} = (\gamma)\left\{-\left(\frac{n+1}{2}\right)^{1/2}\delta_{n',n+1} + \left(\frac{n}{2}\right)^{1/2}\delta_{n',n-1}\right\} \qquad \text{(D-15)}$$

The second delta function gives zero if n = 0. Substituting (D-9), (D-10) and (D-2) into (D-8) and simplifying we get

$$J^{(2)}_{n',n} = \left(\frac{\gamma^2}{2}\right)\left[-2\left(n+\tfrac{1}{2}\right)\int_{-\infty}^{\infty}\Phi_{n'}(\xi)\,\Phi_n(\xi)\,d\xi + \frac{1}{\sqrt{2^{n+n'}n!\,n'!\,\pi}}\int_{-\infty}^{\infty}e^{-\xi^2}\xi^2 H_{n'}(\xi)\,H_n(\xi)\,d\xi\right]$$

or

$$J^{(2)}_{n',n} = \left(\frac{\gamma^2}{2}\right)\left[-\left(n+\tfrac{1}{2}\right)\delta_{n',n} + \frac{\sqrt{(n+2)(n+1)}}{2}\delta_{n',n+2} + \frac{\sqrt{(n)(n-1)}}{2}\delta_{n',n-2}\right] \qquad \text{(D-16)}$$

where we used (D-3) and (D-13) to arrive at the final result. The last delta function in (D-16) makes no contribution if n = 0 or 1. Substituting (D-14), (D-15), (D-16) in (D-5) the power series expansion for $J_{n',n}(a)$ up to second order in the expansion para-

meter γ is,

$$J_{n',n}(a) \simeq \delta_{n',n} + (\gamma)\left\{-\left(\frac{n+1}{2}\right)^{1/2}\delta_{n',n+1} + \left(\frac{n}{2}\right)^{1/2}\delta_{n',n-1}\right\}$$

$$+\left(\frac{\gamma^2}{2}\right)\left\{-\left(n+\frac{1}{2}\right)\delta_{n',n} + \frac{\sqrt{(n+2)(n+1)}}{2}\,\delta_{n',n+2}\right. \qquad \text{(D-17)}$$

$$\left. + \frac{\sqrt{(n)(n-1)}}{2}\,\delta_{n',n-2}\right\}$$

APPENDIX E

APPROXIMATE EVALUATION OF TWO IMPORTANT INTEGRALS

(i) We wish to evaluate the definite integral

$$I_1 = \int_{\beta}^{\infty} \frac{1}{4t^{1/2}} \exp\left(-\frac{4}{3} t^{3/2}\right) dt$$

where $\beta >> 1$. Following the procedure used by Fritsche[75], for evaluating similar integrals, we introduce a new variable λ through the relation

$$t - \beta = \frac{1}{2} \beta^{-1/2} \lambda^2$$

Then

$$t^{3/2} = \beta^{3/2} \left(1 + \frac{\lambda^2}{2\beta^{3/2}}\right) \simeq \beta^{3/2} + \frac{3}{4} \lambda^2$$

and

$$t^{1/2} \simeq \beta^{1/2}$$

where the second term in the expansion of $t^{\frac{1}{2}}$ has been neglected. Thus

$$I_1 \simeq \frac{1}{4\beta} \exp\left(-\frac{4}{3} \beta^{3/2}\right) \int_0^{\infty} e^{-\lambda^2} \lambda \, d\lambda$$

By a simple change of variables, we immediately arrive at the final result:

$$I_1 \simeq \frac{1}{8\beta} \exp\left(-\frac{4}{3} \beta^{3/2}\right)$$

(ii) Next, we want to evaluate approximately the integral

$$I_2 = \int_0^b \frac{1}{t^{1/2}} \sin^2\left(\frac{2}{3}t^{3/2} + \frac{\pi}{4}\right) dt$$

where $b \gg 1$. Writing the sine function as cosine of double the angle and splitting the resulting expression into two parts we get

$$I_2 = \frac{1}{2}\int_0^b \frac{dt}{t^{1/2}} - \frac{1}{2}\int_0^b \frac{1}{t^{1/2}} \cos\left(\frac{4}{3}t^{3/2} + \frac{\pi}{2}\right) dt$$

$$= b^{1/2} + \frac{1}{2}\int_0^b \frac{\sin(4/3\, t^{3/2})}{t^{1/2}} dt$$

To complete the remaining integral, define a new variable $x = t^{\frac{1}{2}}$ and extend the upper limit to infinity, thus

$$I_2 \simeq b^{1/2} + \int_0^\infty \sin\left(\frac{4}{3}x^3\right) dx$$

$$= b^{1/2} + \Gamma(1/3)\sin(\pi/6)\Big/3(4/3)^{1/3}$$

where we made use of the standard integral

$$\int_0^\infty \sin(a x^p)\, dx = \frac{\Gamma(1/p)\sin(\pi/2p)}{p\,(a)^{1/p}}$$

Now

$$\Gamma(1/3) \simeq 2.679$$

$$\therefore \quad I_2 \simeq b^{1/2}\left(1 + \frac{0.4}{b^{1/2}}\right)$$

Hence $$I_2 \simeq b^{1/2} \quad \text{for} \quad b \gg 1$$

APPENDIX F

DERIVATION OF FRANZ-KELDYSH EFFECT USING TUNNELING METHOD

Here we wish to derive an expression for the electro-absorption coe 'icient, for photon energies below the band gap. In the main body of the thesis, we discussed this phenomenon using a different method, here we find it instructive to view this as a tunneling process. A strong electric field tilts the energy bands and makes photon-assisted tunneling [the Franz-Keldysh (F-K) effect] possible, (see Fig. 23). We will follow the method used by Haering and Adams[37] and work in the one-band effective mass approximation. These authors used the W.K.B. treatment, since it provides a good physical picture of the tunneling process, and we will employ the same in our subsequent calculations.

In Fig. 23 we have taken the electric field along the Z-direction and measure energies from the conduction band edge. The valence electron tunnels from the turning point Z_v to Z_m and finally tunnels to Z_c by absorbing a photon energy $\hbar\omega < E_g$. The motion of electrons and holes in the presence of a potential $V(z) = - e\mathcal{E}_z z$ (where $\mathcal{E}_z \equiv \mathcal{E}$ is electric field), is governed by (in E.M.A.)

$$\left[\frac{1}{2m_c} \hat{p}_c^{z}(z) + V(z) \right] F_c(\vec{r}) = F_c F_c(\vec{r}) \qquad \text{(F-1)}$$

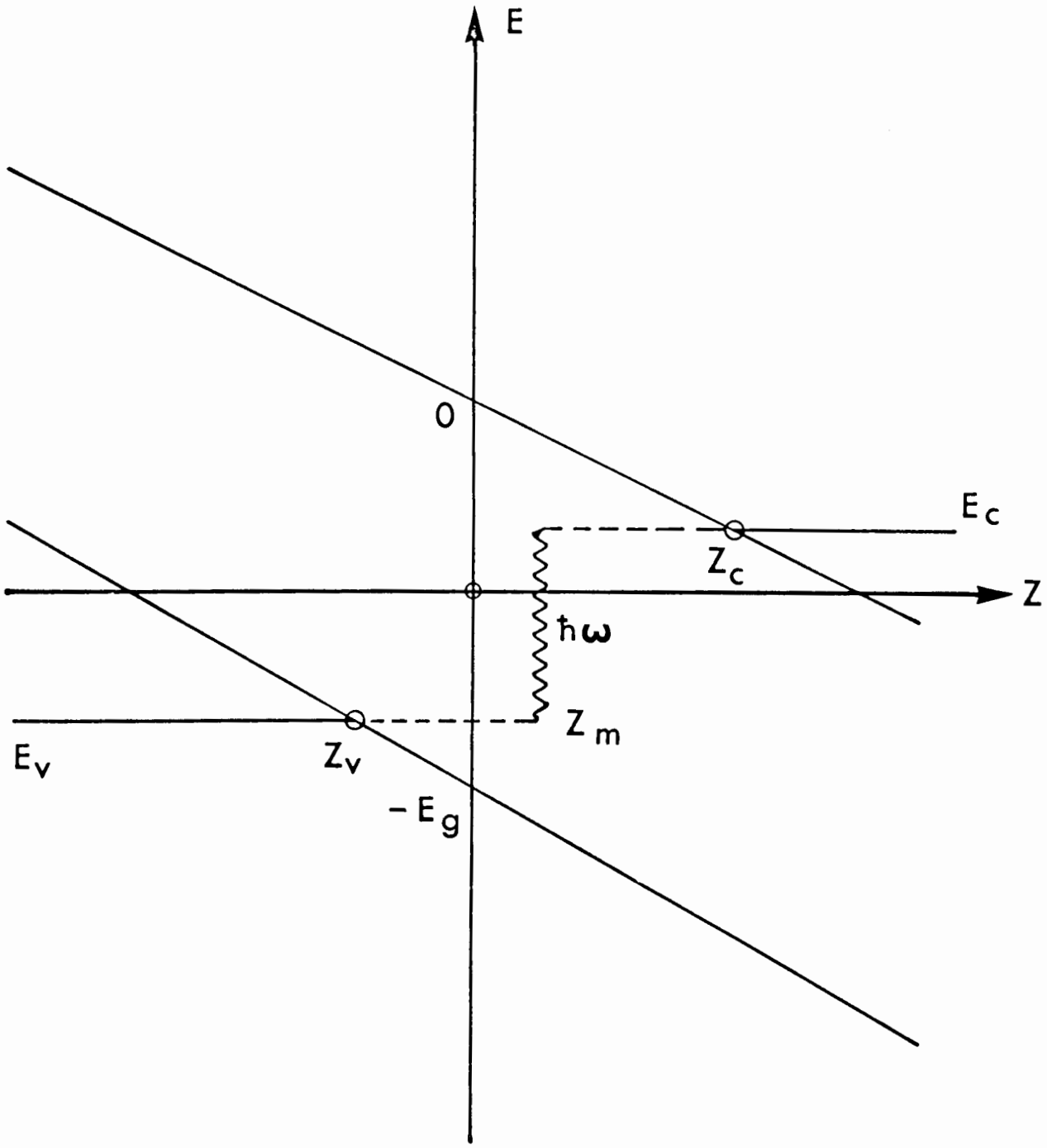

Figure 23. Photon-assisted tunneling in the presence of an electric field.

and

$$\left[-\frac{1}{2m_v} \hat{p}_v^2(z) - E_g + V(z) \right] F_v(\vec{r}) = E_v F_v(\vec{r}) \qquad \text{(F-2)}$$

In equations (F-1) and (F-2) m_c and m_v are the effective masses for the two bands. The equation (F-1) has a solution of the form

$$F_c(\vec{r}) = \frac{1}{\sqrt{L_x L_y}} e^{i(k_x x + k_y y)} \Phi_c(z) \qquad \text{(F-3)}$$

where $\Phi_c(z)$ is the normalized solution of

$$\Phi_c''(z) + \left(\frac{p_c(z)}{\hbar} \right)^2 \Phi_c(z) = 0 \qquad \text{(F-4)}$$

with

$$p_c^2(z) = 2m_c \left[E_c - E_{c\perp} - V(z) \right]$$

and

$$E_{c\perp} = \frac{\hbar^2}{2m_c} \left[k_x^2 + k_y^2 \right]$$

The normalized solution of (F-4) in the W.K.B. approximation[16] is given by

$$\Phi_c(z) = 2\left(\frac{m_c}{T_c}\right)^{1/2} \frac{1}{\sqrt{p_c(z)}} \cos\left[\frac{1}{\hbar}\int_{z_c}^{z} p_c(z)\,dz - \frac{\pi}{4}\right], \qquad z > z_c \qquad \text{(F-5a)}$$

$$= \left(\frac{m_c}{T_c}\right)^{1/2} \frac{1}{\sqrt{|p_c|}} \exp\left[-\frac{1}{\hbar}\int_{z}^{z_c} |p_c(z)|\,dz\right], \qquad z < z_c \qquad \text{(F-5b)}$$

where T_c is the classical period of the motion and z_c is the classical turning point obtained from $p_c(z_c) = 0$. The wave function $F_v(\vec{r})$ for the valence band is similar and can be obtained from the expression for $F_c(r)$ by replacing $p_c \rightarrow p_v$, where

$$p_v(z) = (2m_v)\left\{ V(z) - E_g - E_v - E_{v\perp} \right\} \qquad \text{(F-6)}$$

The turning point, z_v, for the valence band is obtained by setting $p_v(z) = 0$. Notice that $E - E_\perp$ is the kinetic energy along the field direction and will be denoted by ϵ_z, where required. From our previous analysis (see for example, equation (3-13)), we can write the expression for absorption coefficient as follows:

$$\eta = \frac{2(2\pi)^2 e^2 \left|(\vec{P}_{cv}\cdot\hat{\xi})\right|^2}{c\, m^2 n_0 \omega V} \times \sum_{\mu,\mu'} \left|I_{\mu'\mu}\right|^2 \delta(E_c - E_v - \hbar\omega) \tag{F-7}$$

where μ', μ stand for the quantum numbers of the final and initial states respectively ($\mu \equiv E_v, k_x, k_y$) and

$$I_{\mu'\mu} = \int_V F^*_{c\mu'}(\vec{r})\, F_{v\mu}(\vec{r})\, d\vec{r}$$

From (F-3) we can write

$$I_{\mu'\mu} = \delta_{k'_x, k_x}\, \delta_{k'_y, k_y} \times \int_{-\infty}^{\infty} \Phi^*_c(z)\, \Phi_v(z)\, dz$$

The integral

$$I = \int_{-\infty}^{\infty} \Phi^*_c(z)\, \Phi_v(z)\, dz \tag{F-8}$$

has been evaluated in Appendix G, by the method of steepest descent, and thus we have

$$I_{\mu'\mu} = \delta_{k'_x, k_x}\, \delta_{k'_y, k_y} \left(\frac{\pi\hbar}{T_c T_v e\mathcal{E}}\right)^{1/2} \left(\frac{2\mu}{E_g - \hbar\omega}\right)^{1/4} \times \exp\left[-\frac{p^3(z_m)}{3\hbar\mu e\mathcal{E}}\right] \tag{F-9}$$

where

$$p^2(z_m) = (2\mu)\left[E_g - \hbar\omega + E_\perp\right] \qquad \text{(F-10)}$$

and

$$E_\perp = E_{c\perp} + E_{v\perp} = \frac{\hbar^2}{2\mu}\left(k_x^2 + k_y^2\right) = \frac{\hbar^2 k_\perp^2}{2\mu} ,$$

μ being the reduced mass. Substituting (F-9) in (F-7) and including the density of initial and final states we get

$$\eta = \frac{2(2\pi)^2 e^2 \left|(\vec{P}_{cv}\cdot\hat{\xi})\right|^2}{c\, m^2 n_o \omega V}\left(\frac{\pi\hbar}{T_c T_v e\mathcal{E}}\right) \times \left(\frac{2\mu}{E_g - \hbar\omega}\right)^{1/2}\left(\frac{T_c}{2\pi\hbar}\right)\left(\frac{T_v}{2\pi\hbar}\right)\int_{-e\mathcal{E}L_z/2}^{e\mathcal{E}L_z/2} d\epsilon_z \times \int_{-\infty}^{\infty}\frac{L_x\, dk_x}{(2\pi)}\int_{-\infty}^{\infty}\frac{L_y\, dk_y}{2\pi}\ \exp\left[-\frac{2}{3}\frac{p^3(z_m)}{\hbar\mu e\mathcal{E}}\right]$$

$$= R\,\frac{\hbar}{8\mu(\omega_g - \omega)^{1/2}}\int_0^\infty 2k_\perp\, dk_\perp\ \exp\left[-\frac{2}{3}\frac{p^3(z_m)}{\hbar\mu e\mathcal{E}}\right]$$

where

$$K = \frac{\pi e^2 \left|(\vec{P}_v\cdot\hat{\xi})\right|^2}{\hbar\omega\, n_o\, c\, m^2}\left(\frac{2\mu}{\hbar}\right)^{3/2} , \quad \hbar\omega_g = E_g$$

To complete the integral, we expand

$$p^3(Z_m) \simeq (2\mu)^{3/2}(E_g - \hbar\omega)^{3/2}\left\{1 + \frac{3}{2}\frac{E_\perp}{(E_g - \hbar\omega)}\right\}$$

and redefining variables, we finally obtain

$$\eta = R\,\frac{\Theta_F^{3/2}}{\delta(\omega_g - \omega)}\exp\left[-\frac{4}{3}\left(\frac{\omega_g - \omega}{\Theta_F}\right)^{3/2}\right] \qquad \text{(F-11)}$$

where

$$\Theta_F = \left(\frac{e^2\mathcal{E}^2}{2\mu\hbar}\right)^{1/3}$$

This is the expression we were after and, agrees with earlier results.

APPENDIX G

THE EVALUATION OF THE TUNNELING INTEGRAL BY THE METHOD OF STEEPEST DESCENT

We wish to evaluate the integral

$$I = \int_{-\infty}^{\infty} \Phi_c^*(z)\, \Phi_v(z)\, dz \qquad \text{(G-1)}$$

where the functions Φ_c and Φ_v have been defined in previous Appendix F. From the disucssion given there it should be quite clear that the product, $\Phi_c^* \Phi_v$ is quite small in the regions $Z < Z_v$ and $Z > Z_c$ (see Fig. 23 of the Appendix F). Thus we need to evaluate the above integral carefully only in the region $Z_v < Z < Z_c$, where the product of two wave functions is still appreciable. In this region of space

$$\Phi_c(z) = \left(\frac{m_c}{T_c}\right)^{1/2} \frac{1}{\sqrt{|p_c(z)|}} \exp\left[-\frac{1}{\hbar}\int_z^{Z_c} |p_c(z)|\, dz\right], \quad z < z_c \qquad \text{(G-2)}$$

and

$$\Phi_v(z) = \left(\frac{m_v}{T_v}\right)^{1/2} \frac{1}{\sqrt{|p_v(z)|}} \exp\left[-\frac{1}{\hbar}\int_{Z_v}^{z} |p_v(z)|\, dz\right], \quad z > z_v \qquad \text{(G-3)}$$

The turning points Z_c, Z_v satisfy the relations $|p_c(Z_c)| = 0$ and $|p_v(Z_v)| = 0$, respectively, where

$$|p_c(z)| = (2m_c)^{1/2} \left[V(z) - (E_c - E_{c\perp})\right]^{1/2}, \qquad \text{(G-4)}$$

$$|p_v(z)| = (2m_v)^{1/2} \left[E_g + E_v + E_{v\perp} - V(z) \right]^{1/2} \qquad (G\text{-}5)$$

and

$$V(z) = - e \mathcal{E} z \qquad (G\text{-}6)$$

Furthermore the integral (G-1) is required only for $E_c = E_v + \hbar\omega$, because of the delta function in the equation (F-7). Now the method of steepest descent consists in writing the integrand in an exponential form and making the Taylor series expansion in the exponential. Substituting (G-2) and (G-3) in (G-1) we get

$$I = \left(\frac{m_c m_v}{T_c T_v} \right)^{1/2} \frac{1}{\sqrt{|p_c(z_m)|\,|p_v(z_m)|}} \int dz \; e^{f(z)} \qquad (G\text{-}7)$$

where

$$f(z) = - \frac{1}{\hbar} \int_{z}^{z_c} |p_c(z)|\, dz - \frac{1}{\hbar} \int_{z_v}^{z} |p_v(z)|\, dz$$

and the slowly varying quantities have been evaluated at the matching point Z_m, to be determined from the relation $f'(Z_m) = 0$. Now

$$f'(Z_m) = \frac{1}{h}\left[\ldots\right] - \frac{1}{h}\left[\ldots\right] \qquad \text{(G-8)}$$

Setting $f'(Z_m) = 0$ and using (G-4), (G-5) and (G-6), we get

$$Z_m = -\frac{1}{2\beta}\left[\Gamma + \frac{m_v}{m_c + m_v}\left(\ldots\right)\right] \qquad \text{(G-9)}$$

and

$$|k(Z_m)| = |k_v(Z_m)| = p(Z_m) = (2m)^{\frac{1}{2}}\left[E_g - E_0 + E_\perp\right] \qquad \text{(G-10a)}$$

with

$$E_\perp = \frac{\hbar^2}{2\mu}\left(k_c^2 + \ldots\right) \qquad \text{(G-10b)}$$

One can easily convince oneself that $Z_v < Z_m < Z_c$ and thus the point Z_m lies in the forbidden gap as shown in Fig. 23 of Appendix F. Further

$$f''(Z_m) = -\frac{e\mathcal{E}(m_c + m_v)}{\hbar\, p(Z_m)} \qquad \text{(G-11)}$$

Now Taylor expanding the exponential in (G-7) about the point Z_m and making use of equations (G-8) through (G-11) we get

$$I = [illegible]$$

where

$$\sigma = [illegible]$$

We can extend the limits of integration on z to $\pm\infty$, without making any serious error and then the Gaussian distribution integral contributes unity. Also if we take $p(Z_m) \simeq (2\mu)^{\frac{1}{2}} \times (E_g - \hbar\omega)^{\frac{1}{2}}$, we get

$$I \simeq [illegible] \qquad \text{(G-11)}$$

It is lengthy, but rather straight forward calculation to evaluate $f(Z_m)$, and one can show that

$$f(Z_m) = -\frac{1}{\hbar}\int_{Z_m}^{Z_c} |p(Z)|\, [illegible]$$

$$= [illegible]$$

$$= -\frac{[illegible]\ (Z_m)}{3\hbar\, [illegible]}$$

Hence

$$= \left(\frac{\pi \hbar}{T_c T_v e^{\varepsilon}} \right)^{1/2} \left(\frac{}{F_q} \frac{}{\hbar\omega} \right)^{1/4} \exp\left[\frac{}{} \right] \qquad \text{(G-12)}$$

where $p(Z_m)$ is given by the equation (G-10).

APPENDIX H

A RECENT DEVELOPMENT IN MAGNETO-OPTICS

H.1 Introduction

The magneto-optic experiments that we have discussed so far were restricted to semiconductors, where one typically shines infra-red or visible radiation to promote the carriers across the forbidden gap. High magnetic fields ($\sim 10^4$ gauss) are required to satisfy the condition $\omega_c \tau > 1$, as no structure can be resolved otherwise. In any case no structure is expected below several kilogauss even if one goes to the lowest achievable temperatures. This certainly does not appear to be the case in metals, where lots of structure has been observed[76,77,78,79] in the microwave region for magnetic fields less than one hundred gauss. In this chapter, we theoretically analyse the observed low field structure in metals and also investigate the possibility of observing similar effects in semiconductors. It is convenient to discuss the cases of metals and semiconductors separately.

H.2 Low Field Structure in Metals

The experimental conditions for which the low field effects are observed in metals are basically the following. One shines microwaves onto a single crystal of a pure metal and also applies a small magnetic field ($\sim$ 0.1 to 100 gauss) parallel to the

surface. The geometry is similar to the one used in studying Azbel-Kaner[80] cyclotron resonance. The experiment is done at low temperatures (1 to 20° K) and the microwave frequencies range from 10 to 70 GHz. The conditions are always such that $\omega\tau > 1$ and $\omega_c\tau < 1$ (because low magnetic field), where ω and ω_c are the microwave and cyclotron frequencies respectively, and τ, the relaxation time for the electrons. The absorption lines observed were exceedingly narrow and for a given peak $B \propto \omega^{3/2}$. Until recently no theory could explain the cause of this weak field structure in metals.

Since the microwave field can penetrate only a very short distance δ ($\sim 10^{-5}$ cm.) in metals, it became quite clear that the effects were essentially due to the electron trajectories in the skin layer, because it is only those electrons whose orbits pass through the skin layer, can interact with the incident microwave and cause absorption. For electrons moving with the Fermi velocity V_F

$$m V_F = \hbar k_F \simeq 10^8 \hbar \ (\text{cm}^{-1}) \qquad \text{(H-1)}$$

the cyclotron radius

$$R_c = \frac{V_F}{\omega_c} = \frac{\hbar k_F}{m \omega_c}$$

or using (H-1)

$$R_c = \frac{v_F}{\omega_c} \quad (\text{cm.}) \qquad \text{(H-2)}$$

At B = 10 gauss, $R_c \sim 1$ cm. which is very much greater than the penetration depth δ. A single traversal of the skin layer by the electrons in a skimming trajectory (Fig. 24) ($R_c \sim 1$ cm.) could not possibly account for the observed narrow lines. On the other hand, the electrons could not be expected to make several traversals and still stay in phase with the microwave field, because this would require the condition $\omega_c \tau > 1$, which is certainly not fulfilled at the low fields, under consideration. Thus we need a mechanism that would confine the electrons in the surface layer for considerable time, even when $\omega_c \tau < 1$.

A convincing explanation in terms of magnetic field induced surface quantum states has been put forward by Nee and Prange[81,82]. The surface states can be visualized in terms of a skipping orbit trajectory (Fig. 24). In the presence of a magnetic field, an electron striking the surface, if specularly reflected, will continue to move parallel to the surface in successive bounces. Such a skipping trajectory describes an electron bound to the surface region. It is trapped in a potential well formed on one side by the vacuum-metal interface potential, on the other by the

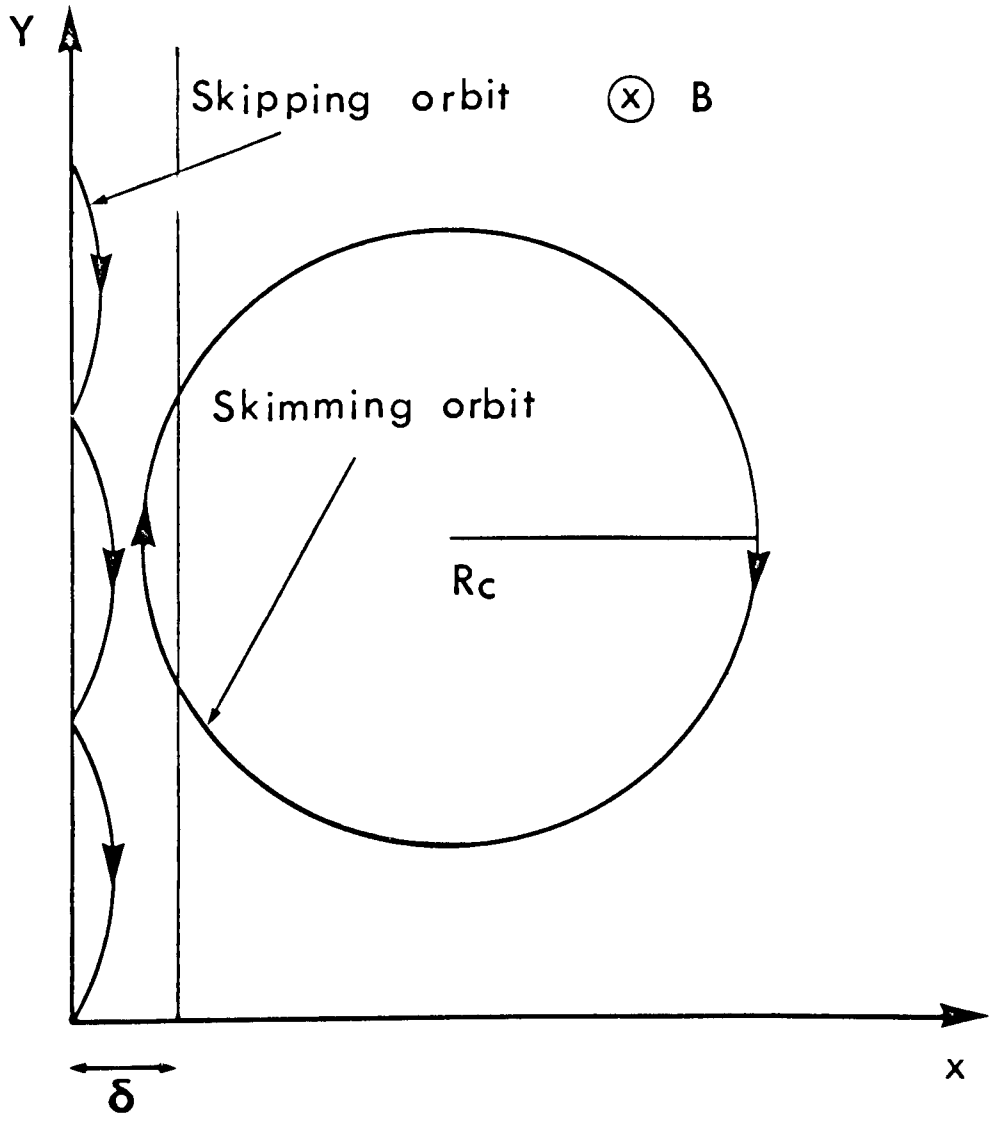

Figure 24. Electrons in skimming and skipping orbits in the X-Y plane, when the magnetic field is directed parallel to the Z-axis. The skipping orbits give rise to the magnetic field-induced surface quantum states.

magnetic field confining it to within the classical turning points of the circular motion. The quantum mechanics of an electron in this potential well, leads to a discrete energy level spectrum for the surface quantum states if $R_c > \delta$ (see Appendix I). We have worked out the energy level spectrum for $R_c > \delta$ in Appendix I and have shown that the transitions among these discrete sets of levels successfully account for the microwave impedance oscillations in metals. If $R_c < \delta$, the energy spectrum is continuous and the structure due to surface states cannot be seen. For the details of the calculations and the theoretical explanation of the observed low field structure in metals, we refer the reader to Appendix I.

H.3 Low Field Structure in Semiconductors

Now, we are ready to discuss the possibility of observing impedance oscillations in semiconductors at low magnetic fields. In semiconductors we could use infra-red or visible radiation to create free carriers and then study the absorption of microwave radiation by these carriers, in an ettempt to see surface states. Alternatively we can study the interband absorption as a function of frequency and under high absorption condition, this curve may show structure due to surface states. It will be found below, that the microwave experiments in semiconductors will not show any structure at low fields ($\omega_c \tau < 1$) because microwave absorption

requires the condition $\omega_{cT} > 1$.[83] Thus there is not enough absorption to satisfy the condition $R_c > \delta$ which is essential for the observation of surface states. The structure due to surface states may exist in the interband absorption spectrum under high absorption conditions. We discuss these two types of experiments below.

(i) Microwave Absorption

It is pointed out in Appendix I, that for surface states to be observable, the condition $R_c > \delta$ must be satisfied. We will argue in this sub-section that such a condition cannot be satisfied for the microwave absorption in semiconductors. Let us assume that the carriers in the conduction band are thermalised and possess energy, $kT = 2.5 \times 10^{-4}$ eV, at 3° K. The cyclotron radius for an electron of effective mass m_c and cyclotron frequency ω_{cc} is given by

$$kT = \frac{1}{2} m_c k_c^2 \omega_{cc}^2$$

or

$$k_c = \sqrt{\frac{2kT}{m_c \omega_{cc}^2}}$$

where

$$\omega_{cc} = \frac{eB}{m_c c}$$

Alternatively we can write

$$R_c = \sqrt{\frac{2kT}{\hbar\omega_{cc}}}\,\lambda \qquad \text{(H-3)}$$

Now for $kT = 2.5 \times 10^{-4}$ eV ,

$m_c = \frac{1}{10} m$, $\delta = [illegible]$,

$\hbar\omega_{cc} = 1{\cdot}1 \times 10^{-8} \frac{B}{(m_c/m)}$ (eV) = [illegible] V for above values

and $\lambda = 9{\cdot}5 \times 10^{-4} B^{-1/2}$ [illegible] cm. for above values

Hence

$$R_c \simeq 1{\cdot}6 \times 10^{-5} \text{ cm.}$$

The microwave absorption coefficient under the condition $\omega_c \tau < 1$ is very small ($< 10^2$ cm^{-1}) and thus the penetration depth is quite large. So the essential condition $R_c > \delta$ cannot be fulfilled and hence no structure can be observed at low magnetic fields at microwave frequencies.

(ii) Interband Absorption

It was derived in Chapter 4 that the interband absorption coefficient increases proportional to the square root of the

frequency, measured from the direct band-gap frequency. Even when we apply a magnetic field of about ten gauss, there is no doubt that such a relationship will be obeyed, because the magnetoabsorption structure does not appear until the magnetic field arises up to several kilogauss. Thus at high frequencies, the absorption would be quite strong ($\sim 10^5$ cm^{-1}) and it may be possible to get into the region $\delta < R_c$. We can take over the entire formalism as developed for metals in the Appendix I, if we replace the Fermi energy E_F, by ε, the energy of the carrier measured from the conduction band edge (i.e. excitation energy of the electron in the conduction band). The energy ε, can be related to the measureable quantities in the following fashion. We know

$$E_c(\vec{k}) = E_c^0 + \frac{\hbar^2 k^2}{2m_c} \qquad \text{(H-4)}$$

and

$$E_v(\vec{k}) = E_v^0 - \frac{\hbar^2 k^2}{2m_v} \qquad \text{(H-5)}$$

The energy, $\hbar\omega$, of the external photon which raises an electron from energy state, E_v, into a conduction band state, E_c, can be written as,

$$\hbar\omega = E_c(\vec{k}) - E_v(\vec{k}) = E_g + \frac{\hbar^2 k^2}{2\mu} \qquad \text{(H-6)}$$

Now, the desired quantity

$$\epsilon = E_c(k) - E_v = \frac{\hbar^2 k^2}{2 m_c}$$

$$= \frac{m_v}{m_c} (\hbar\omega - E_g)$$

where we used (H-6) for k^2. Finally

$$\epsilon = \frac{\hbar\omega - E_g}{\left(1 + \frac{m_v}{m_c}\right)} \qquad \text{(H-7)}$$

For $\epsilon \simeq 0.2$ eV, the absorption coefficient is of the order of 10^5 cm^{-1} and hence the penetration depth is only 10^{-5} cm. The cyclotron radius can be determined from the relationship

$$\epsilon = \frac{1}{2} m_c R_c^2 \omega_c^2$$

or

$$R_c = \left(\frac{2\epsilon}{\hbar\omega_c}\right)^{1/2} \lambda$$

With $\epsilon = 0.2$ eV, and the values of the other parameters being the same as in part (i), we discover that

$$R_c \simeq 5 \times 10^{-2} \text{ cm.}$$

Thus the cyclotron radius is about a thousand times more than the penetration depth and it appears that the surface state effects might be observable. Now let us see what the experiment

demands by the way of resolution.

In Appendix I, it is estimated that the energy separation between surface states is

$$\Delta E_{s.s.} \simeq (E_F)^{1/3} (\hbar\omega_c)^{2/3}$$

For the present case

$$\Delta E_{s.s.} \simeq (\epsilon)^{1/3} (\hbar\omega_c)^{2/3}$$

If $\epsilon = 0.2$ eV and $\hbar\omega_{cc} \simeq 1.1 \times 10^{-6}$ eV, imply

$$\Delta E_{s.s.} \simeq 10^{-4} \text{ eV}$$

Now we are probing the spectrum with typically one electron volt photons and this demands a resolution of one part in ten thousand or higher, which is not hard to obtain experimentally, especially if a single mode, stabilized laser is used. The resolution condition can be made a slightly less severe by choosing a semiconductor with low effective mass e.g. InSb for which $m_c \simeq \frac{1}{20}$ m and using a slightly higher field value. ϵ cannot be increased very much because for $\epsilon \geq 0.5$ eV, the non-parabolic effects become important and the energy relation (H-4) is no longer valid.

Further the condition $E_{s.s.} > \frac{\hbar}{\tau}$ must be satisfied because the structure would be smeared otherwise. It implies that the relaxation time $\tau > 10^{-11}$ sec. This requirement can be satisfied

by a relatively pure sample of InSb at low temperatures. Unfortunately we have not been able to estimate the magnitude of the effect and are thus unable to say as to whether or not the structure will be smeared out due to phonons and non-monoenergetic injection of the electrons in the conduction band. However, by analogy with the metals case we expect such influences to be small and expect that the structure due to surface states should be observable in semiconductors under the experimental conditions discussed above.

APPENDIX I

MAGNETIC SURFACE STATES IN METALS

Here we wish to understand theoretically the observed structure in the surface impedance of metals at low magnetic fields. The theory of Azbel-Kaner cyclotron resonance does not allow for any structure below 200 gauss. However, it has now been established beyond doubt that some unusual structure appears in the microwave impedance of metals at magnetic fields well below 100 gauss. The effect consists of a complicated oscillatory pattern of peaks (in $\frac{dR}{dB}$ or $\frac{dX}{dB}$, where R and X are real and imaginary parts of surface impedance respectively) and the magnetic field value for a given peak in the pattern is accurately proportional to the 3/2 power of the experimental frequency ($B \propto \omega^{3/2}$).

Nee and Prange[81,82] have successfully accounted for the observed structure on the basis of a magnetic field induced quantum surface states which is quantum analogue of skipping trajectory. The quantum mechanical treatment of the skipping trajectory leads to a discrete energy level spectrum and the transitions among these levels are responsible for the observed structure. We calculate the energy level spectrum using the Bohr-Sommerfeld quantization rule. Suppose the magnetic field B, directed along the Z-direction is described by the vector potential $\vec{A} = (0, Bx, 0)$. The electrons would then execute

a circular motion in the X-Y plane. An electron on the Fermi surface having energy E_F and momentum $k_F \sim 10^8$ cm^{-1} has a cyclotron radius $R_c \simeq \frac{10}{B}$. Thus for a magnetic field B ~ 10 gauss, $R_c \sim 1$ cm, which is very much greater than the microwave penetration depth $\delta \sim 10^{-5}$ cm. With the above choice of gauge, the expression for the Hamiltonian can be written as

$$H = \frac{1}{2m}\left(p - \frac{e}{c}A\right)^2$$

or defining

$$E \equiv H - \frac{\hbar^2}{2m} = \frac{1}{2}mv_c^2\left(x - x_0\right)^2 + \frac{p_z^2}{2m} \qquad \text{(I-1)}$$

where

$$x_0 = \frac{\hbar q}{mv_c} \qquad \text{(I-2)}$$

is the centre of the parabolic potential well and the X-directed motion of the particle is simple harmonic motion (Fig. 25a). Those electrons for which x_0 lies well inside the metal cannot take part in the absorption (Fig. 25a) and will not be considered any more. Only those orbits which penetrate a distance $x_n \sim \delta$ are effective in absorbing and for such orbits the centre of the potential well due to the magnetic field, and hence the centre of circular motion is at a distance less than the cyclotron radius R_c from the surface. These electrons suffer specular reflection at the surface (because their X-directed momentum is small and the

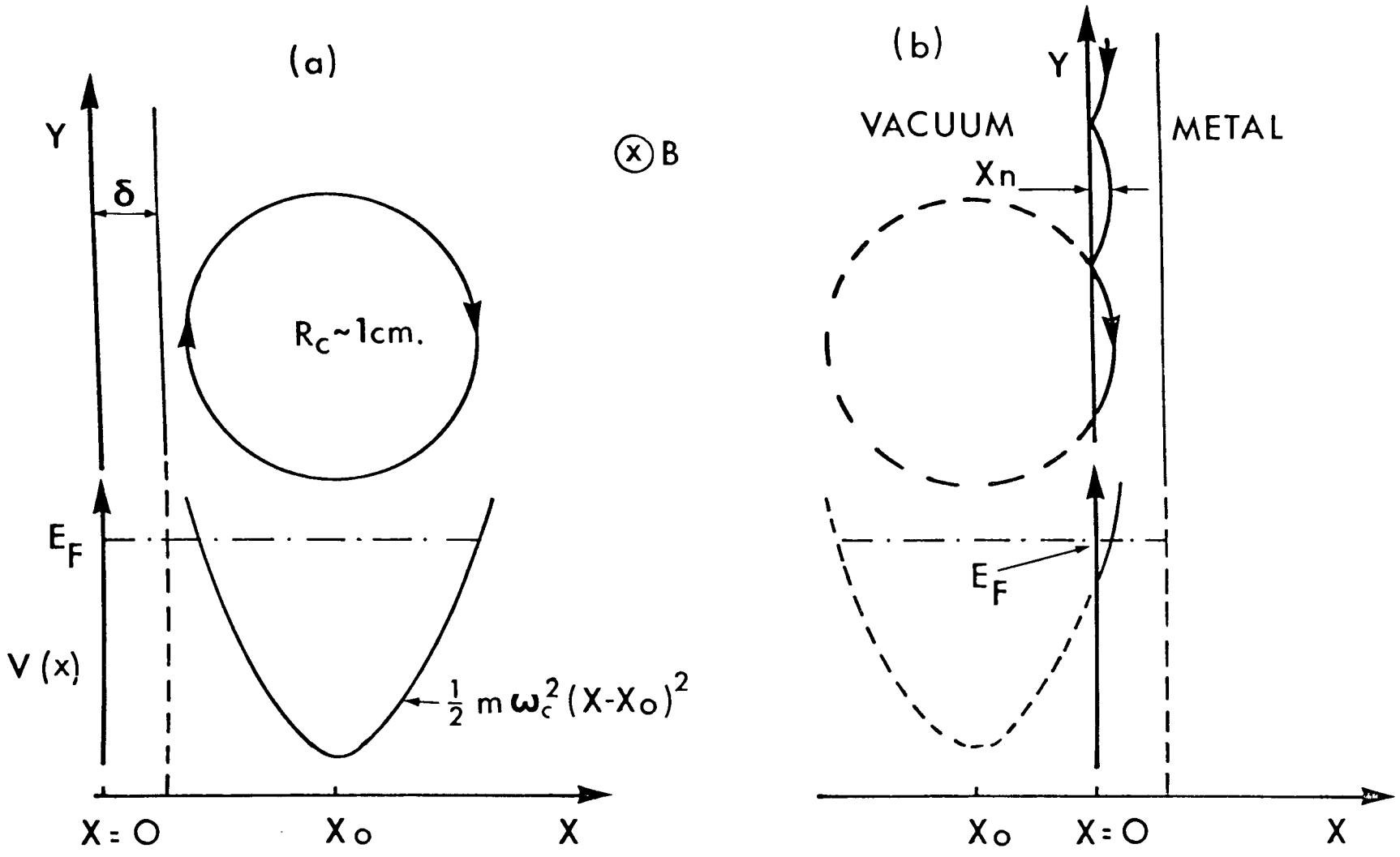

Figure 25(a). An electron in a cyclotron orbit described as a particle in a parabolic potential well.

(b). An electron in a skipping orbit trajectory described as a particle trapped between the surface potential and portion of the parabola.

corresponding wavelength is large) and they go wandering off in the negative Y-direction at nearly the Fermi velocity. (I am considering particle of charge +e.) (See Fig. 25b.) Such electrons do indeed encounter microwave radiation for considerable length of time and are responsible for the observed spectrum.

In microwave transitions the centre of the orbit is not moved, but the electron moves to an orbit of higher energy and consequently larger radius. This means that we need to derive the energy level scheme for a fixed value of p_y, and hence for a parabolic well fixed relative to the surface. Further we assume that the small portion of the parabola that lies inside the metal can be approximated by a straight line. Then

$$E \simeq \frac{p_x^2}{2m} + \frac{1}{2} m\omega_c^2 x_o^2 - m\omega_c^2 x_o \epsilon$$

Remembering in this case that x_o is negative, we write

$$\epsilon = E - \frac{1}{2} m\omega_c^2 x_o^2 = \frac{p_x^2}{2m} + m\omega_c^2 |x_o| \epsilon \qquad (I\text{-}3)$$

As stated above, the particle moves parallel to the Y-direction at nearly Fermi velocity, so we fix $p_y = p_F$. For this particular choice of p_y, the centre of the well moves out to $x_o = \frac{-p_F}{m\omega_c}$ and intersects the surface $x = 0$ at an energy $E = E_F$.

The energies of levels measured from E_F appear as

$$E - E_F = \epsilon \qquad \frac{p_x^2}{2m} + (\quad)x \qquad (I\text{-}4)$$

$$E_F = \frac{1}{2}\,m\,\omega_c^2$$

Clearly at $x = 0$, $T = V = 0$ and hence $\epsilon = 0$. As we shine microwave radiation $\hbar\omega$, the electron moves higher up in the triangular potential well (Fig. 26). We will show below that the particle can only possess a discrete set of eigenvalues. We will restrict ourselves to very small values of ϵ, so that the shallow trajectory approximation holds. This is not a restriction, since the microwave energy $\hbar\omega \ll E_F$, and all transitions occur in the vicinity of E_F. From (I-4)

$$p_x(x) = \pm \sqrt{2m(\epsilon - p_1 x)} \qquad (I\text{-}5)$$

We note that $p_x(0) = p_x(x_c) = 0$, indicating that the classical turning points of the motion are $x = 0$, x_c and the particle executes periodic motion along the X-direction. Further $p_x(x)$ is positive for the outward journey from 0 to x_c and negative for the return motion. Applying the Bohr-Sommerfeld quantization condition to this periodic X-motion we have[79]

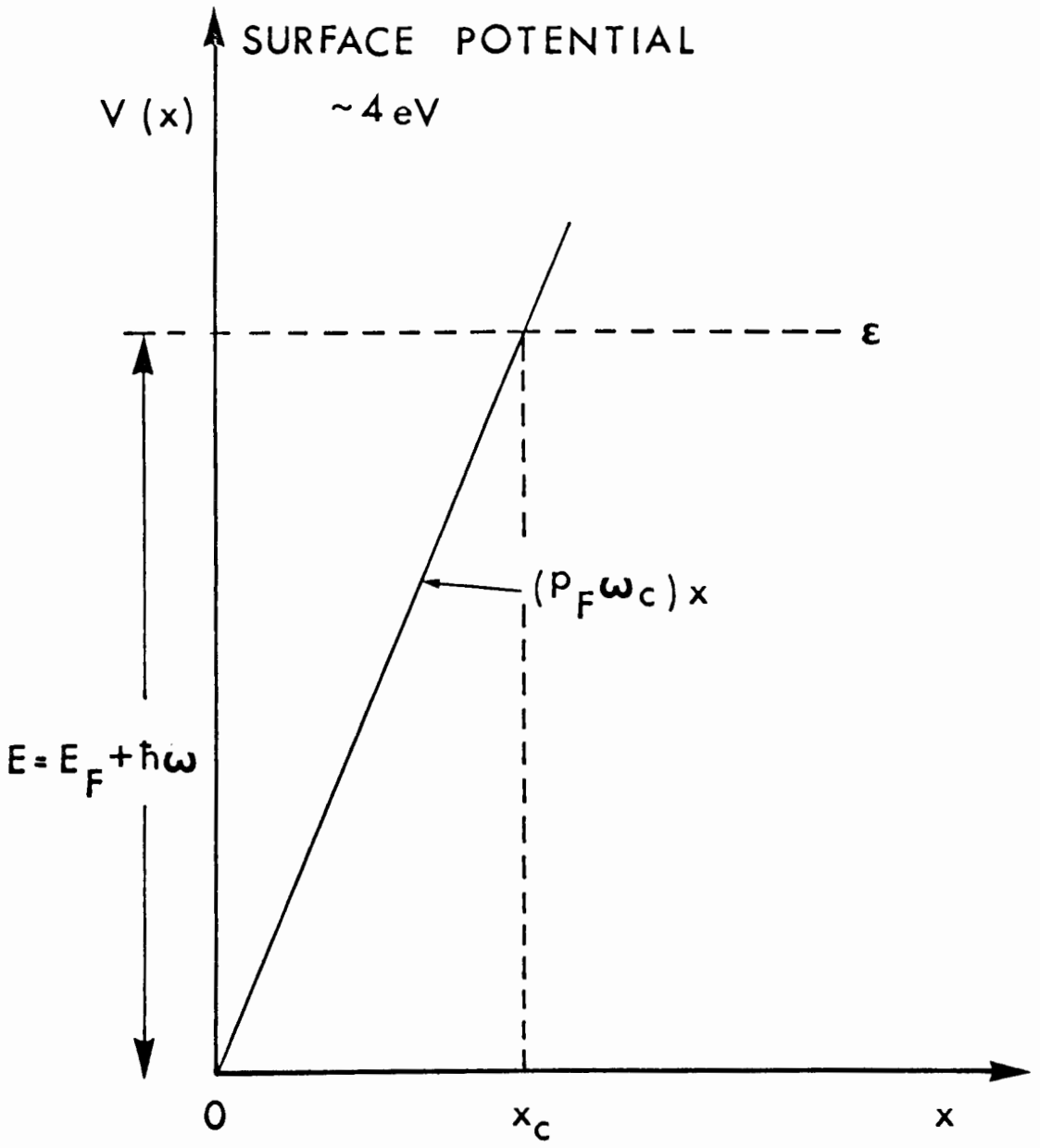

Figure 26. Portion of the parabola approximated by a straight line so that the particle is in a triangular potential well.

$$\oint p_x(x)\,dx = 2\int_0^{x_c}\left[2m\epsilon - 2p_F\frac{eB}{c}x\right]^{1/2}dx$$

$$= (n+\beta)\,2\pi\hbar$$

Completing the integral we obtain

$$\frac{2}{3}\frac{c}{p_F eB}(2m\epsilon)^{3/2} = (n+\beta)\,2\pi\hbar$$

or

$$E_n = E_F + \left\{\frac{e\hbar^{1/2}}{c}\right\}^{2/3}\frac{V_F}{(2k_F)^{1/2}}B^{2/3}C_n \qquad \text{(I-6)}$$

where

$$p_F = m V_F = \hbar k_F$$

and

$$C_n = \left|\frac{2\pi}{2}(n+\beta)\right|^{2/3} \qquad \text{(I-7)}$$

The microwave radiation of energy, $h\nu$ will be absorbed resonantly if it can promote a particle from level n to m. This occurs at the magnetic field value satisfying the equation

$$\hbar\omega = E_m - E_n = \left\{ \frac{e\hbar}{c} \right\}^{2/3} \frac{V_F}{(2k_F)^{1/3}} B_{nm}^{2/3} (\epsilon_m - \epsilon_n) \quad \text{(I-8)}$$

In actual practice however, one keeps, ω fixed and varies the magnetic field. The resonances appear at field values satisfying the relationship

$$B_{nm} = (\epsilon_m - \epsilon_n)^{-3/2} \left\{ \frac{\hbar c}{e} \right\} \left\{ \frac{2k_F}{V_F^3} \right\}^{1/2} \epsilon_n^{3/2} \quad \text{(I-9)}$$

Thus the resonant B values are characterized by the value of n, the lower of the two states between which the absorption takes place. Hence, we expect a series of transitions starting at the n = 1 ground state, going to successively higher states, at field values B_{12}, B_{13}, B_{14}, etc. Similarly there will be other series beginning at n = 2, 3, 4, etc. The agreement between theory and experiment is excellent as shown in Fig. 27. Also equation (I-9) predicts, $B \propto \omega^{3/2}$ which is in accord with the experimental findings. Recently the concept of magnetic-field induced surface states has been extended[84] to superconducting phase, but we will not go into that.

Let us compare the separation between surface state levels

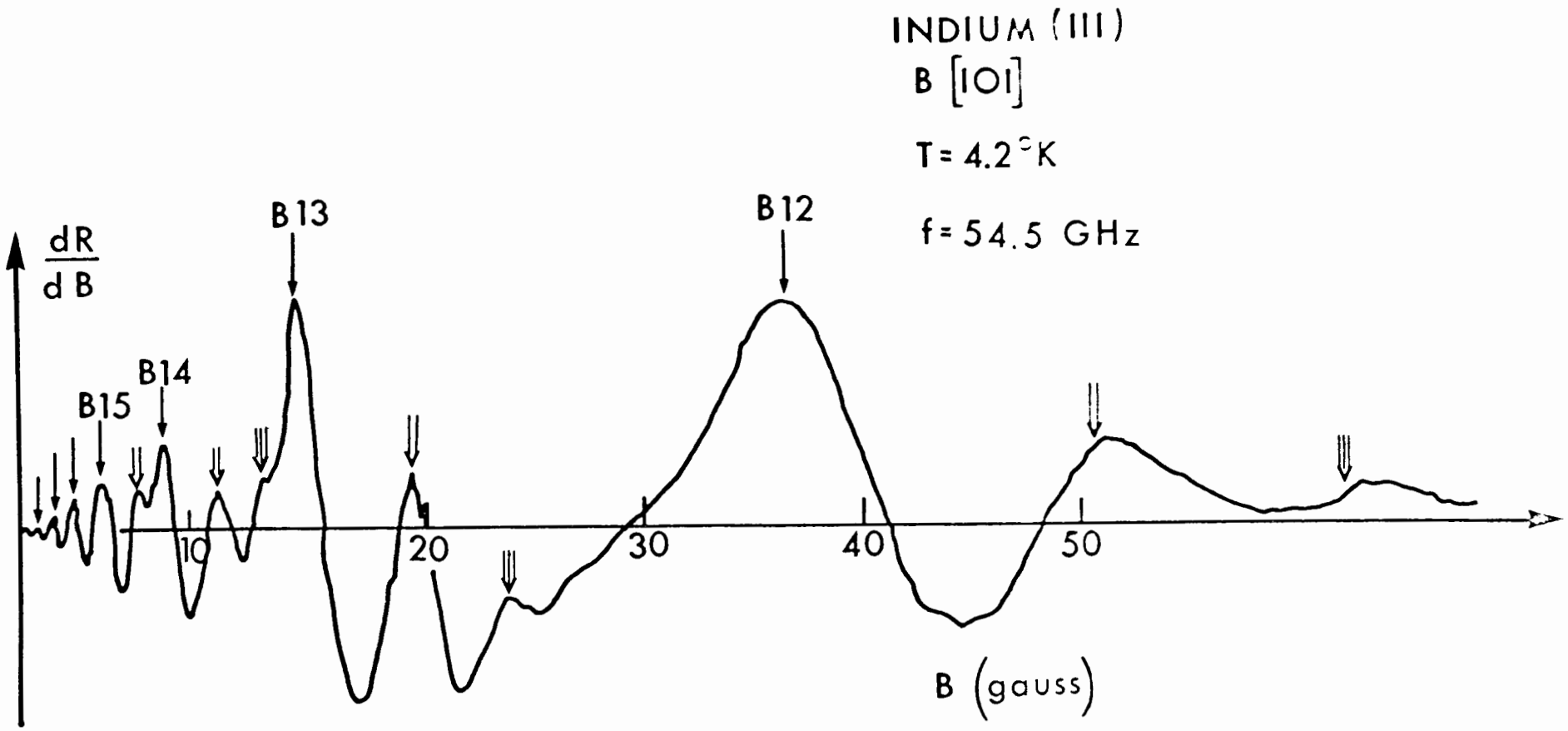

Figure 27. Microwave absorption spectrum in indium. The single peak at 36.4 gauss has been identified as B_{12} and fitted to the equation for B_{nm}. The arrows then predict other resonant field values from the equation in agreement with the dR/dB maxima as in the experimental trace. The single arrows denote the series B_{1m} that correspond to transition from the n = 1 state to successively higher states. Double and triple arrows denote the series B_{2m} and B_{3m} respectively. (J. Jensen, Ph.D. thesis, Univ. of Maryland).

($\Delta E_{s.s.}$) with the cyclotron separation ($\Delta E_{c.R.}$). For this purpose we write (I-6) in the form

$$F_n = F_F + C_n F_F^{1/3} (\hbar\omega_c)^{2/3} \qquad \text{(I-10)}$$

Then

$$\Delta F_{s.s.} \simeq F^{1/3} \hbar\omega_c^{2/3} \qquad \text{(I-11)}$$

Now $\Delta E_{c.R} = \hbar\omega_c$ and hence the relative separation

$$\frac{\Delta E_{s.s.}}{\Delta E_{c.R}} \simeq \left(\frac{F_F}{\hbar\omega_c}\right)^{1/3} >> 1 \qquad \text{(I-12)}$$

Thus the surface states are widely spaced as compared with the cyclotron resonance separation and the condition $\Delta E_{s.s.}\ \tau >$ can be easily satisfied. Incidentally, it should be noticed that at 10 gauss, $\Delta E_{s.s.} \sim 10^{-4}$ eV. Hence a resonance will be observed at 10 gauss field only if we shine 30 GHz microwave radiation. This indeed checks with the experiment.

In the end it must be emphasized once again that the surface states can be observed if $R_c > \delta$. If $R_c < \delta$, the energy spectrum is continuous and thus there is no structure due to surface states.

REFERENCES

REFERENCES

1. J. Bardeen, F. J. Blatt and L. H. Hall, Photoconductivity Conference, 1954 (John Wiley, Inc., N. Y., 1956) p. 146.

2. F. Urbach, Phys. Rev. 92, 1324 (1953).

3. T. S. Moss, J. Appl. Phys. 32, 2136 (1962).

4. B. O. Seraphin and R. B. Hess, Phys. Rev. Letters 14, 138 (1965).

5. B. O. Seraphin and N. Bottka, Phys. Rev. 139, A560 (1965).

6. W. P. Dumke, Phys. Rev. 108, 1419 (1957).

7. V. Roberts and R. Quarrington, J. Electronics 1, 152 (1955).

8. Dennis Dunn, Phys. Rev. (To be Published 1968).

9. G. D. Mahan, Phys. Rev. 145, 602 (1966).

10. I. P. Batra and R. R. Haering, Can. Jour. Phys. 45, 3401 (1967).

11. J. M. Luttinger and W. Kohn, Phys. Rev. 97, 869 (1955).

12. J. Zak and W. Zawadzki, Phys. Rev. 145, 536 (1966).

13. H. N. Spector, Phys. Stat. Sol. 22, 185 (1967).

14. A. K. Rajagopal, Il Nuvo Cimento, 46, 46 (1966).

15. L. I. Schiff, Quantum Mechanics (McGraw Hill, Inc., N. Y., 1955).

16. L. D. Landau and E. M. Lifshitz, Quantum Mechanics: Non-Relativistic Theory (Addison-Wesley Inc., Reading, Mass., 1958).

17. For the crossed field situation, the effect of including photon wave vector, has been considered by F. P. Kapron and R. R. Haering, Can. Jour. Phys. 43, 1921 (1965).

18. L. M. Roth, B. Lax and S. Zwerdling, Phys. Rev. 114, 90 (1959).

19. D. E. Aspnes, Phys. Rev. 147, 554 (1966).

20. T. S. Moss, Optical Properties of Semiconductors (Butterworths Publications Ltd., London 1959).

21. E. Burstein, G. S. Picus, M. A. Gebbie and F. Blatt, Phys. Rev. 103, 826 (1956).

22. S. Zwerdling, R. F. Keyes, S. Foner, H. N. Kohn and B. Lax, Phys. Rev. 104, 1805 (1956).

23. R. J. Elliott, T. P. McLean and G. G. Macfarlene, Proc. Phys. Soc. (London) 72, 553 (1958).

24. E. Burstein, G. S. Picus, R. F. Wallis and F. Blatt, Phys. Rev. 113, [illegible] (1959).

25. S. D. Smith, Handbuch der Physik, XXV/2a, 234 (1967).

26. B. Lax and S. Zwerdling, Progress in Semiconductors (John Wiley, Inc., N. Y. 1960) vol. 5, p. 221.

27. B. Lax, Proc. Int. Conf. Semiconductors Physics, Paris (1964) p. 253.

28. B. Lax and J. G. Mavroides, Applied Optics 6, 647 (1967).

29. For complete bibliography of magneto-optics of solids see, E. D. Palik and B. W. Henvis, Applied Optics 6, 603 (1967).

30. S. Zwerdling and B. Lax, Phys. Rev. 106, 51 (1957).

31. E. Burstein and G. S. Picus, Phys. Rev. 105, 1123 (1957).

32. S. Zwerdling, B. Lax and L. M. Roth, Phys. Rev. 108, 1402 (1957).

33. K. Tharmalingam, Phys. Rev. 130, 2204 (1963).

34. J. Callaway, Phys. Rev. 130, 549 (1963).

35. W. Franz, Z. Naturforsch, 13A, 484 (1958).

36. L. V. Keldysh, Soviet Physics - JETP 7, 788 (1958).

37. R. R. Haering and E. N. Adams, J. Phys. Chem. Solids, 19, 8 (1961).

38. A. Frova, P. Handler, F. A. Germano and D. E. Aspnes, Phys. Rev. 145, 575 (1966). (Also see references given in it.)

39. Y. Hamakawa, F. Germano and P. Handler, Proc. Int. Conf. Phys. Semiconductors (Kyoto) 1966, p. 111.

40. A. G. Aronov, Soviet Physics - Solid State 5, 402 (1963). (His results are in error by some numberical factors.)

41. Q. H. F. Vrehen, Phys. Rev. 145, 675 (1966).

42. H. N. Spector, Physica 30, 1917 (1964) and 32, 1551 (1966).

43. In literature (see ref. (41)) such transitions have sometimes been called 'forbidden transitions'. We avoid using this name because it can cause confusion.

44. Q.H.F. Vrehen and B. Lax, Phys. Rev. Letters 12, 558 (1965).

45. Q.H.F. Vrehen, Phys. Rev. Letters 14, 558 (1965).

46. Q.H.F. Vrehen, W. Zawadzki and M. Reine, Phys. Rev. 158, 702 (1967).

47. M. Reine, Q.H.F. Vrehen and B. Lax, Phys. Rev. Letters 17, 582 (1966). (They choose $\nu = \sqrt{\pi}$).

48. M. Reine, Q.H.F. Vrehen and B. Lax, Phys. Rev. 163, 726 (1967).

49. M. H. Weiler, W. Zawadzki and B. Lax, Phys. Rev. 163, 733 (1967).

50. R. S. Knox, 'Theory of Excitons', Supplement No. 5 to Solid State Physics, Ed. by F. Seitz and D. Turnbull, (Academic Press, Inc., N. Y. 1963). (Also see the references cited there.)

51. D. Redfield, Phys. Rev. 130, 916 (1963).

52. Y. Toyozawa, Inst. for Solid State Physics, University of Tokyo, Technical Report No. A119, 1964 (Unpublished).

53. T. H. Keil, Phys. Rev. 140, A601 (1965).

54. Y. Toyozawa, Progr. Theoret. Phys. (Kyoto) 22, 455 (1959).

55. D. L. Dexter, Phys. Rev. Letters 19, 1383 (1967). (Also see references cited there.)

56. D. Redfield and M. A. Afromowitz, Appl. Phys. Letters 11, 138 (1967).

57. T. P. McLean, in Progress in Semiconductors, edited by A.F. Gibson (John Wiley, Inc., N. Y. 1960) Vol. 5, pp. 55-101.

58. D. G. Thomas, J. J. Hopfield and M. Power, Phys. Rev. 119, 570 (1960).

59. B. Segall, Phys. Rev. 150, 734 (1966).

60. G. E. Hite, D.T.F. Marple, M. Aven and B. Segall, Phys. Rev. 156, 850 (1967).

61. S. Zwerdling, B. Lax and L. M. Roth, Phys. Rev. 108, 1402 (1957).

62. Dennis Dunr and I. P. Batra, Can. Jour. Physics (In Press).

63. I. P. Batra and R. R. Haering, Bull. Am. Phys. Soc. 12, 639 (1967).

64. G. L. Pearson and M. Tanenbaum, Phys. Rev. 90, 153 (1953).

65. H. Ehrenreich, Phys. Rev. 120, 1951 (1960).

66. G. Dresselhaus, A. F. Kip, C. Kittel and G. Wagoner, Phys. Rev. 98, 556 (1955).

67. E. D. Palik, J. R. Stevenson and R. F. Wallis, Phys. Rev. 124, 701 (1961).

68. W. Spitzer and H. Y. Fan, Phys. Rev. 99, 1891 (1955).

69. W. Cochran, S. J. Fray, F. A. Johnson, J. E. Quarrington and W. Williams, J. Appl. Phys. 32, 2102 (1961).

70. C. Hilsum and R. Barne, Proc. Phys. Soc. (London) 71, 676 (1958).

71. C. Hilsum, Progress in Semiconductors, edited by A. F. Gibson (John Wiley, Inc., N. Y. 1965) Vol. 9, p. 135.

72. E. O. Kane, J. Phys. Chem. Solids 1, 249 (1957).

73. I. M. Boswarva and A. B. Lidiard, Proc. Roy. Soc. (London) A278, 558 (1964).

74. U. W. Hochstrasser, in Handbook of Mathematical Functions, edited by M. Abramowitz and I. A. Stegun (Dover Publications, Inc., New York 1965), Chapter 22.

75. L. Fritsche, Phys. Stat. Sol. 11, 381 (1965).

76. A. F. Kip, D. N. Lagenberg, B. Rosenblum and G. Wagoner, Phys. Rev. 104, 494 (1957).

77. M. S. Khaikin, Soviet Phys. JETP 39, 152 (1961) and JETP Letters 4, 113 (1966).

78. J. F. Koch and C. C. Kuo, Phys. Rev. 143, 470 (1966).

79. J. F. Koch, "Electrons in Metals", Simon Fraser University Summer School (1967), Edited by J. F. Cochran and R. R. Haering (Gordon and Breach, Inc.)(To be Published).

80. M. Ya Azbel and E. A. Kaner, J. Phys. Chem. Solids 6, 113 (1958).

81. T. W. Nee and R. E. Prange, Phys. Letters 25, 582 (1967).

82. R. E. Prange and T. W. Nee, Phys. Rev. 168, 779 (1968).

83. B. Lax, Rev. Mod. Phys. 30, 122 (1958).

84. J. F. Koch and C. C. Kuo, Phys. Rev. 164, 618 (1967).